

A photograph of a person's hand holding a green and yellow robotic device. The device consists of several thin, flexible tubes that wrap around the fingers and the back of the hand. The tubes are primarily green, with some yellow sections. The background is dark blue.

Ard Westerveld

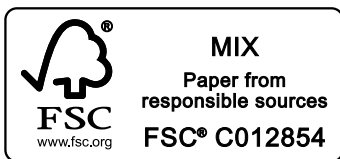
**Robotics
combined with
Electrical Stimulation**

hybrid support of arm and hand for
functional training after stroke

Robotics combined with Electrical Stimulation

hybrid support of arm and hand for
functional training after stroke

Ard Westerveld



The publication of this thesis was financially supported by
the Department of Biomechanical Engineering of the University of Twente

Printed by Gildeprint Drukkerijen

Robotics combined with electrical stimulation
hybrid support of arm and hand for functional training after stroke

Ard Westerveld

ISBN 978-90-365-3600-4

©2014, Ard Westerveld

All rights reserved. No part of this book may be reproduced in any form without
the written permission of the author.

ROBOTICS COMBINED WITH ELECTRICAL STIMULATION
HYBRID SUPPORT OF ARM AND HAND FOR FUNCTIONAL TRAINING AFTER STROKE

PROEFSCHRIFT

ter verkrijging van
de graad van doctor aan de Universiteit Twente
op gezag van de rector magnificus,
prof. dr. H. Brinksma,
volgens besluit van het College voor Promoties
in het openbaar te verdedigen
op donderdag 13 maart 2014 om 14.45 uur

door

Ard Johan Westerveld

geboren op 25 juni 1984
te Gendringen

Dit proefschrift is goedgekeurd door de promotoren:

Prof. dr. ir. H. van der Kooij

Prof. dr. ir. P. H. Veltink

en door de assistent-promotor:

Dr. ir. A. C. Schouten

ISBN 978-90-365-3600-4

Copyright 2014

Contents

1	General introduction	1
2	Selectivity and resolution of surface electrical stimulation for grasp and release	10
3	Control of thumb force using surface functional electrical stimulation and muscle load sharing	28
4	Grasp control in stroke patients using functional electrical stimulation and model predictive control	54
5	A robotic end point manipulator for rehabilitation exercises after stroke	76
6	Passive reach and grasp with functional electrical stimulation and robotic arm support	98
7	General discussion	114
	References	124
	Summary	138
	Samenvatting	142
	Dankwoord	146
	Curriculum Vitae	150
	Publications	152



General introduction

Stroke strikes all over the world. "As if the integrity of my mind/body connection had somehow become compromised", according to dr. Bolte Taylor (2009) who describes her own stroke as a "step by step deterioration of the intricate neurological circuitry". Although each stroke is unique (see Box 1.1), the common part is a compromised oxygen supply to certain brain regions resulting in cell death and loss of function.

As each brain region is responsible for a specific function, the effects of a stroke are highly dependent on the location and size of the region in which the stroke occurred. In the first period after her stroke, dr. Taylor could not understand language, read, write, walk or talk. Impairments caused by stroke include compromised contralateral motor control, muscle weakness, spasticity, memory deficits, loss of sensation, visual impairments and compromised bladder and bowel control (Roth and Harvey 2002). In addition to these physical impairments, a stroke can also influence psychological functions and can lead to depression, fear and anxiety.

Box 1.1: Stroke

Strokes are either ischemic (about 80% of all strokes) or hemorrhagic (figure 1.1). An ischemic stroke is characterized by obstructed cerebral blood flow. Either by thrombosis, embolism or lacunes (Roth and Harvey 2002).

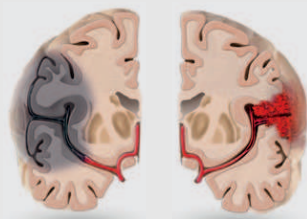


Figure 1.1: Schematic representation of ischemic (left) and hemorrhagic (right) strokes.

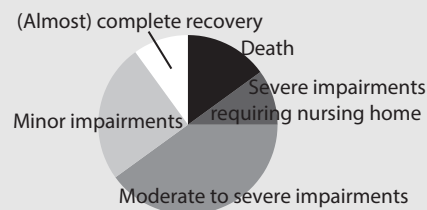


Figure 1.2: Prognosis after stroke^a

Hemorrhagic strokes are caused by rupture of a blood vessel (Donnan et al. 2008) either inside the brain (intracerebral hemorrhage) or in the space around the brain (Subarachnoid hemorrhage). Only 10% of the stroke victims will fully recover, others either die shortly after stroke or have to cope with minor to severe impairments, see figure 1.2.

^adata obtained from <http://www.uhnj.org/stroke/stats.htm>, December 2013

1.1 Influence of stroke on daily life

Worldwide, every three seconds a new stroke survivor (and his/her family) has to cope with some of the functional impairments described above. Imagine not being able to communicate or express your feelings, cannot remember things from your life before the stroke or become dependent on others for daily movement tasks. According to ES Lawrence et al. (2001), 77.4% of acute stroke patients have upper limb motor deficits and 72.4% have lower limb motor deficits. Compromised human motor control (Box 1.2) will lead to various limitations during activities of daily living, like eating, drinking and personal hygiene, and diminish the patient's independency.

In a healthy situation, we are not consciously involved in moving our limbs or in opening and closing our hands. Unconsciously we predict the weight of a cup of coffee and pick it up to bring it to our mouth to drink. That is, if you like coffee of course, otherwise you would probably think twice. Many stroke patients have to work very hard to move their arm contralateral to the brain lesion in a desired way. Over time this may improve due to the compensatory strategies (Roby-Brami et al. 2003) or plasticity of the brain, i.e. the brain's ability to rearrange and let other regions take over functions from lost and affected regions (Johansson 2000; Nudo et al. 2001; Barsi et al. 2008).

Box 1.2: Cortical motor control

Voluntary movements are initiated to achieve a desired goal. The brain integrates sensory information from the body and its environment to drive the appropriate muscles to accomplish a certain task. During the task, sensory signals from muscles and skin are fed back to the brain and used to control the movement (Kandel et al. 2000). Muscle activation is driven from the primary motor cortex (M1). M1 is classically divided in subsections responsible for distinct body parts (Nudo et al. 2001) commonly referred to as the homunculus ("little man") as shown in figure 1.3. Cortical drive from M1 is projected to the alpha motor neuron in the spinal cord through the corticospinal tract.

The corticospinal tract crosses to the opposite side of the spinal cord: right sided movements are controlled by the left hemisphere and vice versa. The nerve endings of the alpha motor neuron in the spinal cord innervate the muscles to generate the desired movement (Kandel et al. 2000).

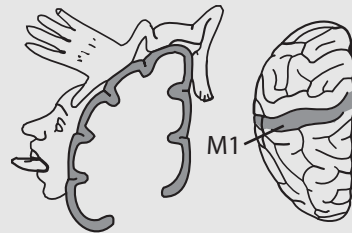


Figure 1.3: Anatomical divisions of the primary motor cortex (Redrawn based on Penfield and Rasmussen 1950)

1.2 Motor (re)learning

People learn their whole life. The basis of learning is the formation of new neural pathways and modification of existing pathways. After stroke, patients have to (partially) relearn motor control. Motor learning is described by Bastian (2008) as the "formation of a new motor pattern that occurs via long-term practice (i.e. days, weeks, years)." A concept closely related to motor learning is motor adaptation, which describes the modification of a movement due to perceived errors. For instance, adaptation to be able to use a computer-mouse set to a different speed as one is used to. This adaptation process can turn into a "learned" calibration for the new environment. In rehabilitation, patients who can only move slowly or inaccurate "do not need to learn the movement from scratch but do need substantial recalibration for their altered neural control" (Bastian 2008).

Integration of sensory information is an important factor for (re)learning. In monkey experiments, in which the primary sensory hand area was ablated, monkeys were able to perform previously learned movements, but were not able to learn new movements (Krakauer 2006). For generalization of tasks learned by training to tasks in daily life, repetitive training of the same movement seems insufficient. When patients are asked to pick up a glass at variable positions, they will probably learn the movement of reaching for a glass in a specific place to a lesser extent, but they might be better in generalizing the task to real life and also retention of the learned movement is expected to be higher in the variable setting (Krakauer 2006).

1.3 Therapy after stroke

Some spontaneous recovery can occur after stroke (Nudo 2006). To further reduce impairment and enhance functional independence of stroke survivors, additional therapy is commonly provided. Stroke therapy either exploits brain plasticity to relearn movement by extensive training or focuses on strategies to compensate for lost functions. Applied training paradigms include arm ability training, constraint-induced movement therapy, bilateral arm training, functional electrical stimulation (box 1.3), interactive robot therapy and virtual reality based therapy (Krakauer 2006; Timmermans et al. 2009). These therapies should focus on task-oriented training (skill learning) to obtain better generalization from rehabilitation setting to daily life activities (Timmermans et al. 2009).

1.4 Functional electrical stimulation

The principles of functional electrical stimulation (FES) are explained in box 1.3. FES is successfully applied as a prosthetic system to replace lost functions, mainly after spinal cord injury (Sheffler and Chae 2007; Snoek et al. 2000). FES can also be used as therapeutic system to improve motor function after stroke. FES training can increase muscle strength and thereby reduce weakness due to non-use (Powell et al. 1999; Rosewilliam et al. 2012) and can reduce pain and contractions

(Malhotra et al. 2012). In a systematic review of randomized clinical trials, de Kroon et al. (2002) identified positive training effects of FES training on motor control. Barsi et al. (2008) showed increased cortical excitability after post stroke FES training, which indicates regeneration of neural pathways.

1.5 Rehabilitation robotics

Robots are inexhaustive and therefore an ideal partner for intensive repetitive functional training after stroke. The past decades, several robotic systems for arm and hand therapy have been designed. MIT-manus (Hogan et al. 1992), HapticMaster (Van der Linde et al. 2002), CADEN-7 (Perry et al. 2007), ARMin (Nef et al. 2007), Freebal (Stienen et al. 2009b) and Dampace (Stienen et al. 2009a) are ex-

Box 1.3: Functional Electrical Stimulation

Functional electrical stimulation (FES) evokes neural activity in motor nerve fibers. Generated action potentials will lead to contraction of the muscle, see figure 1.4. An important difference compared to normal neural activity is the reversed recruitment order. With FES the thickest motor nerve fibers are activated first, as opposed to physiological activation in which the smallest-diameter nerves are activated first (Sheffler and Chae 2007), leading to more coarse movement and earlier fatigue. In addition, to obtain smooth contractions with FES, motor units are activated synchronously with relatively high frequency, also leading to relatively early muscle fatigue.

Three types of electrodes can be used to transfer the generated stimulus to the nerve: 1) implanted, 2) percutaneous or 3) surface electrodes. Implanted electrodes have the benefit of properly cuffing the electrode around the nerve leading to very selective activation. However, this highly inva-

sive solution is mainly suitable for permanent FES applications. Surface electrodes are placed further from the target nerve and dedicated electrode placement is required for selective muscle activation. However, current spreads out in the tissue underneath the electrodes and activation of multiple nerves cannot always be prevented. Nevertheless, due to its non-invasiveness, surface electrodes are commonly used in rehabilitation practice, especially in training therapy (de Kroon et al. 2002).

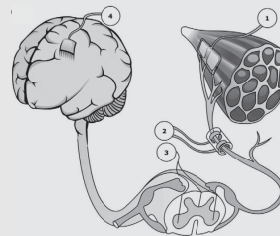


Figure 1.4: Schematic overview of muscle activation with surface FES (1) or invasive alternatives: nerve cuff (2), intraspinal (3) or intracortical (4) stimulation (Stein and Mushahwar 2005)

amples of either robotic exoskeletons or end-point manipulators for arm training. Also some systems for hand training have been developed (Worsnopp et al. 2007; Lambercy et al. 2007; Dovat et al. 2008).

Two recent reviews evaluated the effects of robotic stroke therapy (Prange et al. 2006; Krebs et al. 2008). They both conclude that robotic therapy can improve motor control of the hemiparetic upper limb. Robotic aided therapy gives similar results as conventional therapy (Kwakkel et al. 2008) and robotic manipulators facilitate more intensive training and objective measurements (Lum et al. 2002), without the need of a therapist being continuously present. Thus multiple patients could train simultaneously under supervision of a single therapist or patients might even use robotics without supervision at home for intensive training with the therapist only monitoring progress regularly.

1.6 The MIAS-ATD project: a hybrid approach

Robotics is ideal for intensive and repetitive training. However, from a mechanical point of view, properly actuating the hand and fingers with a robotic device without interfering movements is relatively complex. Functional electrical stimulation has been successfully used for actuation of hand and fingers and might therefore be an excellent extension for a robotic arm support system. A hybrid system will allow for assistance of functional task-oriented movements, focusing on skill-learning and therefore has potential as a rehabilitation device, aiming at generalization to activities of daily life.

The ATD (Active Therapeutic Device) branch of the MIAS (Medical Innovations for an Aging Society) project focuses on the development of a hybrid rehabilitation system. The project is a consortium of Demcon, tic Medizintechnik, Use-Lab, Roessingh Research & Development (RRD) and the University of Twente (UT) funded by Interreg IV-A, part of the European regional development fund. Within the consortium requirements and possibilities for a hybrid rehabilitation system were analyzed. Prototype robotics were built by Demcon and prototype stimulator equipment was provided by tic Medizintechnik. The prototypes were evaluated by Use-Lab, RRD and UT.

1.7 Research questions

The main goal of this thesis is to develop and evaluate control algorithms for a hybrid rehabilitation system combining FES and robotics. The thesis will provide answers to the following questions that arise for proper control of a hybrid rehabilitation system.

- Which muscles involved in grasp and release are available to target with surface FES? And to what extent can these muscles be selectively activated with FES?
- What is the relation between stimulation input and force output of individual

muscles? How can this relation be modeled and used to control the redundant muscular system with FES?

- Can the developed prototype FES system activate hand muscles properly for functional grasp and release?
- Is the developed prototype robotic manipulator suitable for assistance of functional reach movements?
- Is the hybrid rehabilitation system combining robotics for reach and FES for grasp and release effective for passive movement support?

1.8 Thesis outline

In this thesis several experimental studies are described to answer the questions above and evaluate the prototype hybrid system. By the use of an automated system for stroke rehabilitation, which is also applicable in the patient's home, therapy can be intensified. Ideally, an automated system should only support when necessary, thereby maximizing patient effort (Wolbrecht et al. 2008). However, in this thesis the technical feasibility and performance is evaluated and therefore the subjects were asked to relax in the described experiments (i.e. no voluntary movement). A passive subject will be the most demanding situation for the system and is therefore used as evaluation setting.

In **Chapter 2** the possibilities for selective activation of individual fingers by functional electrical stimulation are explored. The main question to be answered is whether it is possible to find specific locations for selective finger movements in different healthy subjects.

Chapter 3 uses selective activation of three thumb muscles to control the forces generated by the thumb in the plane perpendicular to the thumb. A model for the relation between the stimulation parameters and the evoked forces is developed and evaluated in both healthy subjects and stroke subjects. Subsequently, the individual muscle models are used to control the thumb force towards target force vectors by sharing the load among the individual muscles.

A shift towards position control is made in **Chapter 4**, where the relation between muscle stimulation and finger movement is modeled and subsequently used in a model predictive controller. This controller uses the estimated model and predicts the necessary stimulation parameters based on desired finger joint angles. To estimate the performance of this control approach, real objects are grasped and released in healthy subjects and stroke subjects.

In **Chapter 5**, the design and technical evaluation of a new active therapeutic device is presented. This robotic end point manipulator is capable of providing guidance forces and counteracting the weight of the arm to make arm movements easier.

Chapter 6 combines the systems presented in **chapter 4** and **chapter 5**. The combination of robotic supported reach movement and support of grasp and release

by functional electrical stimulation is evaluated during passive reach, grasp and release tasks in healthy subjects and stroke subjects.

Finally, in **Chapter 7** the results of this thesis are summarized and discussed. The discussion focuses on clinical implications of the knowledge currently obtained and the required future steps to translate this knowledge to clinical applications.



Selectivity and resolution of surface electrical stimulation for grasp and release

Published as:
Westerveld, AJ, AC Schouten, PH Veltink, and H van der Kooij (2012). "Selectivity and resolution of surface electrical stimulation for grasp and release." *IEEE Transactions on Neural Systems and Rehabilitation Engineering*. 20 (1), pp. 94–101

Abstract

Electrical stimulation of arm and hand muscles can be a functional tool for patients with motor dysfunction. Sufficient stimulation of finger and thumb musculature can support natural grasping function. Yet it remains unclear how different grasping movements can be selectively supported by electrical stimulation. The goal of this study is to determine to what extent activation of individual fingers is possible with surface electrical stimulation for the purpose of rehabilitation following stroke.

The extensor digitorum communis (EDC) muscle, flexor pollicis longus (FPL) muscle and the thenar muscle group, all involved in grasp and release, were selected for stimulation. The evoked forces in individual fingers were measured. Stimulation thresholds and selective ranges were determined for each subject. Electrode locations where the highest selective range occurred were compared between subjects and influences of different isometric wrist positions were assessed.

In all subjects selective stimulation of middle finger extension and thumb flexion was possible. In addition, selective stimulation of index and ring finger extension was possible in most cases. In 9 out of the 10 EDC subjects we were able to stimulate 3 or all 4 fingers selectively. However, large variability in electrode locations for high selectivity was observed between the subjects.

Within the designs of grasping prostheses and grasping rehabilitation devices, the variability of electrode locations should be taken into account. The results of our study facilitate the optimization of such designs and favor a design which allows individualized stimulation locations.

2.1 Introduction

Grasp and release of objects is an important function in daily life. Both grasping and releasing becomes difficult or even impossible for large numbers of patients from several pathologies. Sufficient electrical stimulation (ES) of finger flexor and extensor muscles, together with the thumb musculature, can help these patients to become more functionally independent (e.g. Shimada et al. 2003) and regain manual dexterity.

Besides directly producing functional hand movement, ES is used to *train* functional movements in stroke patients (e.g. Barsi et al. 2008). For therapeutic ES surface stimulation is preferred above percutaneous stimulation, because of the non-invasive character. During therapeutic training sessions, ES can assist functional movements, leading to motor re-learning of these movements (Krakauer 2006). Especially ES in combination with voluntary effort enhances motor re-learning (DB Popović et al. 2009).

Reduced muscle selectivity, after stroke for example, leads to impaired fine motor skills (Lang and Schieber 2004). If ES can be used to selectively activate muscles, it could be used to train fine motor control. Small electrodes are able to more precisely target muscles or muscle parts for selective activation than are larger electrodes. This precise targeting, however, is increasingly vulnerable to deviations in electrode location. Therefore, electrodes should be positioned precisely, which will be more time-consuming compared to larger electrodes.

The muscle motor point positions relative to the skin are known to vary among different subjects (Nathan 1979; Nathan 1990) and might change during movements of the muscle itself or during the movement of nearby muscles (Cameron et al. 1999). If the inter-subject variation and the variation due to movement both are small, a general location may be determined, leading to near-optimal stimulation for most patients. However, if the inter-subject variation is substantial or stimulation locations vary largely during movement, a search procedure for the individualized location will be necessary. Array electrodes, covering the variations (Popović-Bijelić et al. 2005; M Lawrence et al. 2008; DB Popović and MB Popović 2009) together with an online self-learning algorithm for electrode selection could be a solution in that case.

Numerous objects manipulated during daily life (e.g. coffee cups, bottles, spoons or pencils), require successful movement of the thumb to form a functional grip. In addition, some patients suffer from involuntarily enlarged flexor activity, which hampers extension of individual fingers (e.g. Lang et al. 2009) and therefore the release of objects. Also, controlled closing of the hand by selective flexion of the fingers becomes more difficult. In the pinch grip for instance it is important that the other fingers do not interfere with the active fingers performing the grip. For rehabilitation, where assistance should be applied only when needed, selective finger extension (to counteract enlarged flexor activity) and thumb opposition are the focus when developing effective tools for relearning grasp and release functions.

Anatomically, the extensor digitorum communis (EDC) muscle consists of several parts actuating the different fingers. These parts are innervated by different

nerve branches. Thus, theoretically it should be possible to selectively stimulate extension of individual fingers (Leijnse et al. 2008). However, when voluntarily extending a single finger, some movement of other fingers can be observed (van Duinen et al. 2009). This results from both biomechanical coupling and combined neuromuscular control (Lang and Schieber 2004). When ES is applied to induce movement these couplings can also be expected.

In the past, several neuroprosthetic ES devices have been developed (Micera et al. 2010), including the Bioness H200 (formerly Ness Handmaster) (Hara 2008), Bionic Glove (Prochazka et al. 1997) and MecFes (Thorsen et al. 1999). All of these devices successfully use surface ES to train or aid activities of daily life. In the Bioness H200, electrodes are fixed to the orthosis at appropriate positions. Once these positions are determined, donning and doffing becomes quite easy. Problems with all of these devices include: somewhat limited muscle selectivity and complexity in application due to problems with electrode positioning (Micera et al. 2010).

Keller et al. (2006), assessed selectivity of ES applied to the finger flexors. They observed couplings between the different fingers in all subjects. They were able to selectively activate the middle and ring fingers in all subjects, although this was not expressed quantitatively. Nathan (1990) assessed threshold current levels for both targeted and overflow muscles in bipolar ES. Overflow to other muscles was observed during stimulation of several arm muscles. Different parts of the EDC muscle - for selective finger extension - were not considered.

The goal of the current study is to determine the selectivity and inter-subject variability of ES applied to three muscles involved in grasping and releasing objects: extensor digitorum communis (EDC), flexor pollicis longus (FPL) and the thenar muscle group. The main functions of these muscles are extension of the fingers, flexion of the thumb and abduction/opposition of the thumb, respectively. Knowledge of the selectivity and the variability will give insight in the accuracy needed for electrode placement, which forms important input to the development of new therapeutic tools using ES. The more selective a muscle can be activated, the more possibilities for fine motor control will become available.

2.2 Methods

2.2.1 Subjects

In total 19 healthy subjects participated in this study, divided over two subgroups. Group 1 (N=10; age range 23-27 yr; 5 male) participated in the extensor digitorum communis part of the study and the group 2 (N=9; age range 23-30 yr; 6 male) participated in the thumb musculature part of the study. All measurements were performed on the left hand. Subjects gave informed consent and the experiments were conducted in accordance with the Declaration of Helsinki.

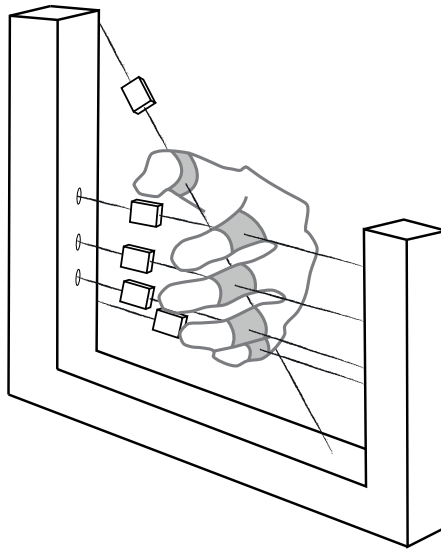


Figure 2.1: Schematic overview of custom-made setup for measurement of finger forces. The subject's five fingers were strapped in pre-loaded wires. Small load-cells measured wire tension and as such finger force.

2.2.2 Experimental setup

A custom-made setup was used, consisting of an electrical stimulator and a setup for measurement of finger forces.

Electrical stimulation

A battery-powered and current-controlled monophasic electrical stimulator with a peak amplitude of 13.5 mA was used. A custom-built Matlab/Simulink (The Mathworks inc., Natick, USA) interface controlled the stimulator wirelessly through a Bluetooth connection. An oval-shaped electrode of 6x4 cm was used as the anode and a round electrode, 1.5 cm in diameter, was used as the cathode. Electrodes with similar size showed good results on both selectivity and comfort in a simulation study by Kuhn et al. (2010).

Force measurement

To measure finger force, a custom-made setup was built, see figure 2.1. This setup consisted of an aluminum frame in which the lower left arm of the subject was strapped just proximal to the elbow and wrist joints. The setup allowed several isometric positions. The fingers were constrained by pre-loaded wires. The tension in the wires was measured by LSB200 load cells (Futek, Irvine, USA), with a maximum force capacity of 45.3 N.

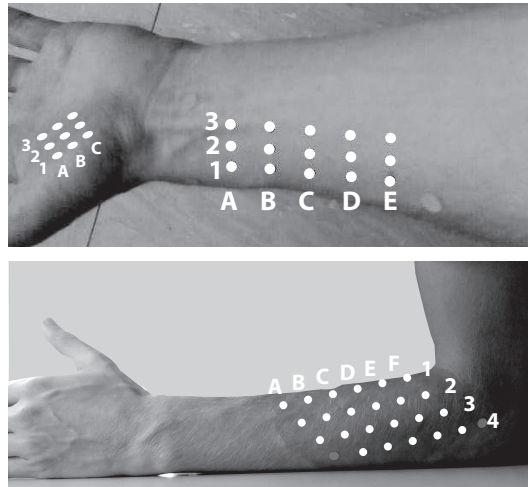


Figure 2.2: To determine the position of the EDC and FPL grid points, small round labels were placed relative to bony landmarks. Equidistant points for electrode placement were drawn between these labels. For the thenar musculature a 3×3 grid of 1 cm spaced points was drawn on the thenar, relative to the metacarpal bone of the thumb.

2.2.3 Experimental protocol

Electrode placement

The anode was placed on the posterior side of the lower arm, just proximal to the ulnar styloid process. To position the cathode at the Flexor Pollicis Longus (FPL) muscle and the Extensor Digitorum Communis (EDC) muscle, a web cam (Philips, Eindhoven, The Netherlands) was added to the setup for virtual projection of grid points. In addition, the webcam was used to take pictures of the electrode location, see figure 2.2. For each subject, the grid points were scaled according to the size of the subject's arm, as the points were defined relative to bony landmarks. For cathode placement on the thenar muscles, a 3×3 grid of 1 cm spaced points was drawn on the thenar.

Stimulation protocol

The muscles were electrically stimulated with single pulses of $350 \mu s$ width. Every second a stimulus was applied. For functional movement pulse trains with a frequency of 12-50 Hz are often used instead of single pulses. We chose to use single pulses to be able to directly connect the measured force response to the applied stimulation pulse, without the need of taking the pulse history into account.

The stimulus amplitude started at 2 mA and was increased by 0.5 mA at two second intervals, until the subject reported unbearable discomfort or the maximum amplitude of 13.5 mA was reached. For most subjects, 13.5 mA was still bearable, but they reported that the intensity was on the edge of painful stimulation.

2.2.4 Recordings

Sensor data was amplified by SG-3016 Isolated Strain Gauge Input Modules (ICP-DAS, Taipei, Taiwan) and acquired by a USB-6259 data acquisition module (National Instruments, Austin, USA) together with a pc running a custom-built Matlab/Simulink (The Mathworks inc., Natick, USA) interface. Force responses were measured at 1.6 kHz.

2.2.5 Data analysis

Force data from each sensor was pre-processed in two steps: 1) a first order Butterworth high pass filter with a cut-off frequency of 1 Hz was applied to remove drift and 2) a 50 ms window moving average filter was applied to reduce noise.

Selection of response thresholds and selective ranges

For each individual finger, the electrode location with the lowest response threshold was determined. A threshold of 0.025 N was used to discriminate between sensor noise and an actual force response. The selective range was determined as the range between the response threshold of the specific finger and the response threshold of any other finger. The size of the selective range gives information about how selectively a single finger can be stimulated. See figure 2.3 for an example of determination of response thresholds and selective ranges.

Variation between subjects

For each subject the electrode location(s) with the lowest response thresholds for a specific finger was determined. This can be multiple grid points when multiple points have the same response threshold. For each subject i , a matrix G_i with the same size as the electrode grid is determined. G_i is one at the lowest threshold location(s) and zero otherwise. Finally, the normalized relative occurrence \bar{G} was determined for all subjects together by summing all G_i 's and division by the number of subjects, N , as described in equation 2.1.

$$\bar{G} = \frac{\sum G_i}{N} \quad (2.1)$$

2.2.6 Influence of altered isometric position

Five different isometric positions were tested, see table 2.1. Threshold and selective range were determined for the index finger (EDC stimulation) and the thumb (FPL stimulation). Threshold levels and size of selective ranges of the different isometric positions were compared to the neutral position using paired t-tests with Bonferroni correction for multiple comparisons.

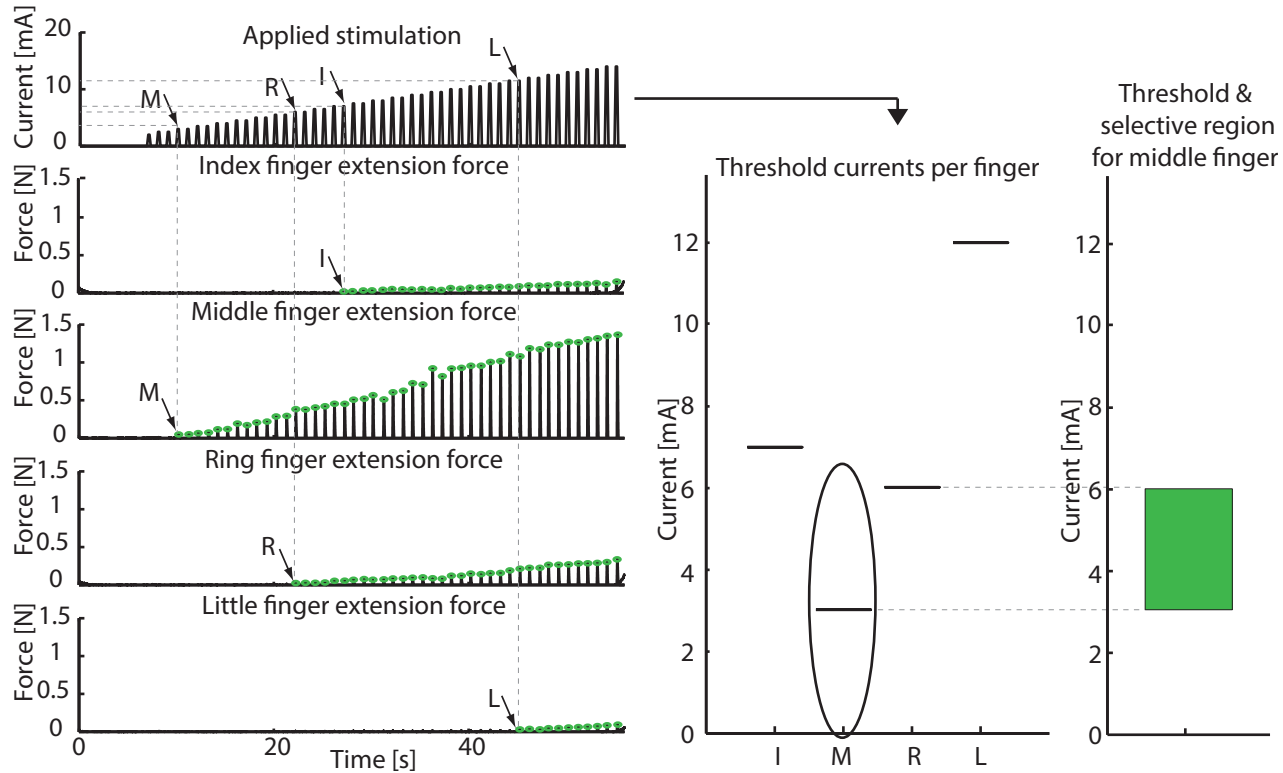


Figure 2.3: Determination of response thresholds and selective range after EDC stimulation for a single grid location. Response threshold was determined for each finger (indicated by the labeled arrows) as the stimulation amplitude where the resulting force exceeded a threshold of 0.025 N. The selective range for a single grid-point was defined as the amplitude range where only one finger responded to the stimulation. In this specific example, the resulting selective range is 3-6 mA.

Table 2.1: Tested isometric wrist positions

Position	Flexion/extension	Pro/supination
1	neutral	neutral
2	45° extension	neutral
3	45° flexion	neutral
4	neutral	90° pronation
5	neutral	90° supination

2.3 Results

2.3.1 Selectiveness of stimulation

Figures 2.4 and 2.5 show plots of the selective ranges for the different fingers of the different subjects. For all subjects, it is possible to selectively stimulate middle finger extension (figure 2.4). In addition, for most subjects, selective stimulation is possible for the index and ring fingers. Selective stimulation of the little finger is achieved in only 4 of 10 subjects. For the stimulation of thumb movement (figure 2.5), all subjects show the possibility for selective stimulation. Selective ranges vary with the electrode locations.

In figure 2.6, box plots of the selective range sizes are shown for the four fingers and the thumb (both FPL and thenar stimulation). For each subject the largest selective range for a specific finger is selected (highest grey bar in each plot of figure 2.4 and 2.5). The selective ranges for index and middle fingers are similar. A decrease in selective range is observed for the ring and little fingers. Selective ranges for the thumb are comparable to those of index and middle fingers.

2.3.2 Variation of response thresholds with respect to grid points

In figure 2.7 the normalized distribution of lowest-threshold grid-points across subjects (see Eq. 2.1) is shown for the EDC muscle (A-D), the FPL muscle (E) and the thenar muscles (F). For the different fingers, clustering of grid-points can be observed. Thus the lowest-threshold points for the different fingers lie close together for the different subjects. However, there was a large overlap between the different fingers. In the thumb muscles, the points with the lowest threshold were more spread over the grid. Thus the electrode location where the stimulation threshold was lowest varied greatly between different subjects.

2.3.3 Influence of altered isometric position

Figure 2.8 shows responses of threshold amplitude and selective range to altered isometric positions for the Index finger and the thumb. Distributions over the subjects compared to the neutral position are shown.

There was a large variation in the responses for the different subjects. For both EDC stimulation and FPL stimulation, no significant systematic change in either threshold amplitude or selective range due to the altered isometric positions was observed.

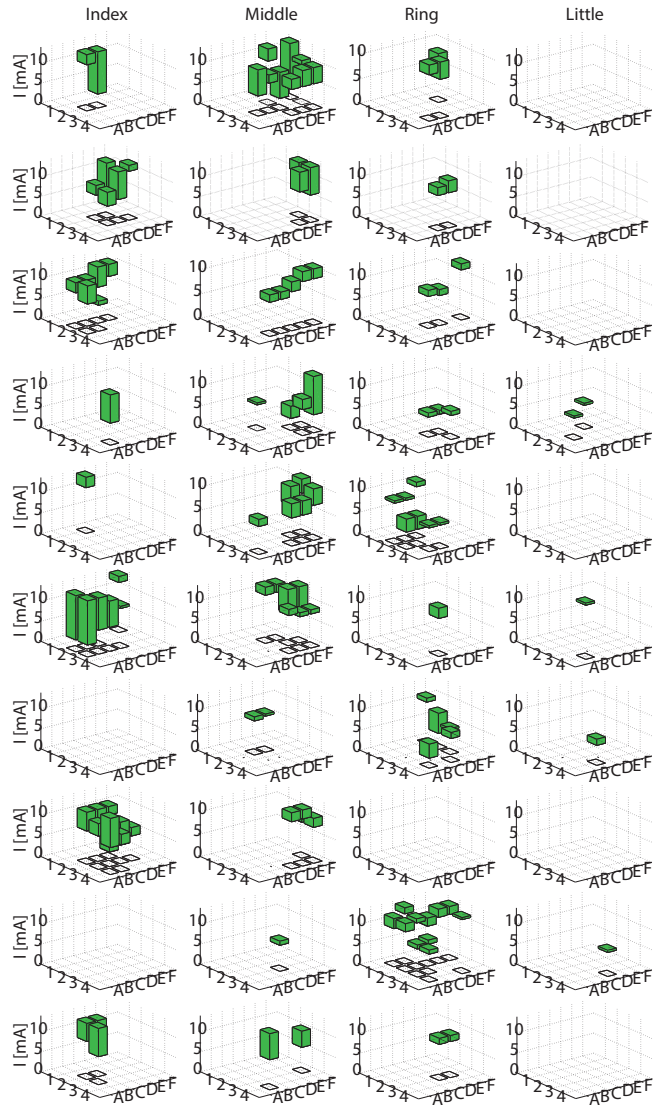


Figure 2.4: Thresholds and selective ranges for the subjects (rows) of group 1 ($N=10$). The columns present responses of each finger to stimulation of the extensor digitorum communis muscle at selected electrode positions (squares). Data represented as explained in figure 2.3.

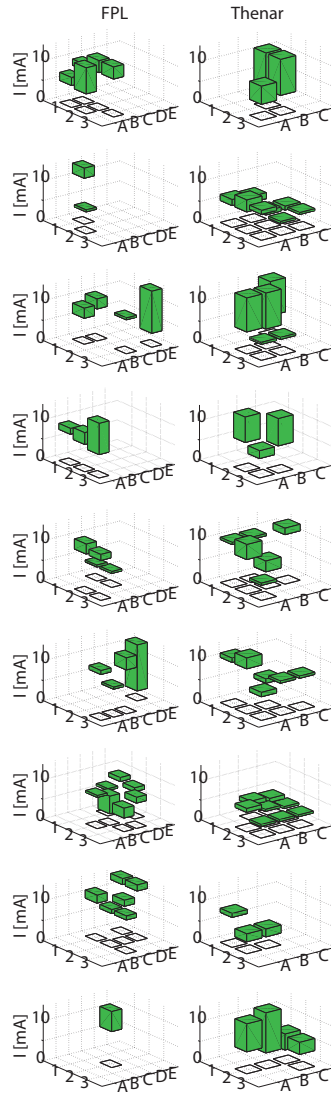


Figure 2.5: Thresholds and selective ranges for the subjects of group 2 ($N=9$). Each row represents a single subject. The columns present responses of the thumb to stimulation of the flexor pollicis longus muscle (first column) and the thenar muscle group (second column) at selected electrode group positions. Dark grey bars denote the selective range, the corresponding squares illustrate the selected electrode position.

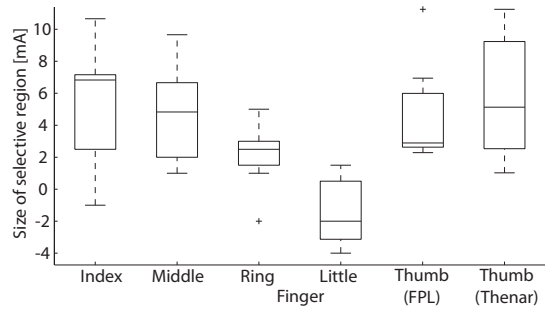


Figure 2.6: Box plots of the maximal selective ranges for each of the fingers (EDC stimulation) and the thumb (both FPL and thenar stimulation) over all subjects. On each box, the central mark is the median selective range, the edges of the box are the 25th and 75th percentiles, the whiskers extend to the most extreme selective ranges which are not considered as outliers, and the outliers are plotted individually.

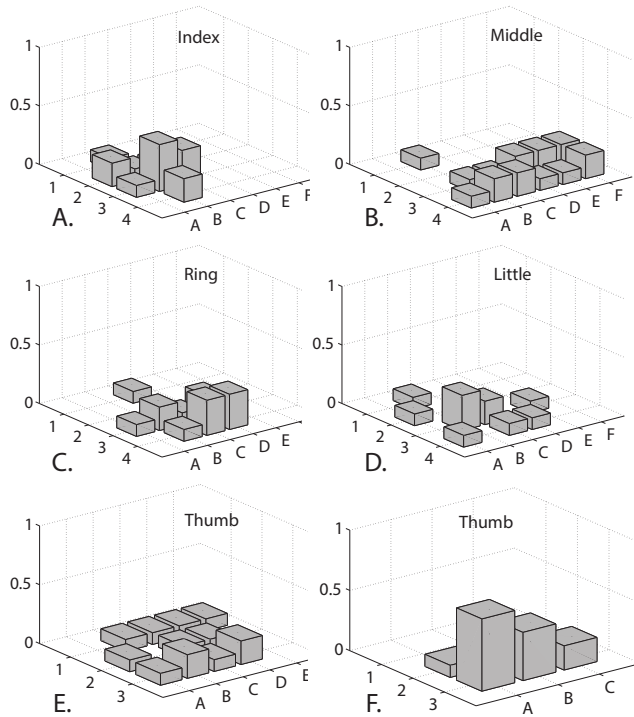


Figure 2.7: Normalized relative occurrence (\bar{G}) of subject-dependent lowest-threshold-positions for (A-D) all fingers based on EDC grid points, (E) FPL grid points and (F) Thenar muscle grid points

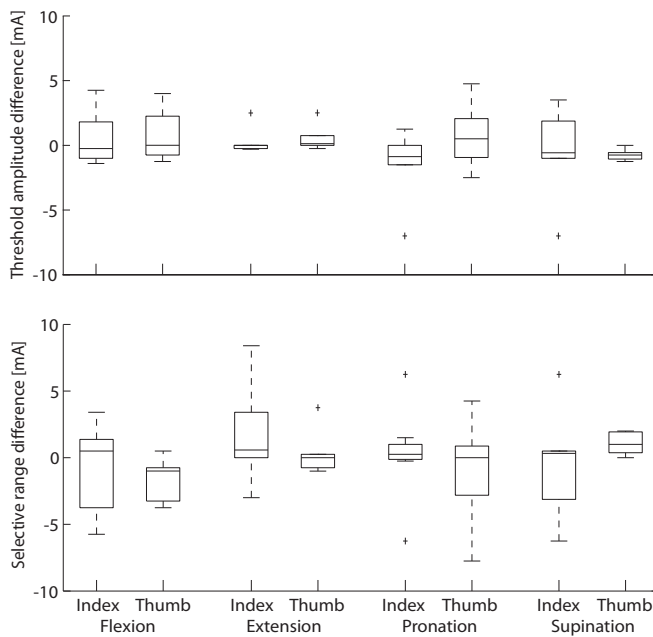


Figure 2.8: Box plots of differences in index finger and thumb activation threshold (top) and selective range size (bottom) with respect to neutral position for different isometric positions. Positions shown are pro/supination combined with 45° of flexion (Flexion) and 45° of extension (Extension) and neutral flexion/extension combined with 90° of pronation (Pronation) and 90° of supination (Supination). On each box, the central mark is the median, the edges of the box are the 25th and 75th percentiles, the whiskers extend to the most extreme data points which are not considered as outliers, and the outliers are plotted individually.

2.4 Discussion

All subjects showed the possibility to selectively stimulate individual finger extension and thumb flexion. We were able to selectively stimulate the thumb in all 9 subjects. In all subjects of the EDC group, we were able to selectively stimulate at least 2 fingers. In 9 out of the 10 EDC subjects we were able to stimulate 3 or all 4 fingers selectively. However selective extension of the little finger was not achieved in 6 of 10 subjects. These results indicate that some fine control of the fingers might be possible with the use of ES. The electrode positions leading to either the lowest threshold amplitude or the largest selective range varied substantially between subjects. Thus, although it is possible to selectively stimulate different fingers, the application of this selective stimulation requires knowledge of the individual properties of the subject. In addition, placement of the stimulation electrode at the location with the lowest response threshold does not necessarily yield the largest selective range. Therefore, the choice of electrode location should depend on the required selectivity of the task. Assisting cylindrical grasp/release for instance will require less selectiveness than assisting the pinch grip or other more complex manual tasks.

2.4.1 Physiological aspects

The fact that selective stimulation is achieved, is likely the result of stimulation of individual muscle parts through individual nerve branches. Leijnse et al. (2008) observed arrangements of different EDC muscle bellies common to different specimens. They observed the muscle part of the little finger was not consistently separable from the ring finger part. In addition, the tendon of this muscle part inserts into both ring and little fingers. This could explain the fact that we were unable to selectively stimulate the little finger in 6 of 10 subjects in the current study.

The relatively small selective ranges of the EDC muscle observed in our experiments might be caused by mechanical coupling of the tendons, by the so called *juncturae tendinum*, which connects the tendons of the different fingers on the back of the hand (Lang and Schieber 2004). In addition, couplings in active neuromuscular control might influence the ability to selectively activate a single digit negatively. Lang and Schieber (2004) observed this neuromuscular coupling to be largest in the control of ring and little fingers, which also might have contributed to the fact that we were unable to selectively stimulate the little finger in our study.

Muscle positions relative to the skin change during wrist movement and one would expect that electrical stimulation parameters vary with this position change. However, under altered isometric positions we did not observe systematic changes in either threshold level or selective range. Our observations do indicate that there is a large variability between the subjects regarding the influence of altered isometric positions. Therefore, an individual approach for identifying influence of altered wrist position and compensation for the possibly altered response is desirable.

2.4.2 Related work

The current study showed similar results to the study of Keller et al. (2006). However they looked at the selectivity of finger flexor muscles, they also succeeded in selective stimulation of most of the fingers, but were unable to selectively stimulate the little finger. Nathan (1990) did not look into the stimulation of individual fingers, but was able to selectively stimulate the thumb by the FPL muscle and the thenar musculature. For the FPL the selective ranges were quite similar. For the thenar musculature he observed much larger ranges. This might be caused by the usage of bipolar electrodes instead of monopolar in our case. In bipolar stimulation, the current can be targeted more precise. This is likely to have more effect in smaller muscles, like the thenar musculature.

Recently, Kuhn et al. (2009) showed that by the use of a proper combination of gel layer resistivity and distance between the electrodes, multiple electrodes in the array can be used to produce a larger virtual electrode, with similar properties of a physically larger electrode. They state that the distance between the electrodes should stay below 3 mm to keep losses small. The larger this size, the larger the gel layer resistivity needs to be. In another study, Kuhn et al. (2010) compared stimulation comfort and stimulation selectivity. The results showed that the most comfortable electrode size depends on the thickness of the fat layer and the depth of the nerve to be stimulated. In thin fat layers and for stimulation of superficial nerves, smaller electrodes were more comfortable. Subjects can tolerate higher current densities on smaller electrodes.

2.4.3 Limitations

For daily life applications, higher frequency stimulation would be more useful instead of single pulse stimulation, because higher forces can be evoked. The goal of the current study was to assess the extent to which individual fingers can be activated using electrical stimulation. This spatial selectivity depends on the geometry of the underlying tissues. The geometry might change due to movement of the wrist or due to contraction of the muscle itself. We did not find any systematic effects of different wrist positions. In higher frequency stimulation the contraction of the muscle will be larger compared to single pulse stimulation. Therefore, the geometry might change more. However, as our results indicate different wrist positions not having a systematic effect on the selectivity, we do not expect much effect of higher frequency stimulation on the muscle selectivity. Enoka and Fuglevand (2001) compared twitch and tetanus data of muscles that control the digits of the hand. Their comparison also indicated that for these muscles the twitch-tetanus ratio does not change systematically with increasing force.

We did not specifically target the EDC muscle, but rather targeted the dorsal skin of the proximal forearm under which the EDC is located. As a result other nearby muscles, like Extensor Carpi Ulnaris (ECU) and EDM, might also be stimulated by the pulses. Since the wrist was fixed in the setup, activation of the ECU (a wrist muscle) should not influence our results. As we were unable to target the

little finger selectively in most cases, it is unlikely that specific activation of the EDM muscle has occurred instead of the EDC muscle.

Here healthy subjects were measured. In the future, this can be extended to subjects from different pathologies mentioned before. Note that muscular properties and (local) innervation of the arm muscles are not affected as a direct result of the mentioned pathologies. At a later stage, due to altered use or even non-use, these properties will change of course. But even after secondary complications geometry of the skin and its underlying muscles will not change much. It is this geometry which is an important factor for spatial selectivity of surface stimulation.

The observed inter-subject variability in both electrode position for selective stimulation and influences of altered isometric positions in a healthy subject population already demand for an individualized approach for each subject. Although the response of the plegic limbs of patients with neurological damage is difficult to predict, it is unlikely that variability will decrease. Thus, designs of future grasp-and-release rehabilitation devices should include the possibility to position the stimulation electrodes according to the needs of the individual patient.

In the current study, we did not take skin thickness or thickness of the subcutaneous fat layers of the individual subjects into account. This variation in fat layer thickness might explain the variability in stimulation levels and selectiveness partially, but it is expected that the fat layers of our subjects had a much smaller variability than the variability of the stimulation responses.

Subject comfort was not explicitly measured in our study. Stimulation was stopped if subjects reported unbearable discomfort. In most cases subjects were able to withstand a stimulation intensity of 13.5 mA, which was the limit of our stimulator hardware. In theory, stimulation hardware with a broader stimulation range, might have led to different results, i.e. larger stimulation ranges. However, in most cases multiple fingers responded at a stimulation intensity of 13.5 mA, thus stimulation was not selective anymore. In addition, most subjects reported the stimulation intensity of 13.5 mA on the edge of painful stimulation. Therefore, we do not think the somewhat small range of the stimulation hardware has limited our results.

2.4.4 Implications for rehabilitation

We measured isometric forces resulting from single pulse stimulation to determine selectivity of surface electrical stimulation. As such we cannot exactly determine whether the selective stimulation is applicable in a rehabilitation setting or in daily life. However, we can relate measured forces to the thumb force needed in lifting a glass filled with water (≈ 0.25 kg) and finger forces needed to overcome enlarged activity of flexor muscles.

Lifting a 0.25 kg object, assuming a coefficient of friction of 0.5, requires a force of 5 N exerted by all fingers together. Kamikawa and Maeno (2008) estimated force distribution ratios across the fingers and their phalanges: a required force of 5 N leads to a desired force of approximately 0.55 N to be exerted by the proximal phalanx of the thumb. Enoka and Fuglevand (2001) estimated a twitch-

tetanus ratio of 1:3 for the muscles controlling the digits. Applying this ratio to the maximum selective forces currently measured, leads to exerted forces of 0.6 N at the proximal thumb phalanx due to tetanic stimulation, which is enough to lift a 0.25 kg object.

At the medial phalanges of the fingers we measured extension forces around 0.1 N. According to Monster and H Chan (1977), the relaxed EDC muscle has a twitch-tetanus ratio of about 1:5. This ratio leads to an estimated tetanic force of 0.5 N at each of the medial finger phalanges. To the best of our knowledge, there exists no literature on flexion forces of individual fingers due to enlarged activity. We believe an estimated tetanic forces of 0.5 N can be used for (at least assistance of) extension of an individual finger suffering from enlarged flexor activity.

Based on these numbers, it is likely that the selective stimulation we observed in our measurements can be useful for application in rehabilitation and daily life. However, direct measurements would give a more clear view on this aspect.

2.5 Conclusion

The goal of the current study was to determine the selectivity and inter-subject variability of ES applied to muscles involved in grasp and release. The results of this study show that it is possible to selectively stimulate a single finger in most subjects. However, the extent of this selective stimulation is highly variable between different fingers and between different subjects. In addition, the possible grid points for this selective stimulation differ strongly between subjects. In our opinion, array electrodes are very useful for future designs of grasping prostheses and grasping rehabilitation devices. The use of array electrodes provides the possibility of automatic customization. So ES, even for more selective stimulation with smaller electrodes, can be applied in a plug and play manner. Because of the possible change of electrode locations during movement and the time variance of the muscular system, an online self-learning algorithm which continuously identifies the best electrode locations for the given task under the changing circumstances can be used. A model which maps electrode locations to produced finger forces under different angles and subject properties will be useful to predict outcomes. Such model can be used in a later stage to control ES of grasp and release in an efficient manner. The results presented here, facilitate the optimization of such techniques and the development of future ES devices in general.



Control of thumb force using surface functional electrical stimulation and muscle load sharing

Published as:
Westerveld, AJ, AC Schouten, PH Veltink, and H van der Kooij (2013). "Control of thumb force using surface functional electrical stimulation and muscle load sharing." *Journal of NeuroEngineering and Rehabilitation* 10 (1), p. 104

Abstract

Stroke survivors often have difficulties in manipulating objects with their affected hand. Thumb control plays an important role in object manipulation. Surface functional electrical stimulation (FES) can assist movement. We aim to control the 2D thumb force by predicting the sum of individual muscle forces, described by a sigmoidal muscle recruitment curve and a single force direction.

Five able bodied subjects and five stroke subjects were strapped in a custom built setup. The forces perpendicular to the thumb in response to FES applied to three thumb muscles were measured. We evaluated the feasibility of using recruitment curve based force vector maps in predicting output forces. In addition, we developed a closed loop force controller. Load sharing between the three muscles was used to solve the redundancy problem having three actuators to control forces in two dimensions. The thumb force was controlled towards target forces of 0.5 *N* and 1.0 *N* in multiple directions within the individual's thumb work space. Hereby, the possibilities to use these force vector maps and the load sharing approach in feed forward and feedback force control were explored.

The force vector prediction of the obtained model had small RMS errors with respect to the actual measured force vectors (0.22 ± 0.17 *N* for the healthy subjects; 0.17 ± 0.13 *N* for the stroke subjects). The stroke subjects showed a limited work range due to limited force production of the individual muscles. Performance of feed forward control without feedback, was better in healthy subjects than in stroke subjects. However, when feedback control was added performances were similar between the two groups. Feedback force control lead, especially for the stroke subjects, to a reduction in stationary errors, which improved performance.

Thumb muscle responses to FES can be described by a single force direction and a sigmoidal recruitment curve. Force in desired direction can be generated through load sharing among redundant muscles. The force vector maps are subject specific and also suitable in feedforward and feedback control taking the individual's available workspace into account. With feedback, more accurate control of muscle force can be achieved.

3.1 Introduction

Stroke has become a major cause of morbidity and mortality in the western world. Incidence of stroke also increases in less developed countries as a result of changing life-styles (Ovbiagele and Nguyen-Huynh 2011). Greying of society and improved health-care are likely to result in an increase of stroke survivors. Functional independence of stroke survivors is highly influenced by their ability to perform a successful grasp. In many activities of daily living, like drinking or opening a door, grasp and release is an essential part of the required movement.

Functional electrical stimulation (FES) of hand muscles can be helpful to train grasp and release in stroke subjects (Crago et al. 1991; DB Popović and MB Popović 2009; Micera et al. 2010). Depending on the ability of the individual patient, the assistance may be selectively (chapter 2) increased or decreased in order to maximize the voluntary activity which is important in relearning movements (Wolbrecht et al. 2008).

Grasping comprises coordinated finger and thumb motion and controlled force exertion on the object to be held. As muscles initiate human movement, accurate control of muscle force is a prerequisite for movement control. For grasping tasks the fingers can be regarded as single degree of freedom (DoF) joints, since movement of the individual phalanges is coupled because of the under actuation of the finger. Furthermore, rotation along the flexion-extension axis of the finger is by far the most important movement for grasping and releasing objects. The thumb, however, requires a different approach as it moves along multiple axes. Controlling force and movement of the thumb will be most challenging and may serve as a model, which may be generalized/reduced to the single DoF case for the other fingers.

A healthy thumb is actuated in several directions by nine muscles in total (Kaufman et al. 1999; Pearlman et al. 2004). However, not all nine muscles can be targeted properly with surface FES. Mainly, because of overlying muscles and nearby sensory nerves making stimulation uncomfortable. Therefore, only a small subset of thumb muscles is available for FES with surface electrodes. This limits the movements which can be controlled with FES. However, thumb movements relevant for grasping (mainly opposition) are feasible with surface electrodes.

Force distribution over multiple muscles is commonly applied in biomechanical modeling, solving actuator redundancy problems for a given task (Happee 1994; Prilutsky and Zatsiorsky 2002). This load sharing approach might also be useful for activating a redundant musculoskeletal system. In addition, by sharing the load over all available muscles we maximize the available range of force. However, to our knowledge, load sharing has not been applied to external activation of muscles with surface electrical stimulation. We will evaluate this possibility and expect this approach to result in accurate force control with a force distribution over the individual muscles optimized by minimizing the sum of squared recruitment over all muscles.

Recently, Lujan and Crago (2009) measured thumb forces evoked by three thumb muscles in healthy subjects and one spinal cord injured patient. Using the

measured forces they trained an artificial neural network (ANN) for feed forward force control. They showed good control of the isometric thumb force in 2D. With the current study we aim at a more transparent approach: using linear combinations of estimated muscle force vectors instead of using a black-box ANN. This approach gives us the benefit of learning more of the underlying physiological system, by comparing combined muscle responses with individual muscle responses. In addition, it might allow for a more generally applicable approach, without the need of training an ANN.

The goal of the current study is twofold: 1) Is it possible to describe thumb muscle responses to FES by a sigmoidal muscle recruitment curve and a single direction of force? And if so, are these so called muscle force maps subject specific, suitable for stroke subjects and time-invariant? And 2) Are muscle force maps suitable for use in 2D thumb force control with FES applying load sharing? And if so, is feed forward control only sufficient and is the approach also suitable for stroke subjects?

3.2 Methods

We will introduce the proposed generalized muscle force model for thumb force control and muscle load sharing first. Thereafter we will describe the experimental evaluation of this model in both healthy subjects and stroke subjects.

3.2.1 Generalized muscle force model

We aimed at predicting muscle force resulting from FES by a relatively simple model. At a specific thumb posture we assumed that the force direction of each muscle, ϕ_i , is constant and that a nonlinear sigmoidal relation exists between the stimulation amplitude and the generated muscle force.

$$|\vec{F}_i(A_i)| = \frac{P_{1i}}{1 + e^{-\frac{(A_i - p_{2i})}{p_{3i}}}} - C, \quad C = \frac{P_{1i}}{1 + e^{\frac{p_{2i}}{p_{3i}}}} \quad (3.1)$$

In Eq. 3.1, $|\vec{F}_i(A_i)|$ is the force magnitude of muscle i at stimulus amplitude A_i ; p_{1i} is related to the force saturation level, i.e. the maximal output force of that muscle, p_{2i} is related to the inflection point of the sigmoidal recruitment curve and p_{3i} is related to the horizontal scaling of the recruitment curve, i.e. the amplitude range. The latter term in Eq. 3.1 is an offset term, ensuring zero force if the amplitude is zero. The muscle force directions, together with the maximal force amplitudes for each muscle represents the force vector map for a system of multiple muscles, see figure 3.1 for an example.

Feedforward thumb force model

We assumed a linear vector summation of the muscle forces acting around the same joint.

$$\vec{F} = \sum_{i=1}^n x_i |\vec{F}_{max,i}| \begin{bmatrix} \cos(\phi_i) \\ \sin(\phi_i) \end{bmatrix} \quad (3.2)$$

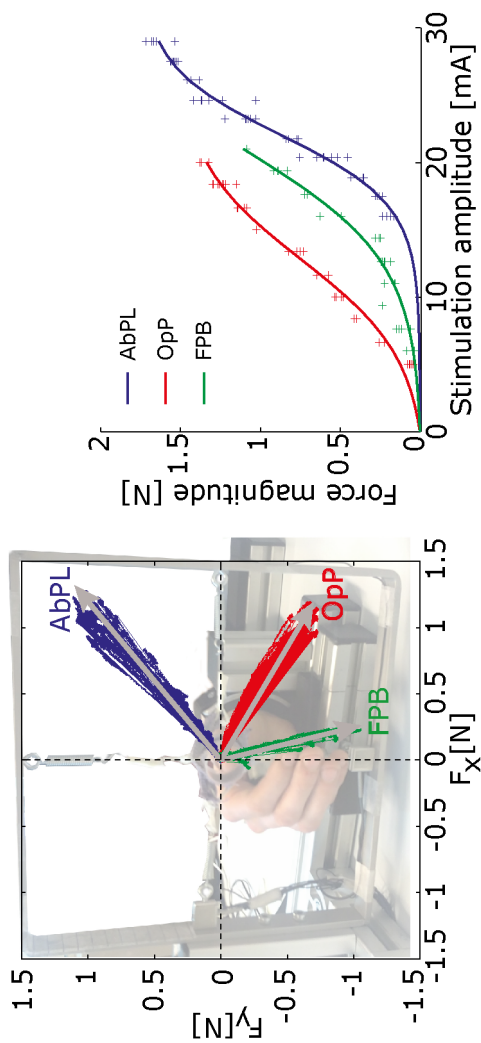


Figure 3.1: An example of the force vector map (direction (left) and magnitude (right)). The colored lines in the left pane show the measurement x - and y -forces for the abductor pollicis longus (AbPL), opponens pollicis (OpP) and the flexor pollicis brevis (FPB) muscles. The determined muscle force directions are indicated by the grey lines. The small variations indicate that the angles are relatively constant throughout the operating range. The force vector map in the left pane is shown on top of an overview of a custom built setup for restraining wrist movements and measurement of thumb forces with two pre-loaded single axis force sensors. The fitted sigmoidal recruitment curves for the three thumb muscles and the individual measurement points (steady state of step responses at different amplitudes) are shown on the right.

In Eq. 3.2, the predicted thumb force vector \vec{F} , is the vector sum of the individual muscle forces ($n = 3$), modelled as a recruitment fraction, x_i , of the maximal muscle force magnitudes, $|\vec{F}_{max,i}|$.

The model of Eq. 3.2 was used to obtain the muscle stimulation levels given a desired thumb force. This inverse problem is redundant: three muscles can be stimulated to obtain a thumb force in two directions. In our (real-time) controller implementation, we addressed this redundancy problem by minimizing the squared muscle recruitment. Minimal summed force is a typical criterion also used in musculoskeletal modeling and load sharing studies (Happee 1994; Prilutsky and Zatsiorsky 2002). The recruitment was modeled as a fraction of the maximal force, thus we obtained a bounded problem which can be formulated as minimizing the vector norm shown:

$$\left\| F_{max}\vec{x} - \vec{F}_r \right\|_2^2 \quad (3.3)$$

In which \vec{F}_r is the [2x1] column vector equal to the reference force and F_{max} is the [2x3] matrix containing the maximal x and y forces of each of the three muscles. \vec{x} is the [3x1] column vector with individual muscle recruitment fractions. To take the bounds on x into account we reformulated the vector norm shown in 3.3 as the equation shown in Eq. 3.4.

$$\operatorname{argmin}_{x \in [0,1]} \vec{x}^T F_{max}^T F_{max} \vec{x} - 2\vec{F}_r^T F_{max} \vec{x} + \vec{F}_r^T \vec{F}_r \quad (3.4)$$

Since the latter term is independent of x , the optimal recruitment, x , minimizing Eq. 3.4 can be written as a quadratic problem of the form as shown in Eq. 3.5, with $Q = F_{max}^T F_{max}$ and $\vec{c} = F_{max}^T \vec{F}_r$.

$$\operatorname{argmin}_{x \in [0,1]} \frac{1}{2} \vec{x}^T Q \vec{x} - \vec{c}^T \vec{x} \quad (3.5)$$

Finally the calculated reference forces for each muscle, $x F_{max}$, are converted to stimulation amplitudes by using the inverse of the sigmoidal recruitment (Eq. 3.1) curve shown in Eq. 3.6.

$$A_i = -p_{3i} \ln \left(\frac{p_{1i}}{|\vec{F}_i| + C} - 1 \right) + p_{2i} \quad (3.6)$$

The combination of obtained stimulation amplitudes, A_i , is the combination which theoretically would produce a force equal to the reference force, \vec{F}_r , or at least the force which is minimizing Eq. 3.3 when the system has reached its boundaries of operation. The constant C represents the offset term as introduced in Eq. 3.1.

3.2.2 Model evaluation

Subjects

Five able bodied subjects (age 32 ± 13 years, 3 men) and five stroke subjects (age 55 ± 18 , 4 men) were included for this study. Table 3.1 summarizes the

Table 3.1: Stroke subjects' characteristics

Subject	Age	Sex	Affected side	Months post-stroke	ARAT
S1	50	M	L	44	52/57
S2	61	M	R	156	3/57
S3	69	M	L	45	24/57
S4	68	M	L	46	17/57
S5	26	F	L	58	2/57

The maximal obtainable Action Research Arm test (ARAT) score is 57 points (normal movement).

characteristics for the individual stroke subjects. The study was in accordance with the declaration of Helsinki and was approved by the local medical ethics committee. All subjects gave written informed consent. During the experiments, the subjects were asked to relax their muscles, in order to avoid voluntary muscle activation.

Experimental setup

Either the dominant arm (healthy subjects) or the affected arm (stroke subjects) was strapped in a custom built device. This setup was used to fixate the wrist and the hand in neutral pronosupination, and to measure the isometric thumb force in two directions perpendicular to the axis of the thumb. Forces were measured by two 45.3 N load cells (Futek, Irvine) preloaded with springs. See figure 3.1.

A special built 3 channel asynchronous biphasic electrical stimulator (TIC Medizin, Dorsten, Germany) was used to apply the electrical stimulation pattern. Stimulation was applied at a constant frequency (30 Hz) and pulse width (150 μ s). The amplitude could be controlled via custom built controllers within the stimulator's range [0–30mA] in steps of 0.125mA. A single 50x50mm anode was used together with 16x19mm cathodes for each channel. Electrodes with similar size showed good results on both selectivity and comfort in a simulation study (Kuhn et al. 2010).

An EtherCAT I/O system (Beckhoff Automation GmbH, Verl, Germany) using Matlab/xPC (The Mathworks, Nattick, USA) as EtherCAT master device was used to control the stimulator parameters and to capture analog data from the force sensors.

Experimental protocol

Preparation

The Abductor pollicis longus (AbPL), Opponens pollicis (OpP) and Flexor pollicis brevis (FPB) muscles were selected for stimulation. We expected to move the thumb sufficiently in directions needed for grasp and release with these muscles. OpP opposes the thumb (pre-grasp), FPB moves the thumb inward (grasp) and AbPL moves the thumb up (release). Electrical stimulation was applied (30Hz; 150 μ s) when electrodes were placed initially. The amplitude was increased to evaluate responses and subject comfort. Electrodes were located at the motor points based on exploration of the responses to electrical stimulation. See figure 3.2 for an example of electrode placement.

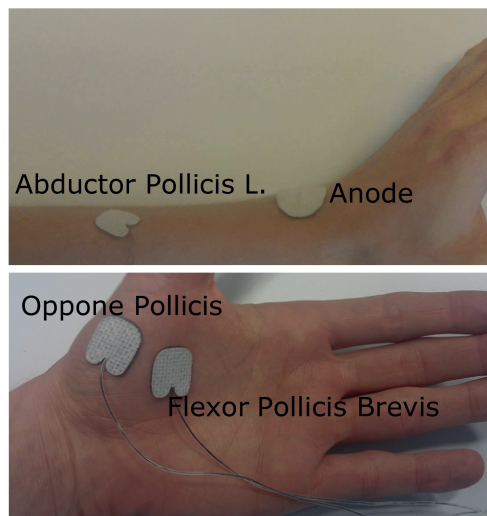


Figure 3.2: Electrode placement. Example of placement of electrode on (top) AbPL and placement of anode at the dorsum of the wrist and (bottom) above FPB muscle and OpP muscle. The AbPL electrodes was placed just medial of the radial bone, approximately 5 cm proximal to the wrist joint, the OpP electrode was placed laterally on the thenar, about 1/3 of the length of the first metacarpal bone, measured from the proximal side. The FPB electrode was placed at about half the length of the first metacarpal bone on the medial side of the thenar. Exact electrode locations were determined experimentally based on observed responses and subject comfort.

Force vector map determination

The subject specific force map (see figure 3.1 for an example) was determined in the isometric setup, with the thumb visually positioned at 30 degrees of abduction and 30 degrees of extension. The threshold and maximal stimulation amplitude for each muscle were determined first: we stimulated (30Hz; 150 μ s) each muscle individually for 1 second, followed by 0.5 second without stimulation. Every 1.5 second the amplitude was increased by 1mA. When either a saturation in the force response was observed or the subject reported unpleasant discomfort, the stimulation was stopped.

The range between the threshold *minus* 1mA and the maximal amplitude was divided in ten equidistant stimulation levels for each muscle. We applied these 30 stimulations (10 amplitudes per muscle) randomly and measured the exerted thumb forces.

From this initialization measurement, we determined the force direction of each individual muscle and the recruitment curve relating muscle stimulation to exerted force. The recruitment curves were described with a sigmoidal function having three parameters, using Eq. 3.1. Parameter values were obtained with a least-squares fit, using the Levenberg-Marquardt algorithm (Seber and Wild 2003). See figure 3.1 for an example of muscle recruitment curves and force directions. This force vector map indicates the ability to control the thumb force in different directions for a specific subject.

Individual muscle controllers

After determination of the force vector maps, the feedback controller gains were determined. Initial gains were obtained from an open loop step response procedure developed by Ziegler and Nichols (1942). The step response reference pattern had the following sequence: [0.5 0.8 0.5 0.2 0.5]| F_{max} |. The reference was held constant for three seconds at each specific level. Thus, excluding the steps at begin and end, this resulted in four step responses in total (two positive and two negative steps of step size 0.3| F_{max} |). The signs of the negative step responses were inverted and then the average of all four step responses was used to determine the open loop gain, K_o .

$$K_o = \frac{X_0}{M_u} \frac{\tau}{\tau_{dead}} \quad (3.7)$$

In Eq. 3.7 the open loop gain, K_o , is calculated from the normalized input magnitude, X_0 , the measured steady state output magnitude, M_u , the time until the output responds, τ_{dead} and the time between the first response and the output reaching the steady state, τ . As suggested by Ziegler and Nichols (1942), the proportional gain, K_c , for each muscle was calculated as 90% of the open loop gain and the integration time for the PI-controller, T_i , was set as 3.3 times τ_{dead} .

For every muscle and subject the inverse of the recruitment curve compensates the non-linear and subject and muscle specific recruitment. In this way the non-linear elements and maximal force levels are compensated within the control loop leading to a linear feedback controller between observed force error and reference force. Furthermore it is expected that range of control gains between the different

muscles and different subjects is relatively small, since the muscle and subject specific recruitment curve transforms the outputs of the PI controllers (forces) into the required stimulation amplitudes.

After determining the initial gains for each muscle, in total four single muscle tests were done for each muscle to be able to analyze performances of the individual muscle controllers: 1) step response reference pattern with feedback control, 2) 0.5 Hz sinusoidal reference pattern with feedback controller, 3) step response reference pattern with a combination of feedforward and feedback control, and 4) 0.5 Hz sinusoidal reference pattern with a combination of feedforward and feedback control.

When oscillatory behavior was observed during the first test, the proportional gain was lowered systematically and the test was repeated until good tracking of the reference was observed without severe oscillations. In some cases the integration time T_i was increased slightly for further fine tuning.

3

3.2.3 2D thumb force targets

For evaluation of the 2D controllers, 5 second constant reference force targets were used. The targets were set at 0.5 N and 1.0 N in different directions within the workspace of the subject. Initially, directions were chosen at -90° , -60° , -30° , 0° , 30° and 60° . Angles outside the theoretical workspace of the subject were not measured. When less than four target directions were theoretically feasible, intermediate angles (15° step size) were also evaluated.

Feedforward thumb force control

The applicability of the thumb force model was evaluated first in an experiment based on feed forward control of the three muscles. In this experiment control was based on the measured muscle parameters and the thumb model described in Eq. 3.2. Based on the previously determined force map, target angles greater than the angle of the long abductor muscle or smaller. The experiment was repeated three times to explore the reproducibility of the methods. The target sequence was the same in each repetition. The sharing of the load was calculated by implementing Eq. 3.5 in a real-time quadratic programming (QP) problem solver using the online active set strategy (Ferreau et al. 2008).

Feedforward and Feedback thumb force control

Control performance might be improved by adding error feedback. This was evaluated in a second set of control trials in which the feed forward control was extended with feedback error compensation. Force targets were the same as in the feed forward control experiments. The error vector between the reference force vector and the actual force vector was used as reference input for a second QP optimizer, which distributed the force error over the individual muscles. Note that due to feed forward muscle activation, forces can also be feedback controlled in the negative direction of the individual muscle axis. The calculated individual muscle force errors were fed back with the individual muscle controllers. A schematic overview of feedforward and feedback control paths is shown in figure 3.3.

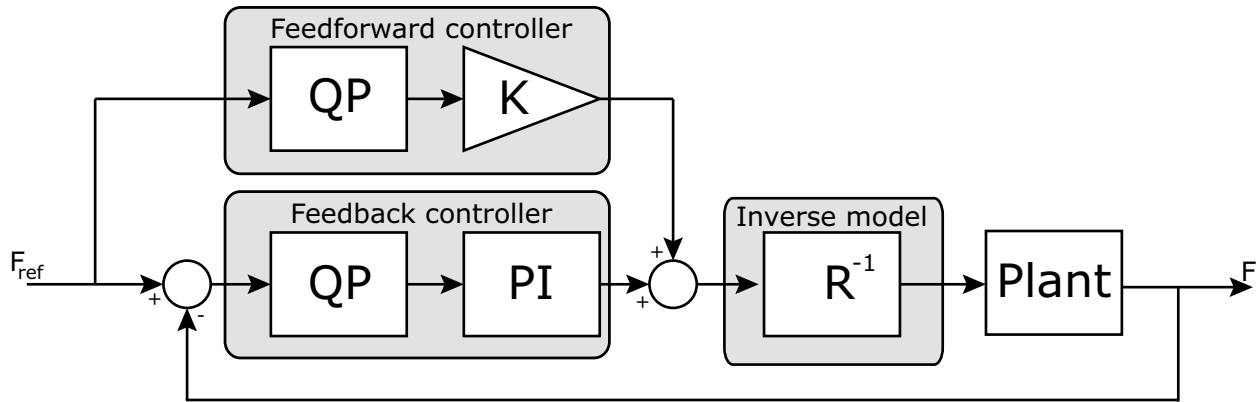


Figure 3.3: Block diagram of feedforward and feedback thumb force controller. Stimulation for three individual muscles is calculated based on a reference force. Force distribution over the muscles is calculated by solving a QP problem as shown in 3.5 indicated by the 'QP' blocks. These QP solvers take the previously determined force map and also boundaries on the recruitment into account. For clarity this is left out in the schematic. The bounds for the feedforward QP problem are $[0,1]$. The bounds for the feedback QP problem depend on the current activation of the muscle (from both feedforward and feedback path) and indicate the remainder of the operating range $([0,1])$ and can thus also be negative when the specific muscle is already active. In the feedback path a PI controller was used for each individual muscle force. When using a combination of feedforward and feedback control, the feedforward path was reduced by a factor $K = 0.8$ to prevent overshoot and let the feedback path compensate for the remainder. When evaluating the feedforward control performance without feedback, K was set to 1.

Performance analysis

RMS errors were calculated from the magnitude of the error vector between measured muscle force during the initialisation procedure and muscle force estimate based on the obtained parameters. In addition, the area of the theoretical work range resulting from the muscle force vectors obtained during the first initialization procedure was calculated and compared between subjects.

An important factor for the controllability is the rate of force change relative to the change of stimulation amplitude for a given muscle. This factor can be expressed by the maximal slope of the recruitment curve, calculated from the derivative of Eq. 3.1, for a give muscle, i :

$$slope_{max,i} = \frac{p_1 i}{4p_3 i} \quad (3.8)$$

At the end of the session, we repeated the initialization procedure to check for possible changes in recruitment properties. In each repetition the sequence of applied amplitudes and selected muscles was kept the same. Time between subsequent initialization procedures was approximately 45 minutes. We estimated the correlation coefficients (Spearman's ρ) between the measured forces and the forces predicted by the initially obtained model for each subjects. This gives an indication of both the prediction ability of the model and the repeatability of the method. To estimate effects of muscle fatigue we compared the force magnitudes in both initialization procedures and calculated the least squares slope, m , for each subject by:

$$m = \frac{\sum |F_{pre}| |F_{post}|}{\sum |F_{pre}|^2} \quad (3.9)$$

In which F_{pre} and F_{post} , are the observed forces during the procedures at the beginning and the end of the session, respectively. The forces are summed over all applied input amplitudes during the initialization procedure. The slope, m , is an estimate of the ratio between initial force generation and final force generation for a given muscle.

Single muscle control performances were evaluated based on the sine tracking tasks. RMS errors between the actual and reference forces were calculated. The 2D controller performances were evaluated based on the stationary error of the responses. This stationary error was defined as the average magnitude of the force error vector during the last 10 percent of the in total 5 seconds lasting step response.

Due to the relatively small sample size, non-parametric statistics was applied. We used Mann Whitney U tests to statistically evaluate improvement with feedback control over feedforward control only and also to evaluate performance in stroke subjects with respect to healthy subjects.

3.3 Results

3.3.1 Force vector maps

Results of the initialization procedures for all subjects and all repetitions are summarized in figure 3.4. Figure 3.5 shows the distribution of theoretical workspace area based on the determined muscle force maps for healthy subjects and stroke subjects. The workspace area was larger in healthy subjects, compared to stroke subjects: $p=0.06$ and $p=0.02$ for first and second initialization procedure respectively. RMS errors for the predicted force vectors were $0.10 \pm 0.02 N$, $0.17 \pm 0.09 N$ and $0.19 \pm 0.11 N$ on average for the healthy subjects for AbPL, OpP and FPB, respectively. For the stroke subjects, the RMS errors were $0.66 \pm 0.12 N$ and $0.79 \pm 0.26 N$ for OpP and FPB, respectively. The AbPL muscle was only activated in S4 and S5, RMS errors were $0.14 N$ and $0.26 N$ for these subjects respectively. Maximal slopes of the recruitment curves in healthy subjects were $0.18 \pm 0.06 N/A$, $0.17 \pm 0.06 N/A$ and $0.70 \pm 0.52 N/A$ for AbPL, OpP and FPB respectively. For the stroke subjects the maximal slopes were $0.09 \pm 0.06 N/A$ and $0.69 \pm 0.43 N/A$ for OpP and FPB respectively. The maximal slopes for the AbPL in subjects S4 and S5 were $0.07 N/A$ and $0.06 N/A$ respectively.

Correlations coefficients between predicted and measured forces are shown in table 3.2 for both initialization procedures. The estimated force generation ratio's between first and second initialization procedure in healthy subjects were 0.87 ± 0.25 , 0.93 ± 0.10 and 0.97 ± 0.06 for AbPL, OpP and FPB respectively. For the stroke subjects the ratio's were estimated at 0.14 ± 0.09 and 0.31 ± 0.14 for OpP and FPB, respectively. For the AbPL muscle, the ratio's were 0.35 and 0.29 for subjects S4 and S5 respectively.

3.3.2 Force controller evaluation

Single muscle controllers

The averaged proportional gain over all healthy subjects was 0.22 ± 0.28 . For the stroke subjects the average proportional gain was 1.04 ± 1.16 , note that these values are dimensionless as the feedback controller has a force both as input and as output, since the inverse recruitment is placed after the controller. The average integral times were $0.56 \pm 0.12s$ and $0.62 \pm 0.45s$ for healthy subjects and stroke subjects respectively.

During the single muscle control experiments, some saturation effects (stimulation reaching predetermined maximal amplitude) were observed, leading to a non-linear feedback system. Disregarding the cases where this saturation occurred, the estimated controller gains were 0.17 ± 0.12 and $0.57 \pm 0.12s$ on average for all subjects for proportional gain and integral time respectively.

Results of the sine tracking experiments for the individual muscle feedback controllers are shown in figure 3.6. Results for healthy subjects and stroke subjects are shown separately. RMS tracking errors for the healthy subjects were $0.30 \pm 0.07 N$, $0.29 \pm 0.06 N$ and $0.50 \pm 0.25 N$ for AbPL, OpP and FPB respectively. For the stroke subjects, RMS errors were similar: $0.31 \pm 0.03 N$, $0.37 \pm 0.10 N$ and

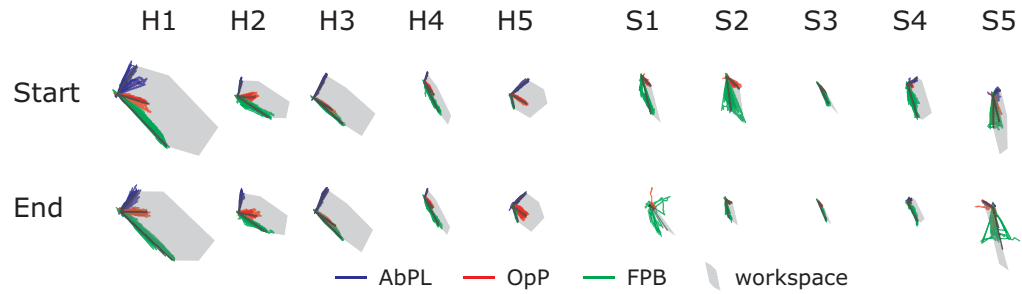


Figure 3.4: Force vector map determination. Force map data in subsequent force map measurements ('Start' and 'End' of experiment) for all (H)healthy subjects and all (S)troke subjects. Grey arrows indicate maximal force for each muscle, obtained from the initialization procedure and the average movement direction. Axes were omitted for clarity, however the axes scaling was the same in all sub figures.

Table 3.2: Force prediction

Muscle	Procedure	Healthy subjects		Stroke subjects	
		F_x correlation	F_y correlation	F_x correlation	F_y correlation
AbPL	initial	0.72 ± 0.19	0.83 ± 0.11	0.95 ± 0.02	0.39 ± 0.09
	final	0.61 ± 0.22	0.77 ± 0.14	0.84 ± 0.22	-0.44 ± 0.79
OpP	initial	0.80 ± 0.13	0.73 ± 0.31	0.51 ± 0.56	0.79 ± 0.09
	final	0.73 ± 0.14	0.63 ± 0.33	0.58 ± 0.28	0.69 ± 0.32
FPB	initial	0.88 ± 0.06	0.92 ± 0.06	0.47 ± 0.20	0.82 ± 0.24
	final	0.86 ± 0.05	0.87 ± 0.10	0.59 ± 0.27	0.78 ± 0.27

Correlations between predicted forces and measured forces during initialization procedures at start (initial) and end (final) of session

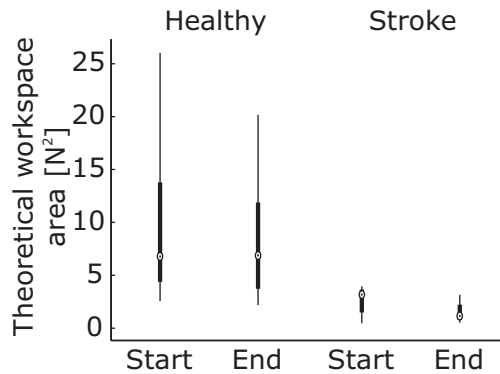


Figure 3.5: Workspace areas. Boxplots of theoretical workspace area for healthy subjects and stroke subjects. Workspaces calculated based on determined maximal muscle forces and muscle directions during the first initialization (Start) and the second initialization procedure (End)

3

0.52 ± 0.22 N for AbPL, OpP and FPB respectively. For subjects S1, S2 and S3 the AbPL muscle could not be targeted properly, therefore the AbPL tracking measurements were skipped for these subjects.

Combined muscle controllers

2D step responses for the best (H5) and worst (H1) healthy subject and best (S4) and worst (S2) stroke subject are shown in figure 3.7. Time series of stepresponses to a single 0.5 N target and a single 1.0 N target for H5 and S4 are shown in figure 3.8. Responses over all subject are summarized in bar plots of stationary errors, shown in figure 3.9. The stationary errors were averaged over all targets within a group. Results were grouped by control type, target magnitude and subject type. With feedback enabled, reduction in stationary errors was observed for the stroke subjects for the 0.5 N targets ($p < 0.1$). Feedforward performance was less in stroke subjects, compared to the healthy subjects ($p = 0.05$ and $p < 0.01$ for the 0.5 N and 1.0 N targets respectively). The stationary errors were larger for the 0.5 N targets compared to the 1.0 N targets when normalized to the target forces ($p < 0.01$) with feedforward control in healthy subjects. No significant differences in stationary errors were observed between the two target levels for the stroke subjects.

3.4 Discussion

We showed the possibility to describe responses to electrical stimulation of individual thumb muscles as a force vector map with a single activation direction and a sigmoidal recruitment curve. As expected the variability between subjects is relatively large (figure 3.4) due to anatomical differences. As a result, force maps always need to be determined for each individual subject. Within subject the results are repeatable, demonstrating the feasibility of our approach (figure 3.4 and

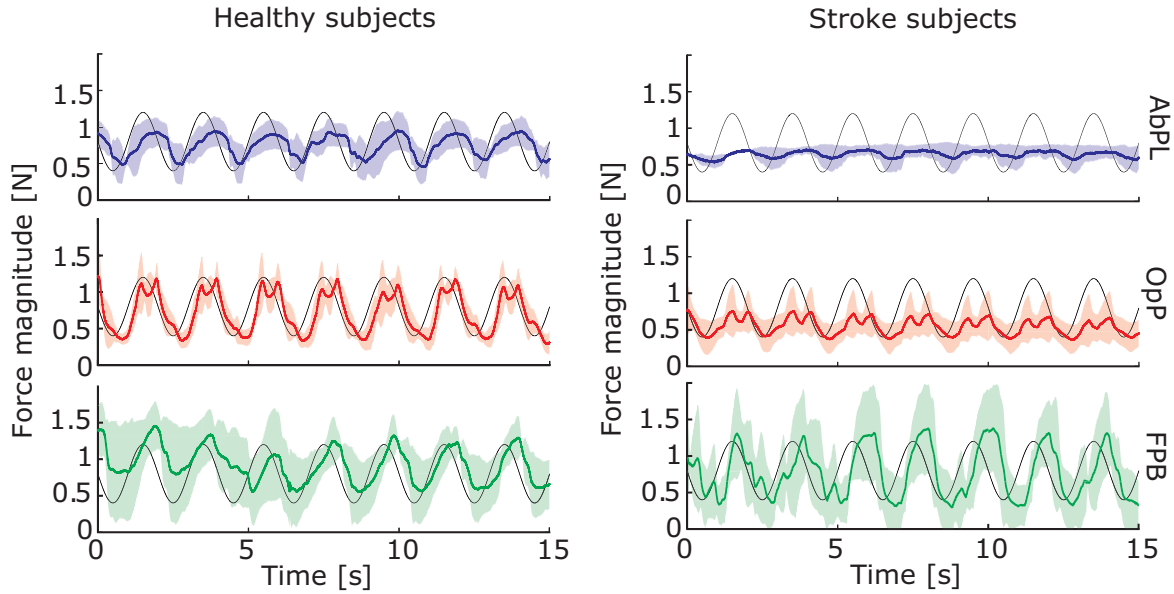


Figure 3.6: Individual muscle control. Sine (0.5 Hz) tracking results averaged over all healthy subjects (left) and over all stroke subjects (right). Results shown for the three selected muscles: Abductor Pollicis Longus (AbPL), Opponens Pollicis (OpP) and Flexor Pollicis Brevis (FPB) and for feedback control only. The mean over all subjects is shown by the solid line, shaded areas indicate the standard deviation. For AbPL only data for S4 and S5 is shown in (b), as in the other stroke subjects this muscle could not be activated.

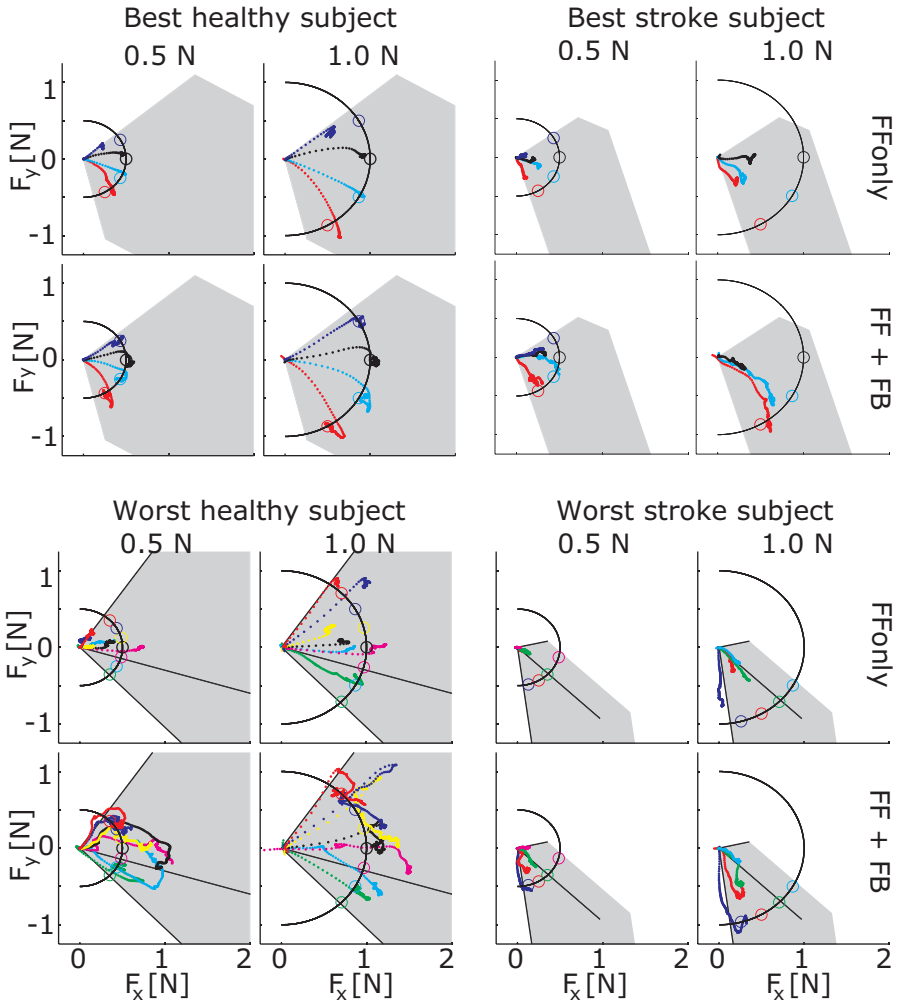


Figure 3.7: 2D force control. Example of responses to the target set points for the best (H5; top-left) and the worst (H1; bottom-left) healthy subject and for the best (S4; top-right) and worst (S2; bottom-right) stroke subject. Top panes of each figure show results of solely feedforward control; bottom panes show results for feedforward and feedback control. 0.5 N targets (left) and 1.0 N targets (right) are shown separately for readability. The colored dotted lines show the measured force response to a target set point shown by the same colored circle in the plane perpendicular to the thumb. For every 100ms in the response a dot was plotted to give an indication of the speed of the force response.

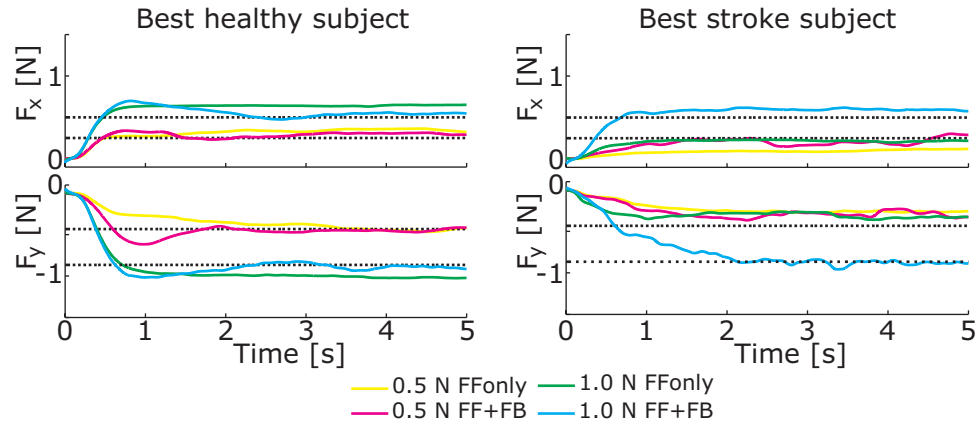


Figure 3.8: Step responses of 2D force control. Time series of responses to a step in target set point for healthy subject H5 (left) and stroke subject S4 (right). Top panes of each figure show forces in X direction; bottom panes show forces in Y direction.

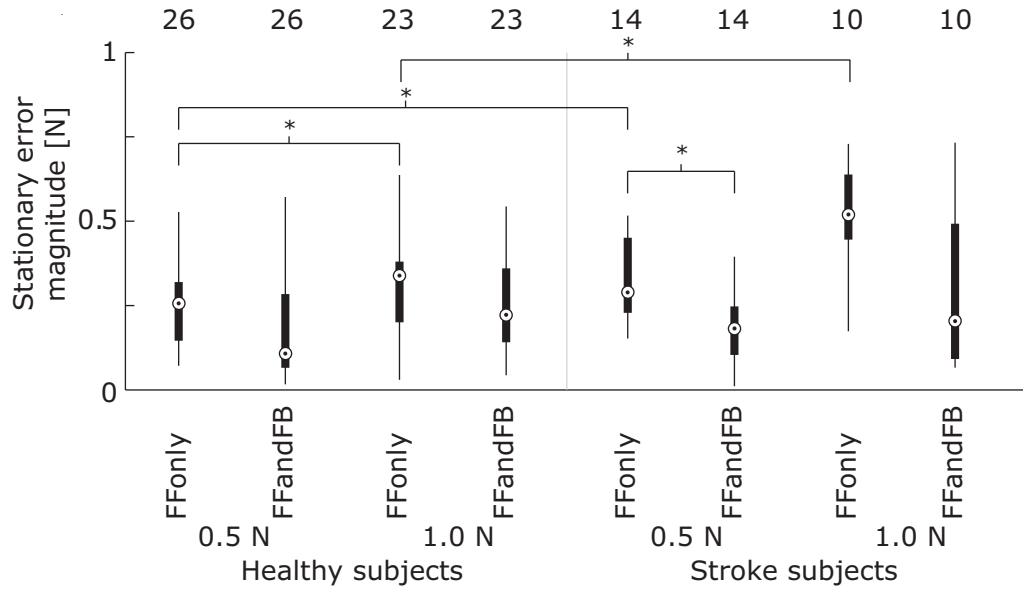


Figure 3.9: Stationary errors in 2D force control. Box plots of stationary errors in 2D force control trials. 0.5 N and 1.0 N targets are shown separately for feedforward control only and the combination feedforward and feedback control and for healthy subjects and stroke subjects. Numbers above the individual box plots indicate the total number of evaluated targets in that group, which was influenced by the workspace area of the individual subjects. Significant differences between groups were calculated by the non-parametric Mann-Whitney U test and indicated by asterisks.

table 3.2). Note that for subsequent sessions it is required to redo the initialization, since the response is highly dependent on exact electrode position (Chapter 2). However, in stroke subjects the AbPL muscle was difficult to target. In the subjects in which we were able to target the muscle initially, the responses during the second initialization procedure differed greatly from the initial procedure as indicated by the low correlation coefficients in table 3.2 and in figure 3.4. Therefore the AbPL muscle seems less reliable for use in 2D force control tasks compared to the other muscles.

The load sharing approach resulted in the muscle being pulled nicely towards the target force by the feedback controller. Since the error vector was used as input for the feedback load sharing, the appropriate ratio of muscle activations was calculated to generate force in the right direction. To our knowledge this load sharing approach is a novel application in electrically stimulated muscle. In our opinion this could be an appropriate solution to solve redundancy problems in activation of multi-dimensional musculoskeletal systems with FES and simultaneously take the boundaries of the individual force sources into account. The variation of controller gains over different muscles and different subjects was low, which gives the possibility to use fixed values for these parameters when applying the methodology presented here. Either as a true fixed value or as a starting point for further fine tuning instead of the methods suggested by Ziegler and Nichols (1942) which were currently used. Thereby further reducing the tunable parameters and setup time.

Performance of the 2D feedforward force controller was worse for the stroke subjects compared to the healthy subjects. For the stroke subjects, adding feedback terms reduced stationary errors. For the healthy subjects the differences between feedforward control only and combined with feedback control were small, see figure 3.9. However, depending on the model accuracy of the individual muscle's input-output relation, the feedback controller also reduced the control performance in certain cases. An example of this can be observed from figure 3.7 where the feedback controller negatively influences the force direction for the 0.5 N targets. This is likely a result of a mismatch in the FPB model, causing the thumb being pulled in a more negative direction than needed. Therefore we recommend estimating model accuracy before starting the control trials, and redo the initialization if necessary.

3.4.1 Limitations

We measured forces in two directions in a plane perpendicular to the thumb. Therefore we neglected the forces perpendicular to this plane. Due to this fact we might have made some errors in absolute force recordings. However, since we are using the same setup in both model identification and control, we expect that the influence of these non-measured forces on our performance observations are minimal.

Forces in unmeasured direction could have led to the relatively low observed forces compared to other studies (Lujan and Crago 2009). However, we expect that these unmeasured forces were small. The stimulated muscles are responsible for thumb movement. Therefore the force component in line with the thumb will be

small compared to the perpendicular force components. A more likely cause is the fact that we aimed at selective activation with small electrodes leading to relatively low current densities and low muscle activation. Even though the observed forces and the evaluated targets of 0.5 N and 1.0 N are relatively low, they are sufficient for positioning the thumb for functional grasping of objects compared to the evaluated force levels during grasping in (Flanagan et al. 1999; Singh et al. 2013). Recently, we have shown applicability of a similar approach during grasp and release of objects (Westerveld et al. 2012).

In all subjects, the FPB muscle showed a steep recruitment curve: when the stimulation came above threshold force increase was high for an increase in stimulation amplitude. This will have resulted in a bigger influence of FPB modeling errors on the output force errors. The steeper recruitment compared to other muscles is likely a result from differences in neural innervation. The FPB muscle is innervated from the recurrent branch of the median nerve which is very superficial before entering the FPB muscle. The OpP muscle is innervated by the same nerve branch, but laterally the branch runs less superficial (Kozin 1998). The AbPL muscle is innervated by the posterior interosseus nerve which is also less superficial.

We reduced the experiment length by only testing specific points along the recruitment curve during the initialization phase. We did not specifically optimize this method of recruitment curve sampling. However, the results in pilot measurements where we compared our current approach with more dense sampling of the muscle recruitment resulted in only minor differences between the obtained recruitment curves. Recently, Scheerer et al. (2012) compared different methods of recruitment curve sampling extensively. Application of methods described there might further improve the accuracy of the obtained recruitment curves of individual muscles, which then could also improve the accuracy of the controllers.

The stroke subjects showed smaller workspaces compared to the healthy subjects (figure 3.5). This is likely a result of non-use after stroke, which could have been overcome partially by additional muscle training prior to the experiment. However, since we only analyzed performance from the trials where the target force vector was within the theoretical workspace, this has not affected our current findings.

The ARAT scores of the stroke subjects had a broad range. Therefore the subjects cannot be considered as a homogeneous group. However, the emphasis of the current approach lies on modeling subject specific recruitment relations. Therefore we did not observe lower stimulation responses related to lower ARAT scores. Furthermore, this is supported by the fact that the subjects with the best ARAT scores showed the smallest theoretical work range for the selected muscles.

3.4.2 Physiological aspects

We expect the remainder of the variation to have a physiological cause. The most likely one is a non-linear additive relation between the individual muscle directions and recruitments. We expect that the linear addition of individual force magnitudes to predict the resulting force magnitude had the largest influence.

3.4.3 Related work

Lujan and Crago (2009) were able to control the thumb forces in two directions by using an artificial neural network. They also observed differences between the measured force of combined muscle activation and the sum of the individual components, which suggested a nonlinear additive relation. Lujan and Crago stimulated different muscles (Extensor Pollicis Longus, Abductor Pollicis Brevis and Adductor Pollicis). The evoked forces in that study are about five times higher than the forces which we found, possibly caused by higher stimulation frequencies (50 Hz compared to 30 Hz in our study) and the different set of stimulated muscles. This makes a good comparison between results difficult. Lujan and Crago only report 2D control RMS errors of one healthy subject and one spinal cord injured (SCI) patient, having implanted electrodes. The RMS error of the SCI patient was 0.89 *N*, which is very low compared to our results in stroke subjects when relating to the achieved force range. However implanted electrodes are known to produce higher muscle selectivity and more direct muscle activation, which makes this comparison unfair. The healthy subject they presented showed an RMS error of 2.65 *N*, which is (taking the factor 5 into account) within the same range as the stationary RMS errors we observed. However, we were able to obtain that similar performance without training and optimizing an artificial neural network but with a more transparent model consisting of only four parameters per muscle.

Scheerer et al. (2012) recently published a single case study on controlling multiple degrees of freedom (in the shoulder) in a SCI subject with implanted electrodes using a feedforward controller. They also solved for redundancy by using a quadratic program and showed initial RMS errors of 5.29 *N*. As shoulder muscles are much stronger than thumb muscles, this value is again difficult to compare with our results. Given the range of their target forces (-18 *N* to 4.5 *N* in the *x* direction, -18 *N* to 22.5 *N* in the *y* direction and -9 *N* to 0 *N* in the *z* direction) one could say that the performance of their controller was slightly better than ours, which seems logical given the fact that the electrodes used by Scheerer and colleagues were implanted. Therefore their stimulation was likely to result in more selective and accurate activation of individual muscles. In addition, Scheerer et al suggest to improve the performance by adding a feedback controller, which is exactly what we did in the current study. We showed that adding the feedback path can indeed improve performance when the feedforward model is not accurate enough.

3.4.4 Clinical implications

This study is a framework for evaluating multi-dimensional control of joints with electrical stimulation. To be clinically applicable in post-stroke rehabilitation, the method needs several extensions. First of all, we currently addressed only thumb muscles. For functional grasp and release training the finger muscles are of course equally important. However, compared to the thumb, those joints do not have the redundancy in actuation: mainly one extensor muscle and one superficial flexor muscle. Therefore the current method could easily be extended to the fingers,

which we also evaluated recently (Westerveld et al. 2012).

When using additional electrodes for (selective) finger flexion and extension, the number of electrodes will increase quickly. Since, electrode placement is subject dependent and can be time consuming, the time required for setup will also increase rapidly. From a practical point of view, time can be gained with the application of electrode arrays and an approach to automatically search for proper electrode locations (Malešević et al. 2012).

Finally, the relations between stimulation and movement and control of movement for grasp and release are also important. However proper force control is a fundamental prerequisite for proper control of movement. Therefore the current study can be seen as an intermediate step towards an approach for assisting grasp and release movements and next steps in our research will focus on directly mapping muscle activation to evoked movements.

Stroke subjects showed a limited workspace in our study. Since they did not have severe spasticity, it is likely that their muscle force have decreased dramatically due to long time non-use after their stroke. Therefore, we expect that results in more acute stroke subjects lie closer to those of the healthy subjects in the current experiment. However, this needs further evaluation and likely a subject specific approach will lead to the best results.

3.5 Conclusion

The aim of this study was to evaluate the possibility to predict thumb muscle force responses to FES and to control thumb muscle force in 2D in both healthy and stroke subjects. For a single muscle, the static relation between muscle force and activation was described by a sigmoidal muscle recruitment curve and a single direction of force. Subsequently, load sharing was used to combine the activation of individual muscles to actively control thumb force in 2D.

From our results we can conclude that it is possible to describe the thumb muscle responses to FES by a single force direction and a sigmoidal recruitment curve. The large variations between subjects indicate that these force maps are highly subject specific, likely due to anatomical differences, requiring an individual approach. The relatively small variation within subjects demonstrates the feasibility and time-invariance of our approach. Effects of muscle fatigue were observed, especially in stroke patients, so the approach presented here is applicable mainly for short sessions (up to 30 minutes).

To our knowledge this is the first study applying a load sharing paradigm in controlling multiple muscles with surface FES in a multidimensional biomechanical system. The load sharing approach controlled the thumb towards the target forces in the 2D control experiments. With feedforward force control only, errors were larger in stroke subjects, compared to healthy subjects. However, with added feedback control, significant differences in control performance had disappeared. Therefore the methodology for multi-dimensional feedback force control presented here has potential applicability as part of post stroke rehabilitation techniques. Especially when applied earlier after stroke and muscles are stronger.



Grasp control in stroke patients using functional electrical stimulation and model predictive control

A Kuck, **AJ Westerveld**, PH Veltink, and H van der Kooij (2013). "Grasp control in stroke patients using functional electrical stimulation and model predictive control." *submitted*

Abstract

Surface functional electrical stimulation (FES) is commonly employed in the rehabilitation of patients with impairments of upper limb motor control due to stroke. In general, a limited number of stimulation electrodes is used mostly in open loop control only. We aim to extend the presently available stimulation techniques to the use of a closed loop model predictive control (MPC) allowing for the use of an extended number of electrodes to achieve selective finger movements and precise position control over different grasp types.

The movements of thumb, index, middle and ring finger were controlled by an MPC algorithm using an underlying state space model which was obtained in a preceding initialization procedure. The system was validated in four healthy and three stroke subjects using setpoint tracking and functional grasping tasks such as hand opening, cylindrical- and pinch-grip.

We show that the proposed system is able to track angular setpoints for each finger with an error of $8.3^\circ \pm 2.9^\circ$ and $6.7^\circ \pm 1.7^\circ$ for stroke and healthy subjects respectively, and successfully generate functional movements to grasp and release a variety of smaller and bigger objects.

With the designed MPC approach, it is possible to assist functional and smooth grasping movements for both stroke and healthy subjects. The approach is therefore highly suitable for application in a functional training environment aimed at regaining hand function after stroke.

4.1 Introduction

Stroke is one of the leading causes of upper limb impairment in the western world. A commonly affected area in the brain is the motor cortex resulting in an impairment of upper and lower limb motor control contralateral to the affected hemisphere. However especially the functioning of the hand is essential for the direct interaction with our environment e.g. object manipulation, eating, drinking, walking, personal hygiene and many other activities. An impairment of those functions represents a major burden to those affected in performing activities of daily life (ADL).

To improve the quality of life after stroke, increasing efforts have been made to extend the available methods for rehabilitation of the impaired neural pathways with the goal of restoring as much as possible of the previously available motor control. Methods which have actively been used in the neural rehabilitation of stroke patients include neurodevelopmental techniques, proprioceptive neuromuscular facilitation, robot assisted therapy, biofeedback, mirror therapy, constrained intensive movement therapy and electrical stimulation (DeLisa 1988).

This paper focuses on the use of functional electrical stimulation (FES) to activate the peripheral motor system. Thereby afferent signals are evoked by the electrical stimulus in addition to efferent signals which activate the muscles. Additionally to directly activating efferent and afferent axons, the resulting movement evokes proprioceptive feedback that stems from Muscle-Spindles and Golgi Tendon Organs. This represents an advantage of FES with respect to methods in which the impaired extremities are only moved passively e.g. when moved manually by a physiotherapist. During FES the muscles are actively involved in performing the desired movement to a much higher degree compared to passive movements. This in turn prevents muscular degeneration and aids a faster recovery of the central nervous system (CNS) (DB Popović et al. 2009). Thereby several studies have reported a positive, statistically significant effect of FES on motor relearning after cerebrovascular accident (CVA) in the acute state and at least minor improvements in a later subacute or chronic state (X Hu et al. 2010; Hara 2008; MK Chan et al. 2009; Shindo et al. 2011; Thrasher et al. 2008; DB Popović et al. 2009).

Present commercially available surface FES systems that are used in the rehabilitation of grasping functions in stroke patients include the NESS Handmaster (NESS Ltd., Ra'anana, Israel), the Bionic Glove (Prochazka et al. 1997) and the Neuromove 900 (Biomotion, Almonte, Ontario, Canada). However all of those developments rely on simple feedforward procedures using only a small amount of electrodes positioned on the forearm. These systems merely evoke simple functional movements such as hand opening and closing without much room for selectivity. This is predominantly related to the complex anatomical nature of the forearm making it challenging to selectively target specific low level functions such as single finger movements. Current research of our group is focusing on extending the present techniques to more sophisticated stimulation procedures. This is achieved by raising the number of electrodes to a total of nine which increases stimulation flexibility to improve the possible training effect of such FES devices and simultaneously increase usability for home application (Westerveld et al. 2012).

Table 4.1: List of all participating subjects.

Subject	Sex	Age	Months since Stroke	ARAT	Affect. Side
Healthy	M	26	n/a	n/a	n/a
	F	21	n/a	n/a	n/a
	F	22	n/a	n/a	n/a
	M	58	n/a	n/a	n/a
Stroke	M	60	147	3	R
	M	68	36	28	L
	M	67	38	25	L

Similar work has been reported e.g. by Keller et. al. who developed a surface FES system that was able to selectively produce finger and wrist forces under isometric conditions based on a previously estimated Hammerstein model. This approach also included a procedure for automatic recognition for the optimal stimulation electrode positions and recursive model adaptation to compensate fatigue (Keller et al. 2006). It however did not include the control of movement.

The present study aims to investigate the feasibility of a model predictive control algorithm (MPC) controlling individual finger movements and a corresponding system model in order to extend the present techniques for functional electrical stimulation in stroke patient rehabilitation. MPC can conveniently be used to control a multiple-input multiple-output (MIMO) system based on the supplied system model. Also additional requirements such as control constraints, recursive model updates due to changing system conditions or system nonlinearities can easily be taken into account and adjusted within a short time period.

In addition to the use of a more complex control procedure, it is investigated whether it is possible to profit from an increased number of stimulating electrodes. This is likely to improve selectivity and therefore making it possible to achieve qualitatively better functional movements during training. Especially movement functionality is important in this matter and represents the core goal of the technique as the goal is to achieve movements for grasping and manipulation of objects. The proposed system is hypothesized to be able to perform two different grasp types, namely pinch and cylindrical grip, which is tested in both pure setpoint tracking tasks, performed in air, and functional grasping experiments.

4.2 Methods

4.2.1 Subjects

Four healthy and three stroke subjects participated in the experimental study. All participants signed an informed consent form and the protocol was approved by the local medical ethical committee. Details of all subjects are provide in table 4.1.

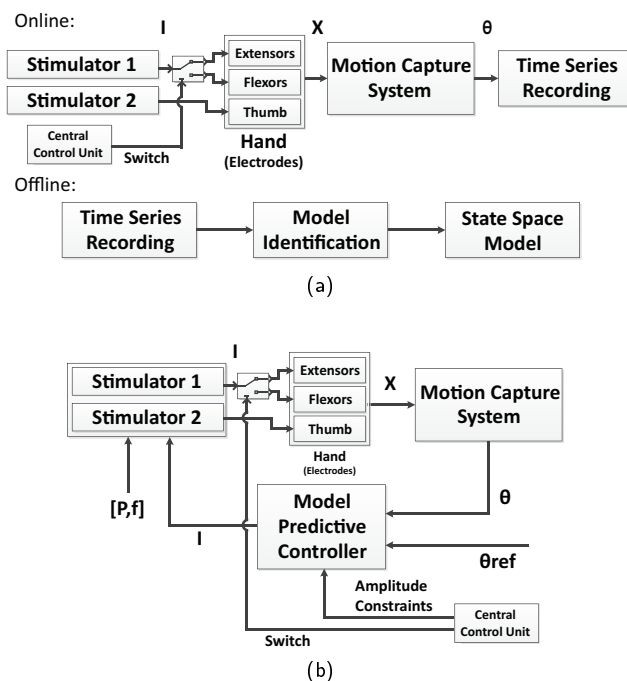


Figure 4.1: Overview of the stimulation system. a) Initialization procedure: the forearm was stimulated by predefined amplitude patterns I while recording the resulting movements x . Subsequently the stimulation amplitudes I and finger angles were used for offline model estimation. b) Feedback control system: The model predictive controller uses the current angular positions θ as well as the setpoint references θ_{ref} to calculate the optimal future stimulation amplitudes I . In both, initialization and control, one stimulator was dedicated to controlling the thumb muscles whereas the other stimulator controlled the flexor and extensor muscles. Switching was controlled by a predefined internal procedure: as needed for initialization (a) or during control, extensors were selected for hand opening, flexors for any grasp type (b). In addition, during control the maximum amplitude constraints of the inactive controller outputs were set to zero to ensure safe operation.

4.2.2 Experimental Setup

Figure 4.1 shows a schematic overview of the overall experimental procedure. It is based on the employment of two electrical stimulators, an optical motion capture system and the model predictive controller which is embedded on an xPc real-time platform. Both electrical stimulators were able to supply three independent current controlled channels for stimulation of the forearm. A more detailed description of these components is given in the subsequent sections.

The entire procedure consists of initialization period during which the forearm were stimulated by predefined amplitude patterns I , while recording the resulting movements x . Subsequently the stimulation amplitudes I and finger angles were used for offline model estimation. Secondly the the model predictive controller uses the current angular positions θ as well as the setpoint references θ_{ref} to calculate

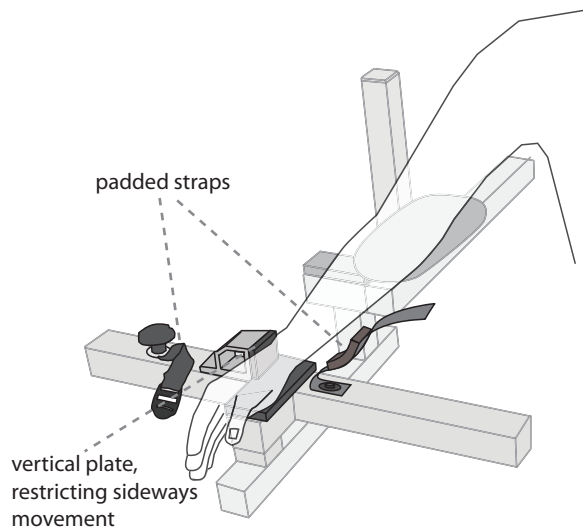


Figure 4.2: Illustration of the arm rest. The elbow as well as the wrist are rested on padded ground whereby most of the forearm is left free of support to improve accessibility for electrode attachment. The wrist is held in place in between a fixed vertical plate as well as padded straps to prevent transverse and rotational movement.

4

the optimal future stimulation amplitudes I .

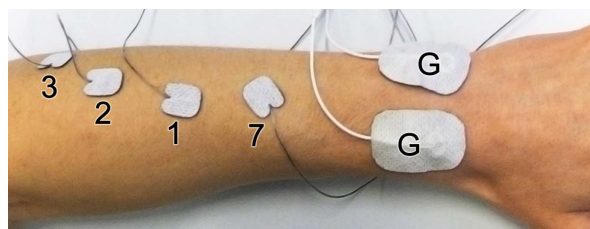
To extend the number of individual channels, given by the two electrical stimulators one stimulator was dedicated to controlling the thumb muscles whereas the other stimulator controlled flexor and extensor muscles, switching between extensor- and flexor- electrodes according to the task (hand movement) or when needed during initialization. Additionally, during MPC control the maximum amplitude constraints of the corresponding controller outputs were set to zero to deactivate the unused outputs and ensure safe operation. Both was handled by a central control unit, which employed predefined rules according to which extensors or flexors outputs were selected for hand opening or closing, as well as setting the appropriate maximum amplitudes.

To constrain the movement of arm and hand, or place the hand in the correct position during the experiment, the arm was fixated in a constraining device, mounted to an ordinary desk chair (figure 4.2). In case of the subjects' inability to keep the hand in a pronated position, the forearm could be fixated to a vertical plate using padded straps. This however did not limit wrist or hand movement in any way.

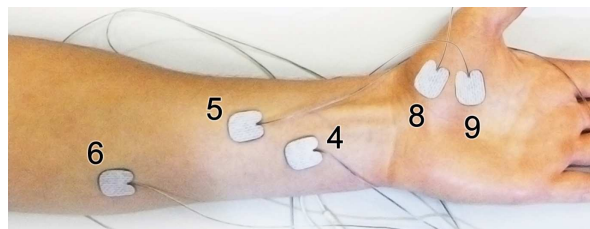
4.2.3 Electrical Stimulation

Hardware

Two custom build stimulators (TIC Medizin, Dorsten, Germany), equipped with an overall of 6 individual physical channels for which the amplitude could be modulated



(a)



(b)

Figure 4.3: Pictures of forearm with electrodes attached. All electrodes are marked with numbers corresponding to the description in table 4.2.

individually. The two stimulators were capable of stimulating with a pulsewidth of $80\mu s$ to $300\mu s$ (incr. of $10\mu s$), amplitudes of $0mA$ to $60mA$ (incr. of $1mA$), frequencies ranging from $2Hz$ to $100Hz$ (incr. of $1Hz$) with amplitude ramp up times of 0 sec to 10 sec (incr. of 0.1 sec). Three channels were designated to target the thumb muscles and the remaining three channels stimulated flexors and extensor muscles. To achieve an overall of 9 possible stimulating channels, flexor and extensor electrodes were pairwise attached to the same channels and switched back and forth for flexion and extension respectively. Pulsewidth and frequency were equal on all channels and left constant. Stimulator pulses were biphasic in order to prevent undesired accumulation of charge at the interface between stimulation electrodes and tissue.

Electrode Placement

Self-adhesive electrodes were placed on the forearm, whereby a squared electrode of 5 cm was used as the anode and a rectangular electrode of 1.6×1.8 cm was used as the cathode. The placement was conducted manually whereby the single electrodes were positioned according to the scheme in figure 4.3 such that the activation of each electrode could evoke movement with maximum selectivity. The term selectivity was defined by maximizing the resulting desired movement of a single finger while minimizing the movement of all other digits. This procedure was conducted manually and controlled by visual inspection. Table 4.2 gives an overview of all placed electrodes, their targeted muscle as well as the desired resulting movement.

Table 4.2: Overview of all stimulating electrodes, their corresponding muscle and resulting movement.

Electrode	Muscle	Desired Movement
1	EDC	Index Extension
2	EDC	Middle/Ring Extension
3	EDC	Ring/Pinky Extension
4	FDS	Index Flexion
5	FDS	Middle Flexion
6	FDS	Ring Flexion
7	AbPI	Thumb Abduction
8	OpP	Thumb Opposition
9	FPB	Thumb Flexion
G	-	Ground

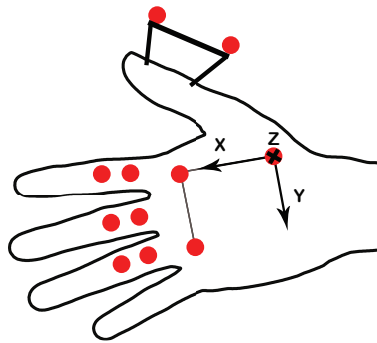


Figure 4.4: Marker positions on all fingers and the back of the hand, which determined the local coordinate system used. Visible is furthermore the extension on the thumb which was included in the setup to avoid marker occlusion during grasping.

4.2.4 Motion Capture and Marker placement

During operation the movement of the hand was recorded and fed back to the MPC using an optical motion capture device (Visualeyez, PhoeniX Technologies Incorporated, Burnaby, Canada) with a precision of 0.015mm at 1.2m distance according to the provided datasheet. Figure 4.4 shows the marker placement on the hand. The three markers on the back of the hand form a local reference coordinate system according to which the angles of thumb, index, middle and ring finger were determined. Each angle was calculated between the vector formed by the two markers on each finger and the x-y plane on the back of the hand. Negative angular movement was defined in direction of finger flexion. To increase the visibility for the camera, the markers for the thumb were not placed directly on the thumb, but were mounted on a small extension approximately 2 cm above and parallel to the thumb. The placement of the markers is mainly due to visibility reasons, as markers placed on the tip of the finger would have been prone to get

out of camera sight as soon as the hand is closed which would have led to angle miscalculations and therefore hamper the control procedure.

4.2.5 System Identification and Control

Preceding the control procedure, a model of the system was obtained, which was subsequently used by the MPC to calculate the inputs needed to reach the desired setpoints. This was achieved by stimulating the finger muscles using step inputs, between zero and the predetermined electrode specific maximum stimulation amplitudes, and recording the resulting movement response for a period of approximately 8 minutes.

The obtained data was preprocessed by subtracting the mean offsets, low pass filtering and piecewise detrending to remove nonlinear offsets and high frequency noise components. During detrending, interpolation points were given by the times at which all input signals were zero and therefore any deviation from zero level was attributed to low frequency noise. Subsequently a piecewise linear interpolation between the consecutive data points was subtracted from the signal and the signal was downsampled to 10Hz.

Subsequently the model calculations were performed using Matlab's System Identification Toolbox (The MathWorks Inc., Natick, MA USA). In the present case, the system was described by a 9 input – 5 output linear state space model of order 15. The model order was determined beforehand by trial and error as well as residual analysis, such that a further increase would not decrease the model residuals to a greater extent and was used constant throughout all experiments.

The MPC, which was implemented using Matlab's Model Predictive Control Toolbox (The MathWorks Inc., Natick, MA USA), operated at a rate of 10Hz, which was restricted by the hardware speed of the real-time computer in use, minimizing the general MPC objective function J (Bemporad et al. 2010) that, in this particular case, can be reduced to the following form:

$$J(\Delta u_j, \epsilon) = \sum_{i=1}^{p-1} \left(\sum_{j=1}^{n_y} |w_{j,y}^y (y_j(k+i+1|k) - r_j(k+i+1))|^2 + \sum_{j=1}^{n_u} |w_{j,u}^{\Delta u} \Delta u_j(k+i|k)|^2 \right) + \rho_\epsilon \epsilon^2 \quad (4.1)$$

J is minimized with respect to $\Delta u(k|k), \dots, \Delta u(m-1+k|k), \epsilon$ and describes the cost function over the control horizon p to find the appropriate stimulation amplitudes u_j for all inputs n_u such that the angles y_j for the number of all outputs n_y reach the desired setpoints r_j . In order to avoid unpleasant or harmful control behavior the inputs u_j and input rates Δu_j are constrained variables with $u_{jmin} = 0$ and u_{jmax} set to the maximum stimulation amplitude of the equivalent electrode which were determined manually before each experiment, and $0 \leq \Delta u_{jmin} \leq 1$ which is equivalent to a maximum change of amplitude of 1mA per control step (100ms).

Control and prediction horizons were set to 0.5s and 0.6s respectively. Input rate weight $w_j^{\Delta u}$ and output weight w_j^y assign the relative importance of input rate constraints Δu_j and setpoint error. Thereby $w_j^{\Delta u} = 0.1$ for all j and $w^y = [1 \ 1 \ 1 \ 2 \ 2]^T$. As the thumb does have a smaller angular movement range, its output weights were set twice as high as for the rest of the fingers in order to aid more accurate setpoint tracking. To add stability to the stimulation behavior and increase subject comfort the overall estimation gain was decreased to 0.4, which is a dimensionless internal variable in the generated MPC object. All remaining settings were left unaltered. The weight ρ_ε penalizes the violation of constraints which is measured by the slack variable ε . As ρ_ε increases relative to the input and output weights, the controller gives higher priority to minimization of constraint violations. Either flexor or extensor control variable outputs (due to the distribution of electrodes across the channels) were made inactive by setting their maximum value constraint to zero, depending on the desired movement. Additionally, internal- and closed-loop controller stability were ensured and tested by calculating the eigenvalues of the controllers unconstrained state space realization and the discrete-time state-space-realization of the closed-loop system. Furthermore, stability of the system model was tested via examination of its step responses. For a thorough documentation of the implemented MPC structure and stability analysis techniques please refer to (Bemporad et al. 2010).

4

4.2.6 Experimental Protocol

Electrode Attachment and Model Initialization

Throughout the experiment the subject was seated in a chair with the affected hand resting on the hand-rest in a neutral pro/supinated position as e.g. when holding a bottle or cup (figure 4.2). Depending on the subjects own ability to supinate the hand, the wrist was fixated using padded straps. Subsequently all 9 electrodes were placed manually according to figure 4.3 whereby correct placement was confirmed matching it to the desired responses in table 4.2. Throughout the experiment the stimulation amplitude was restricted to a range of 0mA to 30mA, therefore during this time also an appropriate stimulation pulse width was determined at which the stimulation showed significant movement responses within a range of 0mA to 15mA. This was merely a preparational step adjusting stimulation intensity and was only changed in case of too little movement response or selectivity in the operating range. Furthermore the stimulation frequency was fixed at 30Hz.

An additional placement criterion was subject comfort, whereby it was assured that the subject's sensation caused by the stimulation was not painful or uncomfortable. As soon as the electrode placement was completed, maximum current amplitudes were determined for each electrode. The maximum amplitude was defined by the amplitude at which any further increase would not lead to any significant change in the desired movement response and did not cause any uncomfortable sensation to the subjects. In cases where further increasing the amplitude led to an unwanted decrease of selectivity the maximum amplitude was set in favor of maintaining selectivity.

Evaluation

In order to assess controller performance in terms of setpoint tracking as well as its ability to achieve functional movements, the controller was set to perform several setpoint tracking tasks in air as well as to grasp a number of objects. The setpoint error is subsequently determined by the root mean squared error of steady state finger setpoint angles and the resulting controlled finger angles.

The four objects with which the ability of grasping and holding was determined were selected from the ARA-test. These were a small cube (2.5cm, 10g), a larger cube (5cm, 90g) as well as a hollow metal cylinder (\varnothing 2x15.5cm, 100g) and a marble (\varnothing 1.7cm, 5g). The objects were manually placed between the subjects' fingers by the experimenter after which the controller was instructed to grasp the object using either pinch grip for the marble and the small cube, or cylindrical grip for the large cube and the cylinder. For pinch grip the object was placed in between index and ring finger or in some cases where selective index finger movement could not be achieved, between thumb and middle finger. Success was determined by holding the object for a period of 10 seconds which was repeated five times for each object.

In terms of setpoint tracking, the controllers' ability for tracking a total of 3 setpoints was assessed. These setpoints were predefined movement patterns corresponding to the functional movement types: pinch grip, cylindrical grip and opening of the hand. Thereby the setpoint tracking was divided into two separate phases: alternating 10 times between 1) hand opening and cylindrical grip as well as 2) hand opening and pinch grip. Each setpoint was held for a period of approximately 10 seconds. Subsequently the measured finger trajectories of all 10 repetitions were lined up to the setpoint change and averaged calculating mean and variance for each timestamp on an interval of -1s to 6s with zero being the change from hand opening to the corresponding setpoint (cylindrical or pinch grip).

4

4.2.7 Data Analysis

Evaluation of Stimulation Selectivity

To determine stimulation quality a new measure for selectivity was introduced. Thereby the selectivity index per electrode is expressed by

$$S_e = \text{var}\left(\frac{M_{e,:}}{\sum_{f=1}^{N_F} M_{e,f}}\right) * N_F \quad (4.2)$$

The selectivity S of each electrode e is given by the maximum response matrix M (with N_e rows and N_F columns) of each digit f to stimulation on this electrode times the number of controlled fingers N_F . Thereby N_F is used as a scaling factor. The intensities were normalized to the sum of their corresponding row which represents the overall response to the stimulus per electrode. In other words, the selectivity of one electrode is the variance of the movements of all fingers evoked by this electrode, normalized by the total movement and multiplied by the scaling factor N_F .

Table 4.3: Results of the system identification procedure using the initialization data. Shown are the mean model fits (eq.4.3) of the estimated state space model for each angular system output.

	Healthy [%]		Stroke [%]	
	mean	sd	mean	sd
Thumb Ext.	56	8.3	55	7.5
Thumb Abd.	67	6.3	74	4.9
Index	68	5.9	51	9.0
Middle	66	12.1	63	6.4
Ring	64	8.8	60	11.2
mean	64	8.3	60	7.5

The hereby used selectivity index is motivated by its practical properties such that in case all resulting movements are equal in amplitude, which corresponds to no selectivity, S is equal to zero. In case selectivity is highest and only one output is activated entirely while leaving all others at zero, S equals one. As thumb extension and abduction are not independent of each other the Euclidean norm was used in order to combine them and obtain a more meaningful, overall activation measure for comparison.

Model and Controller Evaluation

The accuracy of a model output \hat{y} to the previously recorded observed data y with a number of samples N is estimated by the following formula which expresses the similarity of the calculated model outputs to the measured data (Ljung 2013). Thereby \hat{y} and y are vectors of length N .

$$fit = \left(1 - \frac{|\hat{y} - y|}{|y - \frac{\sum_{i=1}^N y_i}{N}|}\right) * 100 \quad (4.3)$$

To assess the controller's potential to be used for performing functional movements, it was set to track the same setpoints as when performing the setpoint tracking task. However this time a number of objects were manually placed in the subject's hand for which setpoints did not depend on the size of the object. A successful grasp was indicated by the controller's ability to hold and release the object for a period of 10 seconds. Thereby the process was repeated 5 times for each object. A single attempt of grasping was awarded with either 1 for success or 0 for failure. In the following the success rate is defined to be the mean of all trial outcomes. To counteract voluntary interference, subjects with much residual hand control e.g. all healthy subjects were blindfolded and instructed to remain relaxed throughout the procedure.

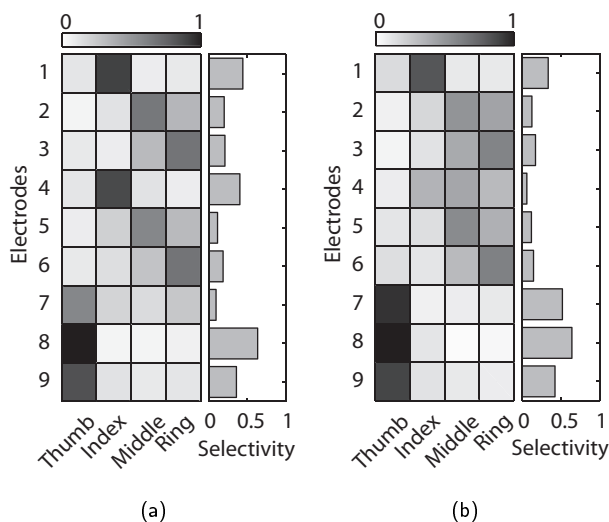


Figure 4.5: Maximum response matrix M , with intensities normalized to the sum of their corresponding row as in 4.2, of all targeted fingers to stimulation on all nine electrodes (rows 1-9) for healthy (a) and stroke subjects (b). Additionally the index of selectivity is given for each stimulating electrode, whereby in case the selectivity $S = 1$ is equivalent to a response of only 1 finger to the stimulus indicating maximum selectivity. Whereas an $S = 0$ indicates an evenly distributed response of all fingers. Electrode targets are equivalent to table 4.2.

4.3 Results

4.3.1 Initialization and System Identification

During model initialization movement on all fingers could merely be elicited by amplitudes near the maximum. This was especially the case for stroke subjects whereas healthy subjects showed lower thresholds at approx. 50% max. amplitude. Maximum amplitudes ranged from approx. 16 - 30mA for extensor- and 6 - 20mA for flexor muscles. Pulswidths ranged from 80 - 120 μ sec for healthy and 200 - 250 μ sec for stroke subjects. During operation a fast onset of diminishing movement response was observed in all stroke subjects such that the pulswidth was often increased several times by an overall of 30 - 50 μ sec in order to counteract this effects. With the thereafter obtained linear state space model, 10 step prediction accuracies given by the model fit of approximately 60-70% were achieved. Table 4.3 shows the average model accuracies for each output, for stroke and healthy subjects respectively. Furthermore, additional analysis and of the MPC objects and real time performance revealed no issues in terms of controller or model stability.

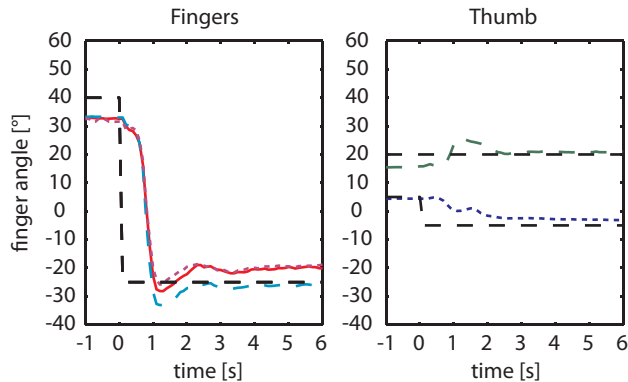


Figure 4.6: Averaged setpoint plot for an exemplary healthy subject with setpoints going from hand opening to a) cylindrical grip and b) pinch grip. Thumb and residual fingers are separated graphically for visibility. Mean variance over all fingers was $1.7^{\circ} \pm 0.25^{\circ}$ for cylindrical and $3.1^{\circ} \pm 2.25^{\circ}$ for pinch grip.

4

4.3.2 Selectivity

Figure 4.5 shows the normalized maximum movement intensity after settling time for each electrode and output. Comparing healthy to stroke subjects both groups show similar selectivity distributions. However the excitation of individual finger movements is degraded in the case of stroke subjects. Particularly it was hardly possible to achieve selective index flexion (resp. to electr. 4 in 4.5b).

4.3.3 Setpoint Tracking

Figure 4.6 shows a typical example for setpoint responses averaged over several trials and obtained for the cylindrical and pinch grip task of one healthy subject. Thumb and finger data are shown separately to increase visibility. The setpoints were tracked with good accuracy for all digits including the thumb. Time zero represents the setpoint change from hand opening to closing. Figure 4.7 shows a similar example for an exemplary stroke subject (ARAT=3). As the subject showed a very limited movement range, the setpoints were adjusted accordingly. Tracking of thumb position hereby showed large offsets in comparison to its movement range. Figure 4.8 shows the average angular range for healthy and stroke subjects. The movement range was defined as the maximum possible movement for each finger or output dimension, elicited by electrical stimulation. Thereby stroke subjects had a smaller movement range in comparison to healthy subjects. Steady state setpoint errors for hand opening, cylindrical, and pinch grip averaged over all fingers of all healthy and stroke subjects can be seen in figure 4.9. In addition to that the steady state error normalized by movement range is shown on a second axis.

Figure 4.10 shows exemplary measured finger angles, angular setpoints including all nine control variables (stimulation currents) and their maximum constraints during a setpoint measurement in air, altering between hand opening and pinch

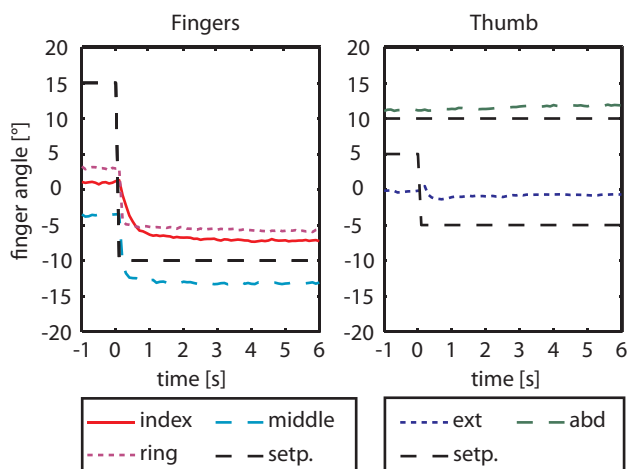


Figure 4.7: Averaged setpoint plot of an exemplary stroke subject ($ARAT = 3$) executing cylindrical grip. Subject showed no residual hand control and a limited angular movement. Mean variance over all fingers was $1.8^{\circ} \pm 0.013^{\circ}$.

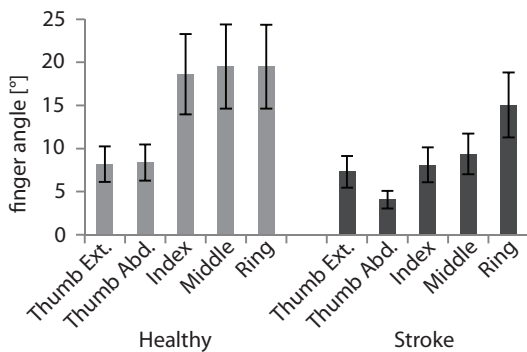


Figure 4.8: Movement range for each finger, averaged over all stroke and healthy subjects. Movement range was defined as the maximum possible movement of each finger elicited by electrical stimulation.

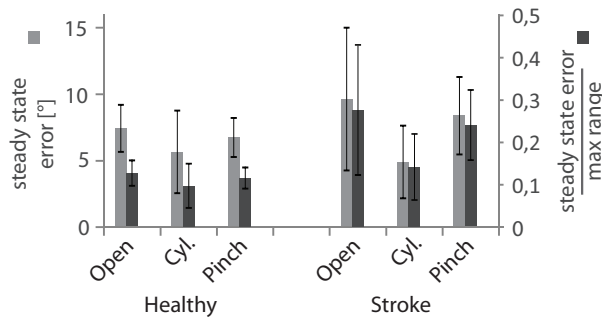


Figure 4.9: Mean steady state errors over all fingers including the thumb during setpoint tracking averaged over all healthy and stroke subjects as well as the mean steady state errors normalized by the movement range.

grip. Visible is also how the constraints of outputs 1-6 are altered to multiplex between flexion and extension. All control variables are normalized by their maximum boundary constraint. As described previously, outputs 1-3 and 4-6 can not be active at the same time. Note how all fingers follow their setpoints adequately. Since the setpoints in this case are aiming for selective index flexion only output 4 and 5 are active during flexion. Hereby output 4 is selective for index flexion, and therefore most active, whereas channel 5 is selective for flexion of the middle finger and shows merely small activity, likely due to a mechanical coupling embedded in the system model (figure 4.5a). Also, whereas all other outputs hardly come close to their maximum amplitude constraints, output nr. 3 alternated between zero and maximum amplitude. The reason for this might be that in this case the maximum amplitude was set slightly too low. This way the maximum current was needed to reach the desired setpoint. This is evident when regarding the setpoint of the ring finger, that output 3 is selective for, which is able to reach the setpoint only with a larger offset compared to other fingers.

Errors are divided evenly over all inputs and it was possible to perform the pinch grip task in all healthy, but merely one stroke subject. On all remaining stroke subjects selective stimulation for index flexion could not be achieved which led to the exclusion of the pinch grip task in those cases.

Generally, both setpoint error and standard deviation is larger in stroke subjects by a factor of about 1.25 and 1.65 respectively compared to the observations in healthy subjects.

4.3.4 Functional Movements

Table 4.4 shows a comparison of the average success rates for grasping for healthy and stroke subjects during electrical stimulation. Thereby the success rate in stroke subjects was slightly lower for heavy or small objects such as the metal cylinder and the marble. Big and small wooden cubes were grasped with 100 % success rate.

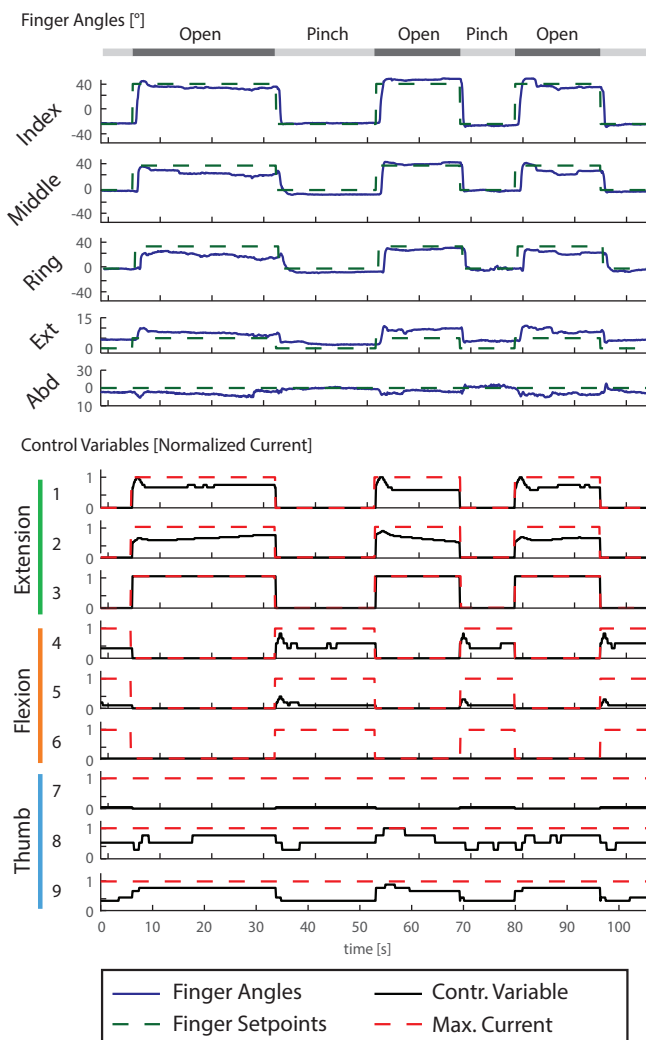


Figure 4.10: Exemplary measured finger angles, angular setpoints, as well as all nine control variables and their maximum constraints during a setpoint measurement in air, altering between hand opening and pinch grip. Note how the constraints of channels 1-6 are altered to multiplex between flexion and extension. All control variables are normalized by their maximum boundary constraint.

Table 4.4: Success rate of grasping experiments in stroke and healthy subjects. The numbers define the percentage of trials in which the object was held successfully.

	Stroke		Healthy	
	mean	sd	mean	sd
Metal Cylinder	75%	21%	95%	1%
Marble	75%	5%	100%	0%
Big Cube	100%	0%	100%	0%
Small Cube	100%	0%	100%	0%

4.4 Discussion

In this paper we investigated the feasibility of a model predictive control approach for the control of fine grasping movements in stroke patients. The aim of this study was to passively generate functional movements to grasp and release objects of different size and shape. We showed that the approach can produce functional movements to grasp and release a variety of smaller and bigger objects (Table 4.4). Performance in stroke subjects was slightly reduced, especially for small and heavy objects.

Additionally, we showed that it is possible to obtain a system model to predict finger movement with accuracies of approximately 60% to 70% which can be used for control. Also it was shown possible to find the desired stimulation positions to achieve selective flexion and extension movements of index, middle and ring finger as well as the thumb in three different angular directions as shown in figure 4.5. The average variability in setpoint tracking of $8.3^\circ \pm 2.9^\circ$ and $6.7^\circ \pm 1.7^\circ$ for stroke and healthy subjects respectively did not have a big impact on movement functionality.

4.4.1 Related Work

In terms of movement control, the precise positioning of individual fingers to achieve a functional movement with the possibility of conveniently implementing a variety of other possible movements for patient training had not been demonstrated so far. However, selective finger activation and feedback control of electrical stimulation have been described thoroughly in literature.

The results regarding selectivity are similar to those obtained in chapter 2 of this thesis, where the possibility to generate selective finger extension and thumb movements by electrical stimulation using electrodes aligned on a grid was shown. Existing control methods mainly focus on gross motor control of wrist and hand (Crago et al. 1996; Hart et al. 1998; Micera et al. 2010). With the MPC approach presented here assistance of fine motor control with selective finger stimulation becomes available.

Current commercially available devices such as the Handmaster or the Neuro-move lack variability in stimulation patterns, number of electrodes and available independent channels. Therefore these devices are limited in their application which could lead to insufficient training paradigms. Our current approach was shown able

to control individual finger and hand movements accurately. This could possibly lead to a better result for the neural recovery of fine motor control functions.

In other systems which make use of a greater number of input electrodes to select the optimal electrode configuration this is implemented as a separate step preceding training similar to the procedure described by us (O'Dwyer et al. 2006; Keller et al. 2006; DB Popović and MB Popović 2009; Hoffmann et al. 2012; Elsaify 2005). Being able to use a system model, the MPC has an inherent electrode selection procedure. Therefore even an initial incorrect electrode placement such as switching electrode order does not have an impact on the robustness of the procedure. Additionally this makes it possible to easily up-or downscale the amount of inputs with minimal additional adjustment time and allows for a patient specific approach.

4.4.2 Possibilities for rehabilitation

Three practical shortcomings of the current methods should be overcome before an approach like this can be applied in post stroke rehabilitation: 1) donning and doffing is cumbersome and time consuming, 2) the motion capture system is only suitable for a laboratory setup and 3) the user remains passive in the current approach. For rehabilitation purposes, the system should be quick and easy to setup by a non-trained user, finger movement should be recorded with a simple and easy to setup system and voluntary effort by the user should be promoted to achieve a positive training effect (Wolbrecht et al. 2008; Reinkensmeyer et al. 2009; Timmermans et al. 2010).

A drawback of the method is the strong dependency on a large number of stable electrodes on the forearm. We had placed an overall of nine electrodes whereby three groups of three electrodes were dedicated to control thumb, flexors and extensors respectively. Preceding the experiments, the electrode positions were searched manually which was subjective, cumbersome and time consuming. Therefore we suggest to replace the many single electrodes by electrode arrays. This has been under development by a number of groups (Malešević et al. 2012; DB Popović and MB Popović 2009; O'Dwyer et al. 2006; Hoffmann et al. 2012). The manual search procedure could subsequently be taken over by intelligent search algorithms to increase usability especially decreasing the time needed for donning and doffing.

The controller used constant position information which was captured by a motion tracking device, mainly suitable for a laboratory environment. For clinical application a more compact and more plug and play solution is needed. Measurement gloves (Williams et al. 2000; Simone and Kamper 2005; Veltink et al. 2012; Oess et al. 2012) or commercially available devices like Microsoft Kinect (Chang et al. 2011) or LEAP motion (Weichert et al. 2013) might be used as a more portable solution for feedback of finger angles.

The present system is preprogrammed strictly independent of subject intention. For application in rehabilitation, feedback mechanisms to detect voluntary subject activity is required to be more effective and increase the possible recovery of motor

function (Sinkjær et al. 2003). This has already been done using e.g. EMG or torque (Hara 2008; Besio 1997; Hincapie and Kirsch 2007; XL Hu et al. 2011; Yamaguchi et al. 1999), but also systems driven by data derived from the cortex using invasive or noninvasive methods are in development (Ethier et al. 2012; Tavella et al. 2010; Schneiders et al. 2011; Pfurtscheller et al. 2005; Muller-Putz et al. 2008).

4.4.3 Limitations

The success-rate in terms of selectivity, functional grasping and setpoint tracking was lower in stroke subjects. Also the pulsewidth used in all stroke subjects was about two times higher to result in a similar activation threshold compared to healthy subjects. This could be attributed to the fact that all of them had already entered the chronic phase which might have resulted in muscular degenerations or other active or passive tissue dysfunctions (Carda et al. 2013). Two of the stroke subjects showed signs of spasticity (ARAT = 28 and 25) and one showed a significant angular movement limitation (ARAT=3). In cases where spasms are present with difficulties to keep the hand in an open/neutral position, the employment of a passive orthosis such as the SaeboFlex system (Saebo Inc., Charlotte, NC, USA) could be used. However, this might be less of an issue when the technique is applied for rehabilitation of acute stroke patients. In that group, the controllers performance is hypothesized to be more similar to that of a healthy subject as no significant muscular degenerations, contractures or spasticity should have occurred at this point in time (Carda et al. 2013; Brainin 2013).

As visible in table 4.1 the age difference between the recruited healthy and stroke subjects was rather high. Therefore one should be cautious in the direct comparison of both groups. Muscles in elderly could be weaker as in younger subjects caused by muscular changes due to age. In addition to that, electrode contact might be different in elderly due to a reduced skin smoothness. However, inter-subject variability in terms of stimulation parameter tuning is always present. The procedure is able to overcome such changes by e.g. increasing stimulation intensity. Therefore we do not expect that differences in age have influenced the outcome of this study to a large extent.

Voluntary subject interference, especially during the conducted object grasping task cannot be excluded with absolute certainty. Despite the fact that all healthy subjects were blindfolded and instructed to remain relaxed, the possibility of subject interference remains. Future work could incorporate EMG measurements, together with methods to subtract the stimulation artefacts (Sennels et al. 1997; Langzam et al. 2006) to ensure that the subject is truly passive.

All controllers showed to be both closed-loop and internally stable, which is essential to ensure safe performance. However mismatch between the model and the biological system can still lead to unstable situations. This could be avoided by tuning the controllers to behave less aggressive which decreases oscillation and subject discomfort and therefore add stability, but this will also hamper setpoint tracking results.

The initialization procedure was kept rather short to reduce the total experiment length. Therefore, all data was used for model calculation. This could have led to overfitting and therefore might have degraded the result of the control procedure.

The control interval had to be set to 100ms because of hardware restrictions this was partly larger than the actual time constants of the system. Normally desirable control intervals are well below the systems time constant. This could have added inaccuracies to setpoint tracking performance, which might be overcome by increased computing power.

Only angles of the first phalanx were measured, to avoid camera occlusion. Therefore most certainly only part of the fingers states were known accurately to the controller during operation. However due to the close relationship between the movement of each fingers joints the measured angles were sufficient to obtain functional movement, which was the main goal of this study.

4.5 Conclusion

We have shown that the designed model predictive control approach can lead to functional and smooth movements suitable to grasp, hold and release a variety of objects in both stroke and healthy subjects. The approach provides the possibility of flexing and extending individual fingers selectively and therefore has the ability to generate a broad range of movements. The procedure has potential for application in a clinical or a home setting supplying a flexible technique for upper limb stroke rehabilitation.



A robotic end point manipulator for functional rehabilitation exercises after stroke

Westerveld, AJ, BJ Aalderink, W Hagedoorn, M Buijze, AC Schouten, and H van der Kooij (2013). "A damper driven robotic endpoint manipulator for functional rehabilitation exercises after stroke." *submitted*

Abstract

Stroke survivors may benefit from robotic assistance for relearning of functional movements. Current assistive devices are either passive, limited to only two dimensions or very powerful. However, for reach training, weight compensation and a little assistance with limited power is sufficient.

We designed and evaluated a novel three dimensional robotic manipulator which is able to support the arm weight and assist functional reaching movements. Key points of the design are a damper based drive train, giving an inherently safe system and its compact and light-weight design.

The system is force actuated with a bandwidth of up to 2.3 Hz, which is sufficient for functional arm movements. Maximal assistive forces are 15 N for the up/down and forward/backward directions and 10 N for the left/right direction. Force tracking errors are smaller than 1.5 N for all axis and the total weight of the robot is 25 kg. Furthermore, the device has shown its benefit for increasing reaching distance in a single case study with a stroke subject.

The newly developed system has the technical ability to assist the arm during movement, which is a prerequisite for successful training of stroke survivors. Therapeutic effects of the applied assistance need to be further evaluated. However, with its inherent safety and ease of use, this newly developed system even has the potential for home based therapeutic training after stroke.

5.1 Introduction

Robotic systems have found their way into rehabilitation practice. Although the exact mechanisms underlying improvement of function after training with robotic assistance are still unclear, several studies have shown benefits of the use of robotic devices for movement therapy after stroke (Prange et al. 2006). Robotic aided therapy gives similar results as conventional therapy (Kwakkel et al. 2008) and robotic manipulators facilitate more intensive training and objective measurements (Lum et al. 2002), without the need of a therapist being continuously present. Influenced by these positive results, more and more devices are being developed for training of both upper and lower extremity movement. Recently, a Swiss randomized clinical trial showed that robotic therapy for the arm can give a significantly larger improvement compared to conventional therapy (Klamroth-Marganska et al. 2013). This is a promising result, although the costs currently hamper the clinical use (Kwakkel and Meskers 2013). Therefore, more simple and affordable robotic devices are desirable for rehabilitation practice.

Three recent reviews (Loureiro et al. 2011; Brewer et al. 2007; Riener et al. 2005) provide an extensive overview of upper extremity rehabilitation robotics. Most of these devices are academic prototypes and not commercially available. A distinction in mechanical design can be made between end-point manipulators like MEMOS (Micera et al. 2005) and InMotion ARM (Hogan et al. 1992) on one side and exoskeleton systems, like Armeo Power (Nef et al. 2007) on the other side. Exoskeletons follow the natural arm anatomy and can deliver joint specific assistance. However with exoskeletons, proper alignment between joint axes and exoskeleton axes is crucial, requiring time and experienced operators. Passive alignment systems have been proposed to prevent misalignment (Stienen et al. 2009a; Schiele and Hirzinger 2011), but will always increase the complexity of the device. Furthermore, the exoskeleton should provide large shoulder torques to compensate for gravitational forces due to the arm and the exoskeleton itself. End point manipulators in general have a more simple mechanical structure. Typically these devices have a single connection with the human arm and therefore cannot assist individual joints.

Existing upper extremity devices can also be categorized according to the amount of assistance (e.g. number of degrees of freedom, actuator power, controllability) they are able to provide, see figure 5.1. There exist very powerful high-end (mostly exoskeleton) devices on one side and passive devices on the other side. Examples of powerful high end devices are Armeo Power (Nef et al. 2007), CADEN-7 (Perry et al. 2007) and MIME (Lum et al. 2006). These devices share properties like large work-range, strong motors and fast actuators. Often these devices are suitable for movement assistance and for diagnosis using system identification techniques (Kooij et al. 2005) These techniques need imposed perturbations of the arm, which leads to increasing demands on the system. Some systems are purposely built with this application in mind (Park et al. 2008; Stienen et al. 2011; Otten et al. 2014). Examples of passive devices are the Dampace (Stienen et al. 2009a), Armeo Boom (Stienen et al. 2009b) and Armeo Spring (Sanchez et al.

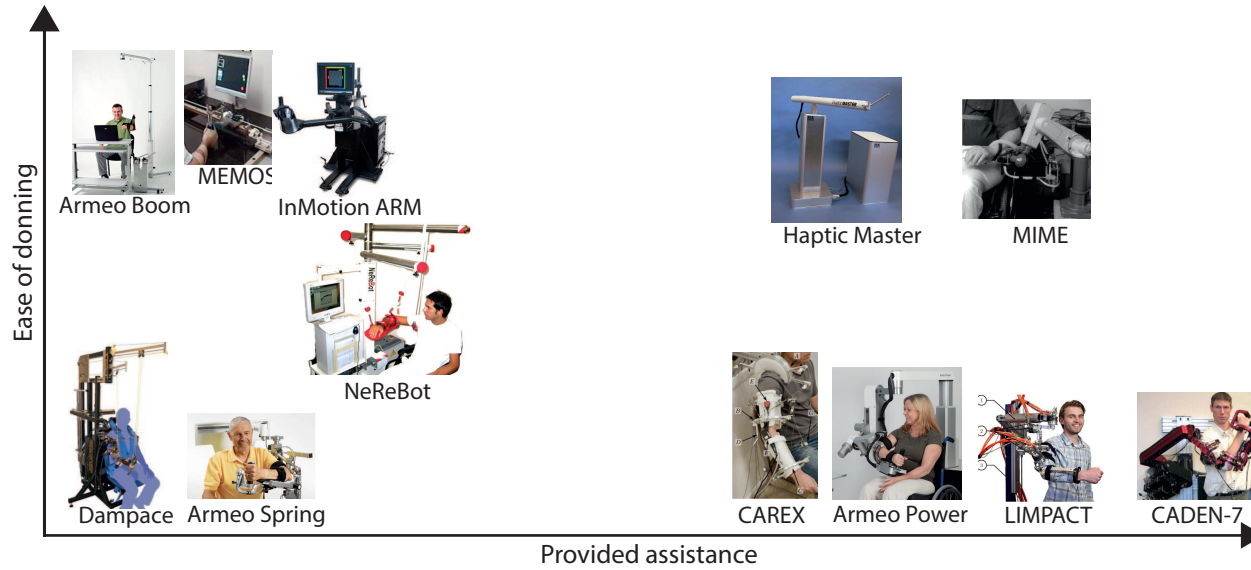


Figure 5.1: Overview of existing commercial arm rehabilitation devices, arranged by their provided assistance (like number of degrees of freedom, actuator power, controllability) and ease of donning. There exist a gap in the middle, for a device with simple donning/doffing and the ability to both counteract gravitational forces and provide some guidance forces to the human arm.

2006). These devices mainly counteract the gravitational force acting on the arm and allow users to use their remaining muscle capacity to move their arm without the load of gravity. In addition, several cable-based systems have been developed to move the arm (Rosati et al. 2005; Mao and Agrawal 2012).

Another important difference between existing devices is the control architecture. Some devices (like MIME) are position controlled. These devices are very stiff and move the arm in a certain position, which has been shown less beneficial for therapy (Reinkensmeyer et al. 2009). Other devices are impedance controlled (In-motion ARM, ARMin) which means that they apply a force to guide the arm based on a measured deviation from a desired position or trajectory. A third category are admittance controlled devices (e.g. Haptic Master). In admittance control, interaction forces are measured and used to control the speed of the actuators such that a certain virtual (haptic) environment is perceived by the user.

For rehabilitation purposes, currently there exists a gap between the high-end active devices and the passive devices. A low power assistive device with a 3D workspace can fill this gap. Thereby allowing for functional task training, when the device is kept inherently safe and easy to operate by a non-expert, possibly even at home.

Compensation for gravitational forces already has shown to be beneficial for rehabilitation after stroke (Beer et al. 2007; Krabben et al. 2012; Prange et al. 2012). However for some patients gravity compensation alone is not enough to complete certain reaching tasks, especially early after stroke. A little extra active guidance in the movement direction additional to gravity support may help these people in completing reaching tasks, which makes therapy much more rewarding. Assistance of reaching tasks does not necessarily require high actuation forces. A small force guiding the patient in the right direction would already be sufficient. A device capable of both counteracting gravitational force and supplying assistive forces in three directions would in potential be a great therapeutic tool to improve reaching movements after stroke.

To fill the gap, we developed a new lightweight active therapeutic device (ATD). This paper presents the design and evaluation of this novel three dimensional end-point manipulator for use in functional training of reaching tasks after stroke. Key features of the system are the ability to provide both gravity support and apply relatively small guiding forces. In addition, the system is inherently safe, simple to install and easy to operate by a non-expert. The design is relatively simple in order to keep the costs low and therefore has the potential to make the final step to clinical or even home use. This will be a big step forward along the way to address intensive after-stroke therapy and effective rehabilitation outcome.

5.2 Hardware Design

5.2.1 Specifications

The ATD is a training system suited for training of either the left or the right arm of a patient, see figure 5.2. Table 5.1 lists the key specifications of the ATD

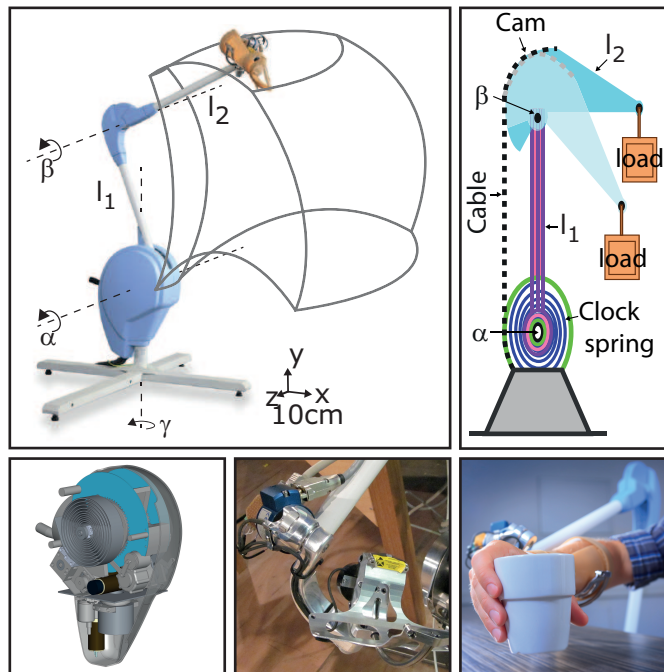


Figure 5.2: Overview of ATD system. The top left pane shows the ATD and its range of motion (grey lines). The top right pane schematically shows the passive gravity compensation mechanism. Interior CAD drawings, end-point gimbal and user interaction are shown in the bottom panes from left to right.

Table 5.1: Overview of key specifications of ATD

Parameter	Value
Stature range of intended patient population	1.46-1.88 m*
Maximum patient weight	120kg (~ 3 kg arm weight*)
Fügl-Meyer/MRC** score of intended patient population	≥ 30 / ≥ 2
Donning time	< 2 min
Size of housing	$0.30 \times 0.23 \times 0.55$ m
Size of ground frame	0.90×1.15 m
Length of links l_1 and l_2	0.6 m
System weight	25.5 kg
Max power consumption	600 W
Maximum actuation force***	$F_x = -16..15$ N
	$F_y = -13..17$ N
	$F_z = -9..9$ N
Bandwidth of force actuation (closed loop)	2.3 Hz
Bandwidth of position actuation (closed loop)	2.1 Hz
Hysteresis	< 2.2 N

* Corresponds to P01 and P99 stature range of Dutch 60+ male and female population (Daanen et al. 2003).

** MRC = Medical Research Council Scale of muscle power;
2 = movement only if gravity is eliminated

*** Determined open loop; negative forces indicate forces in the direction of the negative axis

system. The system is intended to be used by a patient which is seated in front of a table. Due to its compactness and low weight, the system can be transported by a single person. The system is very flexible and allows fast adjustments of the exact training tasks, which is beneficial for the motivation and the overall training effect (Timmermans et al. 2010). Furthermore the amount of support or restriction can be adjusted for each training and person, from resistive 3D forces to compensation of gravitational forces and assistive guidance forces.

The ATD uses a combination of passive gravity compensation and active actuation to reduce required actuator power and thereby costs. The gravity compensation is provided by a clock spring, of which the pre-tensioning is manually adjustable, to provide a nominal vertical force. The end of the clock spring is connected to a cable, which runs parallel to link l_1 , over a cam and is connected to link l_2 of the robot (figure 5.2). The shape of the cam compensates for both rotation of angle β , leading to a reduction of effective length of l_2 , and for the non-linearity of the rotational spring. To optimize the cam shape such that compensation forces are minimally influenced by position changes, the force error was measured by vertical movement of a load using a cylindrical cam. For different angles of α , the

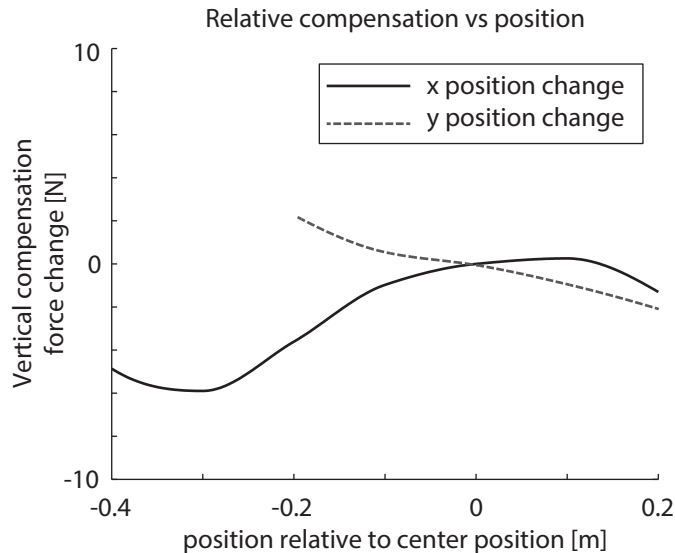


Figure 5.3: Non-linearity of the passive gravity compensation. Imperfections for movement in x and y direction are shown relative to the center xyz -position $[0.6, 1.0, 0.0]$. The actuators will compensate for the imperfections in passive gravity compensation.

5

load compensation error was measured by variation of β with a fixed load. Based on these load curves a new cam was calculated giving the least load variation while varying α and β . Resulting in the passive curve shown in figure 5.3. The remaining deviations can be actively compensated for., while was fixed in the center position. With reverse engineering a new cam is calculated. Before a training session is started, the operator can adjust the spring compensation to provide the desired compensation for a specific patient. The use of a passive gravity compensation keeps the robot in position during donning and doffing, ensuring an intrinsic safe situation.

5.2.2 Actuation and sensing

To meet the actuation demands of a high torque at a low speed with a standard and compact motor, transmission and gearing is needed. The limited back drivability of gears results in unsafe and direct coupling to the actuator. This can be reduced by introducing elasticity in the drive chain, i.e. series elastic actuation (Pratt and Williamson 1995). However, in the ATD this is solved by using a novel damper approach. With a damper the generated torque is proportional with the motor speed. The motor-damper combination makes a fast and stable torque actuator and allows for a very compact, safe (decoupling of subject and motor) and robust design with a relatively high closed loop bandwidth.

The damper in the drive train allows for force control by controlling the rotational speed, similar to the use of series elastic actuators (Pratt and Williamson

1995) where force is controlled by controlling spring deflection. The use of a non-dissipating element like a spring, might however cause unstable oscillations (Oblak and Matjacic 2011). As opposed to the SEA, the rotational damper dissipates energy. This makes application safer for usage in robots interacting with humans at the cost of a reduced efficiency. Furthermore the damper concept has a higher closed loop bandwidth compared to position feedback when using a motor with gearbox or flexible elements. This higher bandwidth is caused by the fact that the closed loop system with a damper is part of the velocity feedback loop, while the spring system is part of the position feedback loop. The former has per definition a higher bandwidth.

All actuators are enclosed in the housing, see figure 5.2. The drive train of the robot has active torque actuators for axes α and β in combination with the passive gravity compensation. The actuator for the γ axis is not influenced by gravitational forces, as the axis is vertical. Therefore, a more compact drive train without damper was chosen for axis γ . All axes are actuated by a DC motor combined with a planetary gearhead with a reduction ratio of 51:1. For the base rotation axis γ , the DC motor drives a tooth belt connected to the robot housing. A mechanical break-out mechanism ensures that the maximum torque in the γ direction is limited to a safe value of 11 Nm. For the other two axes, the DC motor is placed in series with a rotational damper (Kinetrol S-CRD, Kinetrol, Farnham, UK). The use of a rotational damper ensures that the torque is limited due to the maximum speed of the motor and ensuring an intrinsically safe situation. A disadvantage of using a damper is the need for continuous motor rotation to provide a constant force. However, in the ATD system, the majority of the constant force is already provided passively by the parallel spring. Thus the motor damper combination only needs to provide small offset forces.

The combination of passive and active actuation ensures that the required motor power is relatively low as the majority of the gravity compensation is provided by the clock spring. This ensures that the system has a low power consumption and can be connected to a standard mains connection. Furthermore, the system is inherently safe since control errors or controller instability can never lead to large force fluctuations or a risk of hyper-flexion of patient joints. Also the ATD does not depend on an available mains supply to hold its vertical position, preventing the collapse of the robotic manipulator with the patient attached in the case of unexpected power loss.

A six Degree-Of-Freedom (DOF) force sensor (JR3 20E12 100N, JR3, Woodland, CA, USA) and three absolute angular encoders, together with a kinematic model of the actuator allows the measurement of the interaction force vector between the ATD and the subject and also the position vector of the end point position. A passive gimbal is located between the endpoint of l_2 and the arm cuff. The gimbal is equipped with potentiometers to measure the angles and allow for estimation of the hand and elbow orientation.

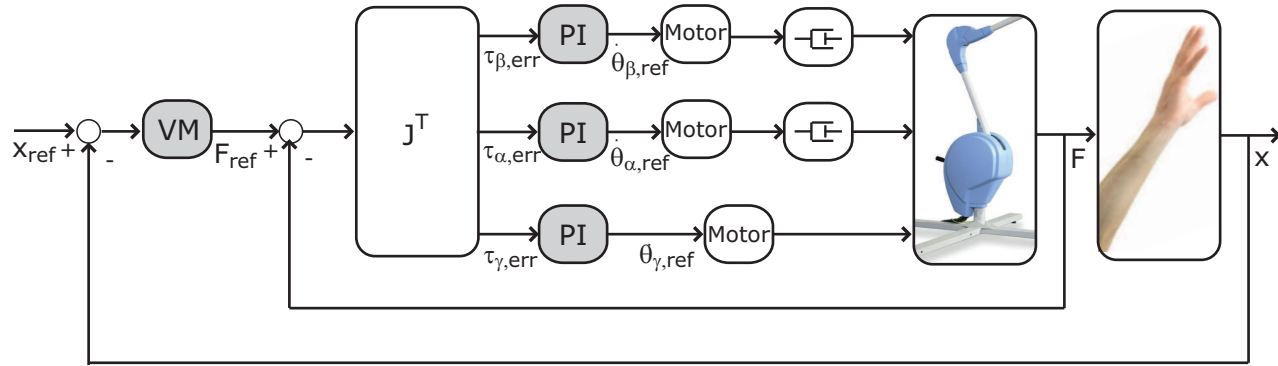


Figure 5.4: Schematic overview of control structure. VM indicates the virtual model used to calculate the reference force. This model consists of stiffness, damping and offset force: $F_{ref} = (bs + k)(x_{ref} - x) + F_{offset}$

5.2.3 Electronic design

The ATD is controlled by means of an embedded computer. In this computer an embedded safety software layer is implemented to check whether values are within acceptable bounds and ensure that possible errors in control do not lead to unacceptably large actuation forces. On top of this embedded software layer, custom controllers can be implemented in Matlab/Simulink (The Mathworks, Natick, USA) and uploaded to the embedded computer system for real time control. In this Matlab/Simulink layer desired variables can be selected for logging, for instance the number of movements, the interval between movements, the quality of a movement (deviation from an ideal path) and the amount of support during a movement. This allows for feedback to patient and physician during and after a training session. Patient feedback is an important motivator during training (Timmermans et al. 2010), while the feedback for the physician allows evaluation of the training performance and on the longer term evaluation of the training effect.

5.3 Controller design

The control scheme is shown in figure 5.4. Two feedback loops are implemented. The inner force control loop is initially used to compensate for small imperfections in the passive gravity compensation (see also figure 5.3). The offset force term (F_{offset}) can be used to compensate pre-measured gravitational forces. In the outer feedback loop, the deviation from a set point trajectory (x_{ref}) is used to implement an impedance controller with a virtual spring-damper system ($bs + k$), leading to a set point force (F_{ref}).

Based on the calculated reference force (F_{ref}) and the measured forces (F) the force errors are calculated and subsequently transformed into joint torque errors ($\tau_{[\alpha,\beta,\gamma],err}$) with the transpose of the Jacobian matrix. As the actuation for the base (γ) is different from the other axes (α , β), this angle is controlled differently. For axes α and β the joint torque errors are used to calculate the desired motor speed ($\dot{\theta}_{([\alpha,\beta],ref)}$), which is proportional to a joint torque as the motors are coupled through a rotational damper, as explained in Section 5.2.2. PI controllers are used to control the speed of the motors. For γ , an inner force control loop is created with PI control of the motor speed ($\dot{\theta}_{(\gamma,ref)}$) based on the determined torque error.

5.3.1 Controller tuning

The torque controllers for the three axes were individually tuned. For this purpose, the endpoint of the robot with the force sensor was fixed to the world in the middle of the work range and the frequency response functions (FRF) for the device were estimated (H_{device}). To estimate H_{device} , a multisine perturbation was applied to one motor directly ($\dot{\theta}_{([\alpha,\beta,\gamma],ref)}$), while the controllers were disconnected and the reference for the other motors was zero.

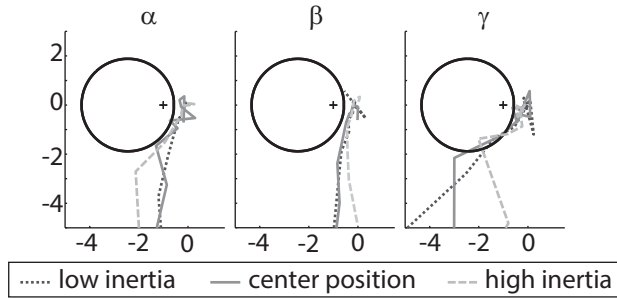


Figure 5.5: Open loop Nyquist diagrams for axes α , β and γ . The open loop response was estimated in the center position (green), with the device in the configurations with the lowest inertia (blue) and highest inertia (red). The black circles denote the $M = 1.3$ M-circle. The black cross denotes the $[-1, 0]$ point in the Nyquist diagram.

Control parameters were set based on the open loop frequency response function (FRF) of each axis. The loop gain for each axis is determined by:

$$H_{loop} = \left(K_p + \frac{K_i}{s} \right) H_{device} \quad (5.1)$$

in which K_p and K_i are the proportional and integral gains of the controller respectively and H_{device} is the transfer function of the device for that specific axis.

The values for the control parameters were set using Nyquist diagrams and M-circles, see figure 5.5 (Maciejowski 1989; Schouten et al. 2006). Briefly, the M-circle denotes a stability margin, where a specific value for M indicates a constant closed-loop gain. When the dynamical open loop response of the system is obtained, theoretical values for the controller can be calculated iteratively such that the closed loop system remains stable. These control values are then applied to ensure the closed loop response of the true system indeed lies outside the selected M-circle. In our case we selected $M=1.3$, which indicates that the highest gain of the closed loop behaviour is 1.3. Bandwidths of the individual axes were determined at 3.7Hz , 6.4Hz and 2.4Hz for axes α , β and γ respectively.

5.4 Performance

5.4.1 Force controller

To evaluate the bandwidth of the force controller, a multisine signal was applied as an offset force (F_{offset}) while the device was fixed to the world. The bandwidth of the system is determined as the -3 dB point in the frequency response function $\frac{F}{F_{ref}}$ obtained from this measurement. The obtained frequency response functions are shown in figure 5.6. The bandwidth was estimated to be 7.0 Hz , 6.1 Hz and 2.3 Hz for F_x , F_y and F_z respectively.

To evaluate the response speed of the ATD, the responses to step force inputs were measured. From these step responses the settling times were calculated for

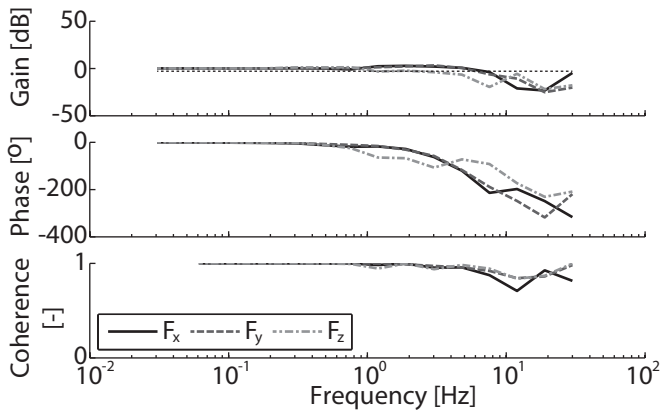


Figure 5.6: Frequency response functions for the force controllers along axes x , y and z . The force control bandwidth was estimated as the frequency where the gain crosses the -3dB line (dotted line). The top pane shows the gain of the frequency response function and the phase is shown in the middle pane. The coherence is shown in the bottom pane.

each direction. In figure 5.7, the responses to step inputs of 1 N , 5 N , 10 N and 15 N are shown. Average settling times were determined at 0.24 s , 0.18 s and 0.40 s for F_x , F_y and F_z respectively.

To evaluate the force tracking accuracy and whether the force directions are properly decoupled, sinusoidal reference force trajectories were applied. RMS errors between the reference and actual trajectories were determined as a measure of performance. Figure 5.8, shows reference and measured forces for all three axis during the sine tracking experiment. RMS errors were estimated at 0.74 N , 0.35 N and 1.47 N for F_x , F_y and F_z respectively.

5.4.2 Position controller

To evaluate the bandwidth of the position controller, a multisine signal was applied as a position perturbation while the reference was set at a fixed (neutral) position. The bandwidth was estimated to be 2.1 Hz , 3.9 Hz and 2.1 Hz for x , y and z respectively.

End point stiffness of the device was evaluated by using a fixed reference position. The device was moved manually away from its reference position while forces and positions are recorded. The measured stiffness was compared to the value of the virtual stiffness, k , which was set in the controller. During the measurement the robot's end point was manually moved.

Figure 5.9 shows the measured and theoretical stiffness values for x , y and z directions during trials with different settings for the position controller. The slope of measured and theoretical lines are similar. Note that the ATD can apply a limited amount of force (also to ensure safety), which causes the saturation effects in the graphs.

Another important observation from figure 5.9 is that the system has little force

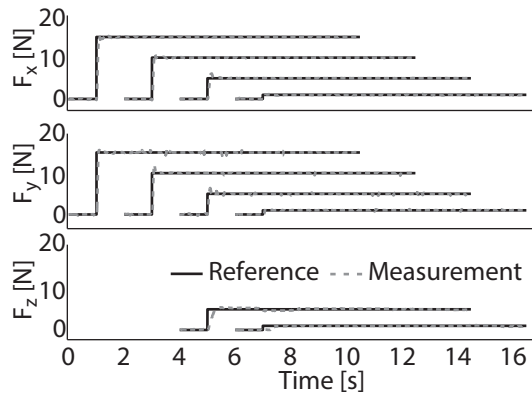


Figure 5.7: Responses to step force inputs for X (top), Y (middle) and Z (bottom). Reference forces are shown in black. Blue lines show the measured response. Step inputs of 1 N, 5 N, 10 N and 15 N were applied. The 10 N and 15 N step were omitted for the Z axis, as these are outside the force range of the Z-axis.

5

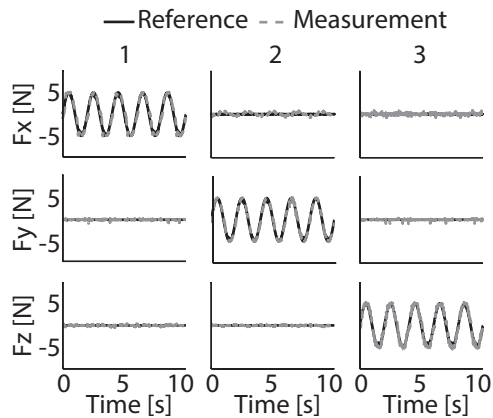


Figure 5.8: Tracking of sinusoidal reference forces. In each trial (1, 2 and 3) the reference for a single axis was a 0.5 Hz sine with an amplitude of 5 N, reference forces for the other two axes were zero. Panes in the same column belong to the same trial, thus indicating the induced errors based on a perturbation of one of the other axes. Reference forces are shown in black, measured forces in blue.

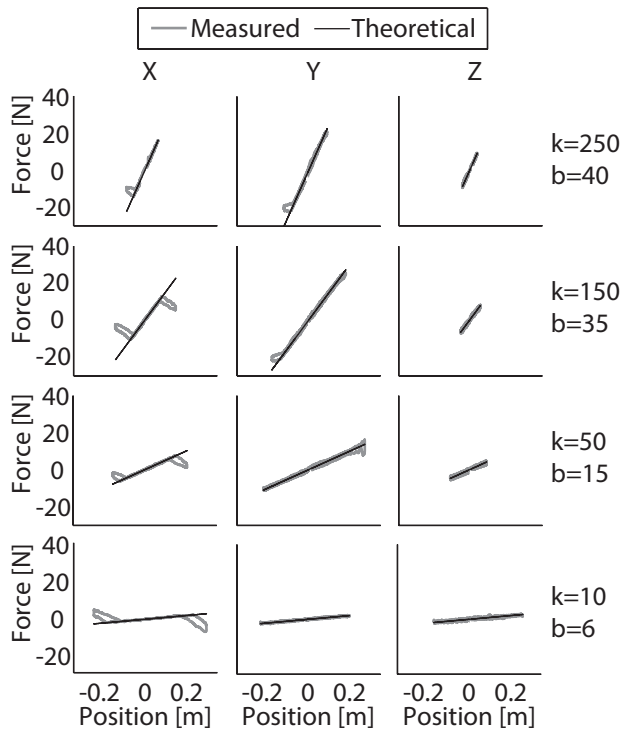


Figure 5.9: Measured stiffness compared with stiffness set in the position controller. Blue lines show the measured stiffness. The black line indicates the theoretical stiffness.

hysteresis. Any hysteresis present induces non-linear behavior of the system and reduces performance. In practice this will cause non-continuous force assistance to a patient when the movement direction of an axis inverts during motion. If the assistive force fluctuates, this may be mistaken for a patient induced deviation from the ideal reference trajectory and will cloud the measurement results.

The hysteresis present in the system was calculated from the measurements shown in figure 5.9. The average hysteresis for the different stiffness settings was estimated at 0.6 N , 1.4 N and 1.6 N for x , y and z respectively.

To evaluate the performance of the position controller, a mass comparable to the weight of a nominal arm (2.3 Kg) was attached to the endpoint of the robot. Passive gravity support was adjusted to compensate for the added weight. Circular reference trajectories were applied to move the weight along a circle in the horizontal plane ($k = 150\text{ N/m}$, $b = 35\text{ Ns/m}$). The results are shown in figure 5.10. RMS errors between the reference and actual trajectories were estimated at 13.1 mm , 2.1 mm and 4.0 mm for x , y and z direction respectively for the circular movement duration of 10 seconds (0.6 rad/s) and at 5.8 mm , 0.86 mm and 3.1 mm for x , y and z direction respectively for the circular movement duration of 20 seconds (0.3 rad/s).

5.4.3 Evaluation in possible application

To evaluate the ability of the device to assist patients, a single case study was performed with a male stroke subject (62 years old) with minimal voluntary arm function (Action Research Arm Test score of 3 points). The stroke subject was

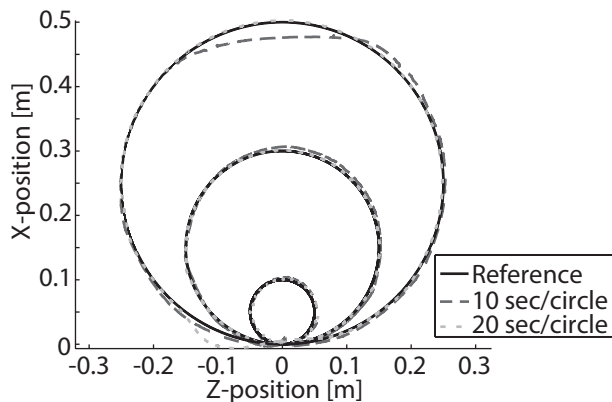


Figure 5.10: Example of position tracking with a circular reference trajectory while moving a 2.3kg weight along a circular reference trajectory with $k = 150\text{ N/m}$ and $b = 35\text{ Ns/m}$. Reference trajectories were set at either 10 seconds per circle or 20 seconds per circle. Three distinct circle diameters were used as reference: 0.1m , 0.3m and 0.5 . For each diameter/speed combination, the averaged resulting movement of five repetitions is shown. Reference positions are shown in black. The colored lines show the measured positions for the different combinations. All starting positions were set at $[0,0]$ for comparison.

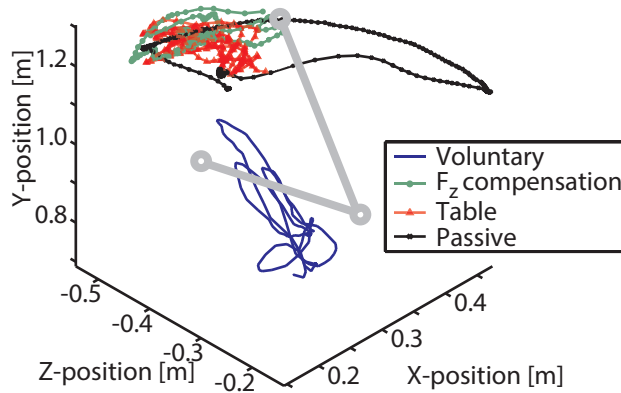


Figure 5.11: Result of circle drawing tasks of the single stroke subject. Results are shown for the following conditions: 1) without support of the device (blue); 2) with gravity support provided by the device (green with dots); 3) with a virtual table pushing the arm upward (red with triangles); and 4) Passive movement pulling the arm towards a circular trajectory with $k = 100\text{N/m}$ and $b = 22\text{Ns/m}$ (black with crosses). The gray circles indicate shoulder, elbow and hand positions. The bars between the circles represent upper and lower arm of the subject.

5

asked to make a circular movement with his hand in the horizontal plane using visual feedback under each of the following conditions: 1) without support of the device, 2) with gravity support provided by the device, 3) with a virtual table pushing the arm upward when moved below a certain position threshold and 4) passively, with the device moving along a circular reference trajectory ($k = 100\text{N/m}$, $b = 22\text{Ns/m}$). For conditions 2, 3 and 4, the weight of the arm was measured beforehand and used as offset force in y -direction.

Figure 5.11 shows the results for all four conditions. Support of arm weight has a clear beneficial effect as the patient is then able to maintain the arm around shoulder level (compare the blue line (voluntary movement) in figure 5.11 with the other lines). Gravity support only (green line with dots) and combined with a virtual table (red line with triangles) gave similar results. The movement range was extended when the robot provides additional movement assistance during the passive condition (black line with crosses).

5.5 Discussion

In this paper we presented and evaluated a novel three dimensional end-point manipulator for use in functional training of reaching tasks after stroke. The system is aimed at assisting patients during functional upper extremity exercises. The system is lightweight (25 kg) and easy to operate by a non-expert, which leads to the potential of making the final step to clinical or even home use.

During the passive movement condition the reference trajectory was a large circle in the horizontal plane. However, the patient's arm did not follow this trajectory and the actual circular path was much smaller than the reference path. This resulted from a combination of imperfect gravity compensation and limited motor power. This led to a saturation of the motor, as this motor was already used partially for compensation of gravitational forces. As mentioned before this can be overcome by implementing a passive spring with a higher stiffness for providing passive gravity compensation around the α axis, which would then also improve the provided assistance.

5.5.1 Comparable systems

Our objective was to develop a device which fills the gap between passive devices and high-end devices. Therefore there are no directly comparable systems. However, we can compare the system presented here to the other (high-end) active devices as shown in figure 5.1, since in theory these devices could provide the same assistance as the ATD system. The ATD system has much lower assistive force capability ($\sim 15\text{ N}$) compared to the Armeo Power ($\sim 75\text{ N}$) and the Haptic Master ($\sim 100\text{ N}$). Also the bandwidth of the ATD's position controller (1.4 Hz) is lower than the bandwidth of the Armeo Power (2.1 Hz) and the Haptic Master ($> 10\text{ Hz}$).

Currently, stiffness values of up to 250 N/m can accurately be rendered with impedance control, which is low compared to the Armeo Power ($> 714\text{ N/m}$) and the Haptic Master (up to 50 kN/m). However, for guidance of movement 250 N/m will be sufficient. Further reducing the stiffness of the position controller can be used to allow the user to deviate more easily from the reference trajectory, which is helpful for rehabilitation purposes.

Although, the ATD system has lower force capability, lower endpoint stiffness and lower bandwidth compared to Armeo Power and Haptic Master, this will not be a limitation when the system is applied for low frequent functional tasks (e.g. reaching movements). Moreover, the ATD system is more compact and has much lower weight ($\sim 25\text{ kg}$) than both the Armeo Power ($> 200\text{ kg}$) and the Haptic Master ($\sim 40\text{ kg}$). This gives the current system the benefit of being more easy to handle, move and transport. Together with the low force capability and inherent safety due to the dampers in the drive train, this makes the ATD perfectly suited for functional training in a home environment.

5.5.2 Clinical implications

The device has two main rehabilitation applications. These can be deployed depending on the ability of individual patients, possibly in a home environment enabling frequent training. The first application is compensation of gravitational forces. Gravity compensation had been shown beneficial for rehabilitation of stroke patients (Beer et al. 2007; Krabben et al. 2012; Prange et al. 2012). Literature reports increased work range due to reduced flexion couplings when compensating for gravitational forces. When patients improve, gravity compensation can be reduced to keep the training challenging.

A second application is the active assistance of motion. When patients have difficulties in reaching the arm towards an object, the device can assist them in reaching the object with the trajectory guidance mode. When patients improve, the assistance can be reduced again. For rehabilitation purposes the virtual stiffness and damping parameters can be used as tuning parameters to make the robot either stiff or compliant, depending on the amount of assistance the subjects needs during the movement. With such an approach, therapy can be both motivating (patients can reach the targets) and challenging (patients should provide sufficient effort to get to the target).

To assist reaching towards objects in a training environment a minimum jerk reference trajectory (Shadmehr and Wise 2005) towards a predefined object position is currently implemented. In addition, circular reference trajectories are implemented, allowing for assistance during circle drawing tasks (Krabben et al. 2011; Sukal et al. 2007). However, the interface also allows for defining custom reference trajectories.

The benefit of both the gravity support and active assistance have been shown in a single case study with a stroke subject with minimal arm function (ARA test score of 3 points). In figure 5.11, differences in movement can be observed between the patient's moving voluntarily without any assistance and moving with support of his arm weight by the ATD. With support of arm weight the patient is capable of lifting the arm at shoulder level. Since the patient had minimal arm function, the size of the movement with compensation was still very minimal. When active assistance was added, the movement size became much larger, indicating the training potential of the device.

However, there was no noticeable difference between compensation of gravity only and the condition with a virtual table surface. This is likely the result of the minimal voluntary function of the patient. We expect that patient's with more voluntary arm function can benefit from the virtual table, by using this feature to get more elbow extension due to the synergies often occurring after stroke (Beer et al. 2007). Additional clinical tests are required to verify this.

5.5.3 Limitations

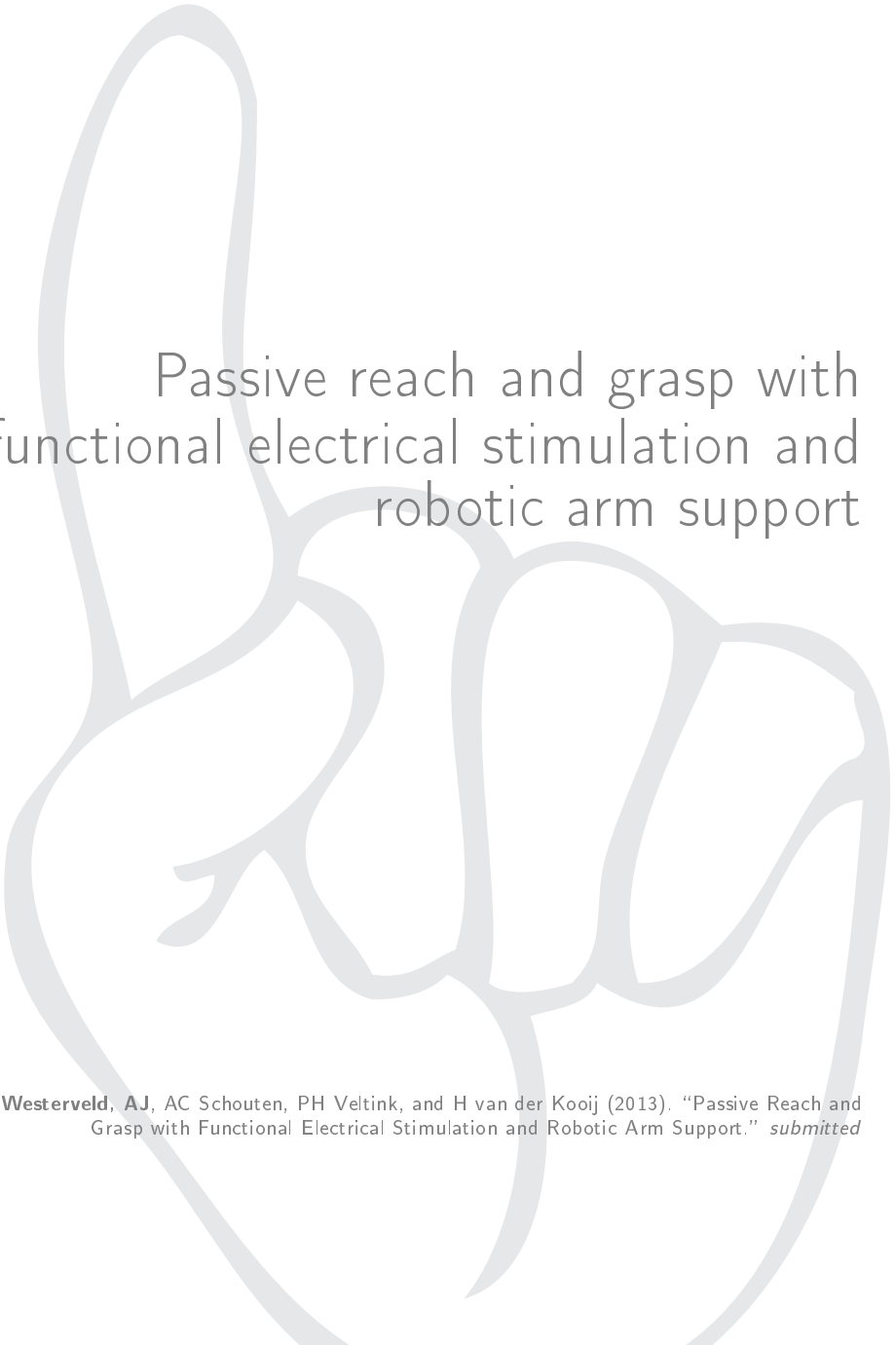
The current design is a first iteration in developing a compact low-power assistive end-point manipulator. The performance was already shown sufficient for assisting functional reaching movements. However, there are some small points which

could easily improve the performance even further. Currently, the γ axis has the worst performance and is therefore the bottleneck. The lower performance mainly resulted from conservative rules to limit the motor speed and torque output on this axis to prevent enabling of the mechanical break out system. This also resulted in a slower response and a lower force bandwidth in the z-direction ($2.3Hz$) compared to the x- and y-direction ($7.0 Hz$ and $6.1 Hz$ respectively). This bandwidth will be sufficient for low frequent, relatively slow movements (e.g. reaching tasks), however with some minor modifications to the design (stronger motor or also use a damper driven solution for γ axis) the potential of the device could be increased even further.

In addition the imperfections in gravity compensation in relation to movement along the x-axis are higher than expected. This results in higher requirements for the motor (α) to eliminate these imperfections. This limits the force range in certain positions and could be overcome by the use of a spring with higher stiffness for the passive gravity compensation around the α -axis, which will be implemented in a follow up design.

5.6 Conclusion

The novel system presented here we are able to fill the gap between high power assistive devices and the passive devices. With its capability of providing both compensation of gravitational forces and assistance during functional tasks, the ATD system is a great assistive tool during the rehabilitation process. Due to the inherent safety, low weight and compactness of the system, intensive functional task training becomes available, potentially even in a home environment.



Passive reach and grasp with functional electrical stimulation and robotic arm support

Westerveld, AJ, AC Schouten, PH Veltink, and H van der Kooij (2013). "Passive Reach and Grasp with Functional Electrical Stimulation and Robotic Arm Support." *submitted*

Abstract

Rehabilitation of both arm and hand function is an important aspect for increasing functional independence of stroke subjects. Robotics and functional electrical stimulation (FES) can support reach and grasp and aid rehabilitation. The aim of this study is to demonstrate the technical feasibility of an integrated device combining robotics and FES for functional manipulation of objects.

To support grasp and release, FES was applied using Model Predictive Control (MPC) to control joint angles of thumb and fingers. In addition, reach support was provided by a novel 3D robotic manipulator. The system's performance was evaluated in both stroke and blindfolded healthy subjects, where the subject's passive arm and hand made functional reach, grasp, move and release movements while interacting while manipulating objects of different sizes.

The success rate of complete functional grasp, move and release movements with different objects ranged from 33% to 87% in healthy subjects. In severe chronic stroke subjects only partial trials were completed successfully. In healthy subjects, overall success rates for the subtasks reach, hand opening, grasping, holding, positioning and releasing the object were 89%, 96%, 96%, 98%, 76% and 100% respectively.

We demonstrated that our developed integrated training system can move the passive arm and hand for functional pick and place movements. In the current setup, the positioning accuracy of the robot with respect to the object position was critical for the overall performance and could be improved by the use of a higher virtual stiffness and by including feedback of object position in the robot control. The system has potential for post-stroke rehabilitation, where support could be reduced based on patient performance which is needed to aid motor relearning of reach, grasp and release.

6.1 Introduction

Stroke survivors often have a diminished arm and hand function, which reduces their ability to interact with objects. In many activities of daily living, like drinking or opening a door, human-object interaction is essential. Therefore rehabilitation of both arm and hand function is an important aspect for increasing functional independence of stroke subjects. Being able to grasp and release without the ability to reach, or being able to reach without the ability to grasp and release, does not lead to a functional movement. From a functional point of view, combining reach support with grasp and release training in a single rehabilitation solution would be desirable.

In the past decades robotic technology has emerged to aid the rehabilitation process of stroke subjects. Robots are particularly useful for support of repetitive tasks with high repeatability and without the need for continuous presence of a therapist. Many robotic systems capable of supporting or training the arm during reach have been developed and evaluated (Loureiro et al. 2011). Some robotic systems targeted at hand support have been developed (Worsnopp et al. 2007; Dovat et al. 2008). However, high complexity is needed to properly actuate the hand with external mechanics. Therefore hand robotics is currently not very applicable for functional movement training, i.e. integrated with arm movement, especially not in a home environment which could be the future of automated rehabilitation systems allow intensive training.

Besides therapeutic robotics also functional electrical stimulation (FES) is being used to restore hand function in stroke survivors. FES of finger and thumb muscles can be beneficial for stroke subjects in relearning functional grasp and release movements (Micera et al. 2010). FES has been used successful for both neuroprosthetic (Sheffler and Chae 2007; Snoek et al. 2000) and therapeutic systems (Powell et al. 1999; Rosewilliam et al. 2012; de Kroon et al. 2002; Barsi et al. 2008; Malhotra et al. 2012). However, current commercially available systems use an open loop approach, which limits performance and requires continuous user input (Lynch and Popovic 2008). Also FES control needs a personalized approach due to the high variability between subjects (chapter 2).

To increase training independence, an approach for training without the need for a therapist being continuously present is preferred. Recently, we have developed a Model Predictive Control (MPC) approach to selectively control fingers and thumb for grasp and release with FES (chapter 4). The strength of this approach is the use of a personalized model relating the stimulation level to the resulting movement. In addition, this method has potential for application in an automated system allowing for therapist-independent training.

The overall goal of our research is to develop an integrated post-stroke training environment for home use by a combination of robotic arm support and FES support of grasp and release. For relearning after stroke a high level of patient involvement is required (Reinkensmeyer et al. 2009), therefore a training system should focus on reducing support based on the ability of the individual patient (Freeman et al. 2009; Wolbrecht et al. 2008). However, as a first step, we will focus on full

Table 6.1: Properties of participating subjects

	S1	S2	H1	H2
Age	62	67	25	28
Sex	M	M	M	M
Hand	R	R	R	R
ARAT	3	11	n/a	n/a
Months +stroke	160	112	n/a	n/a

support of movement (in which the subject is passive) in healthy subjects and chronic stroke subjects. The aim of this paper is to demonstrate the feasibility of a combined robotics-FES rehabilitation system for full support of functional object manipulation tasks. Full support will be the most challenging from a technical point of view and is therefore evaluated here.

6.2 Materials and Methods

6.2.1 Subjects

Two stroke subjects (S1-S2) and two healthy subjects (H1-H2) participated in this study. The affected side for the stroke subjects and the dominant side for the healthy subjects was supported. Subject characteristics are shown in table 6.1. The study was approved by the local ethics committee and all subjects signed written informed consent.

6.2.2 Experimental setup

Robotic device for reach support

A custom-built robotic device was recently developed (Demcon, Enschede, The Netherlands) (Chapter 5). This device (see figure 5.2) is a 3D end effector which can both compensate gravitational forces of the arm and manipulate the arm in space. The device has two key features. Firstly, it compensates gravitational forces passively and secondly, it provides active guidance with damper based drive trains, which makes the device inherently safe by the use of low power motors and decoupling of the motors and the load. In addition to these key features, the device is compact, has low weight and allows for fast donning and doffing.

The device can apply forces to the subject's arm using three active and three passive degrees of freedom. A spring is mounted parallel to the actuator of the β axis (see figure 5.2). The pretension of this spring can be adjusted in order to passively compensate for the weight of the subject's arm. All actuators are mounted in the base. Rotation of the base and rotation of links l_1 and l_2 (see figure 5.2) are actuated. At the end point a passive gimbal is mounted between the linkage and the arm cuff, which allows for arm rotations relative to the linkage. A six degrees of freedom force sensor mounted at the end of the linkage measures the interaction forces between the arm and the linkage. With the encoders on the

active axes and potentiometers on the passive gimbal the arm and hand positions are calculated.

The robot's embedded computer (Bachmann electronic GmbH, Feldkirch, Austria) received reference force setpoints from an xPC target computer (The Mathworks, Natick, USA) through analog communication channels.

MPC and FES to support grasp and release

We recently developed a model predictive controller (MPC) for electrical stimulation of finger muscles to facilitate grasp and release, described in details in (chapter 4). The same method was applied in the current study for control of hand opening and closing and is briefly described below.

An overview of the FES controller is shown in figure 6.3. The obtained system model was used by the MPC (Camacho and Bordons Alba 2004) to calculate the optimal stimulation amplitudes in order to reach the reference finger angles.

Two custom-built electrical stimulators (TIC Medizin, Dorsten, Germany) each having three independent stimulation channels were used to stimulate finger and thumb muscles. Three stimulator channels were used for targeting thumb muscles (abductor pollicis longus, opponens Pollicis and Flexor pollicis brevis), the other three channels were used through a multiplexer for targeting both the flexor digitorum superficialis muscle with three electrodes and the extensor digitorum communis electrodes muscle with three electrodes. During grasp tasks the flexor electrodes were activated and during release tasks the extensor electrodes were activated. Thus, in total nine stimulating electrodes were placed. The flexor and extensor muscles were placed at positions evoking selective movement of individual fingers to allow for more selective finger control. As the ring and little finger were less selective and often respond simultaneously, they were targeted with a single electrode. See figure 6.1 for an example of the electrode placement.

A VisualEyz (Phoenix Technologies, Burnaby, Canada) motion capture system was used to track positions of active LED markers on hand and fingers. Marker placement is shown schematically in figure 6.2. Three markers were based on the back of the hand to represent the hand coordinate frame. In addition, two markers were placed on the proximal phalanges of each finger. From these markers metacarpophalangeal (MCP) joint angles were calculated. For the thumb angles in the plane of the coordinate frame (flexion/extension) and perpendicular to the coordinate frame (abduction/adduction) were calculated.

The measured marker motions were sent to the xPC target computer. The MPC system was implemented on this computer using the marker motions to calculate finger angles and control the fingers towards reference angles. Together with the generation of set point forces for the robotic manipulator, the xPC target computer thereby provided synchronous control of reach, grasp and release.

6.2.3 Experimental protocol

Initially, the electrodes were placed on the target muscles, based on visual inspection of the evoked responses. In addition, maximum stimulation amplitudes were

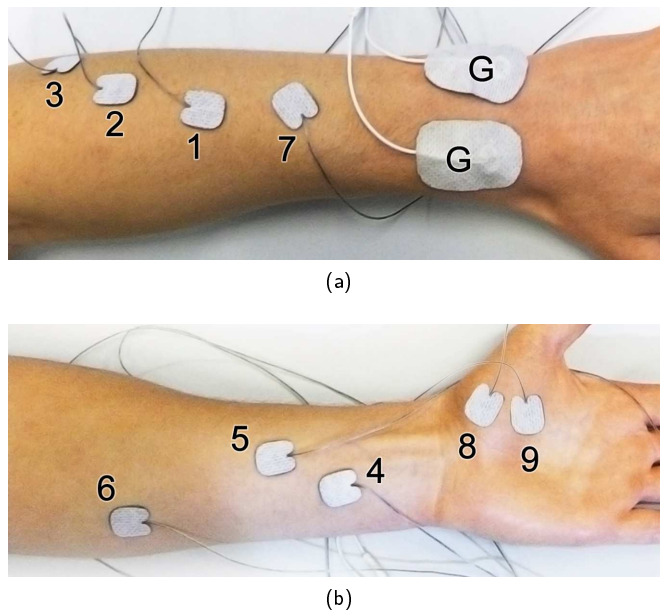


Figure 6.1: Overview of electrode placement on the dorsal (a) and palmar side (b) of the arm and hand. Electrodes are placed above the finger extensors (1..3), finger flexors (4..6), abductor pollicis longus (7), opponens pollicis (8) and the flexor pollicis brevis (9). Two ground electrodes (G) were used for each of the two stimulator devices.

6

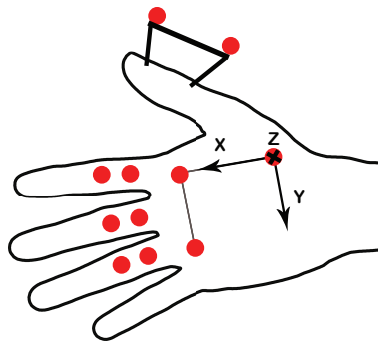


Figure 6.2: Schematic representation of placement of motion tracking markers on the back of the subject's hand (chapter 4).

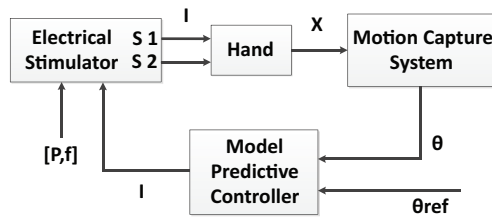


Figure 6.3: FES control system. A MPC approach is used to control the finger movement, which is measured by an optical motion capture system

determined for all electrodes. The maximum was determined by occurrence of one of the following three events: subject discomfort, crosstalk to other muscles or saturation of response, which was in general the first event to occur. When all electrode positions were determined, the arm was fixed in the cuff of the robotic manipulator and the passive weight compensation was adjusted for the subject's arm weight.

Subsequently, an initialization procedure was started to obtain a subject specific model relating the input stimulation amplitude to the resulting finger movement. During this procedure each electrode was activated with random stimulation amplitudes up to the determined maximum while the subject was relaxed. The robot was in a fixed position slightly above the table in front of the subject. This position was later used as a starting position for the functional movements.

The Action Research Arm Test (ARAT) was used as a test bed for passive grasp and release movements. Four objects of the ARAT (the wooden ball ($\varnothing 7.5$ cm) and three cubes: 2.5 cm, 5 cm and 7.5 cm) were selected to evaluate the system with objects of different weight, size and shape. The respective weights of the objects were 0.14 kg, 0.01 kg, 0.09 kg and 0.3 kg, for the ball and the cubes ordered by increasing size. Coordinates representing three positions were pre-programmed into the robot: A) a starting position, B) an object position on the table in front of the subject where the ARAT objects were initially placed, and C) an object target position where the objects had to be moved to.

A minimum jerk trajectory generator was implemented to create reference trajectories to move between two defined positions with a predefined duration. A fixed virtual stiffness of 100 N/m was implemented to let the force controlled robot guide the arm towards the reference trajectory based on the measured position.

Task specification

During the tasks the subjects were asked to relax. The healthy subjects were blindfolded to prevent them from knowing which object they had to grasp and where. Thereby voluntary movement interference was prevented. Tasks were repeated five times for each object for both fast movement (5.5 seconds in total) and slow movement (24 seconds in total). The movement was divided in six subtasks:

1. move from the start position to the object

2. open the hand for grasp
3. close the hand while holding the robot in position
4. move and hold the object
5. position the hand for release, and
6. release the object.

First the robot was set to keep the arm in the starting position. Next, the robot and MPC were set to follow reference trajectories according to the described subtasks. Subtasks 1 and 2 overlapped in time to increase smoothness of movement. After object release the hand was moved back to the starting position to be ready for the next trial. When the object was grasped successfully and released at the target position, the trial was marked successful. Otherwise, the subtask on which the movement failed was logged. When the robot had returned to the starting position, the operator placed the next object at the object position and removed the previous one.

6.2.4 Recordings and data analysis

The primary outcome measure was the success of the functional object manipulation task. Success rates for the different objects were logged for all subjects. In addition the success rates for the subtasks were logged. Trials were aborted when a subtask failed, therefore the number of evaluated trials per subtask depends on the success of all preceding subtasks.

Interaction kinetics was a secondary outcome measure. Kinetic data obtained from the robot's force sensor was used to estimate voluntary interference by the subject. In addition, kinematic patterns of hand position were obtained from the robot's sensors and finger joint angles were obtained from the motion capture data. The performance in tracking the hand and finger reference trajectories was evaluated.

As the robot operates in closed loop and the interaction force depends on both the subject and the robot, we cannot directly separate the amount of force provided by the robot and the user. Therefore, we assessed the energy balance of the interaction between the subject and the robot by integrating the product of force and velocity over time, thus estimating work done between both systems. As the start and the end positions of the movement are the same and at rest, the total kinetic and potential energy changes are zero, thus the work done should be zero if the combination of robot and subject behaved as a conservative system.

The MPC was evaluated by the success in grasp and release of the selected ARAT objects: wooden ball ($\varnothing 7.5\text{cm}$), small cube (2.5cm), middle sized cube (5 cm) and large cube (7.5 cm).

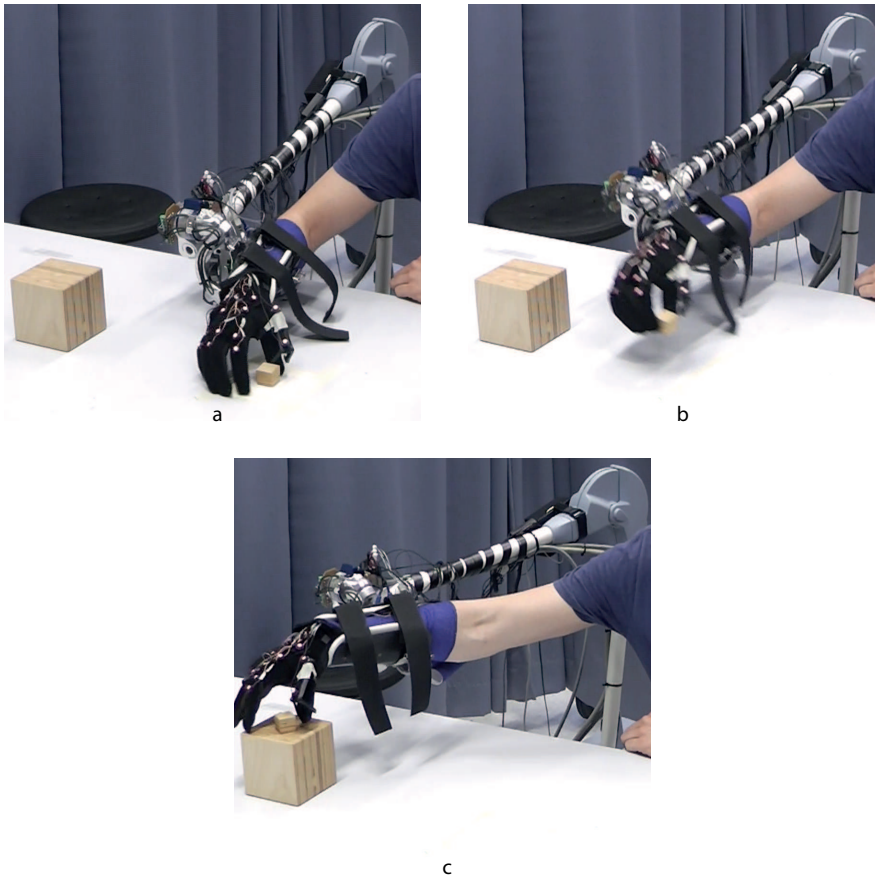


Figure 6.4: Example of the controlled movement in a healthy subject: a) reach to grasp, b) grasp and move and c) objects release.

6.3 Results

Examples of the different hand states (hand open, pinch grip and cylindrical grip) controlled with MPC are shown in figure 6.4. In addition the supplementary video¹ shows the system in action while successfully moving the arm of a passive subject and manipulating different objects.

6.3.1 Success rates

In table 6.2 the success rates of the full reach, grasp, move and release movement sequences with the different objects are shown. In the healthy subjects the majority of trails was finished successfully. In S1 the electrical stimulation was

¹Video available at <http://youtu.be/8w-AhHzpXs8>

Table 6.2: Success rates of complete object manipulation tasks

Object	S1	S2	H1	H2
2.5 cm cube	-	0%	75%	67%
5.0 cm cube	0%	0%	57%	87%
7.5 cm cube	-	-	33%	40%
Wooden ball	-	0%	75%	45%

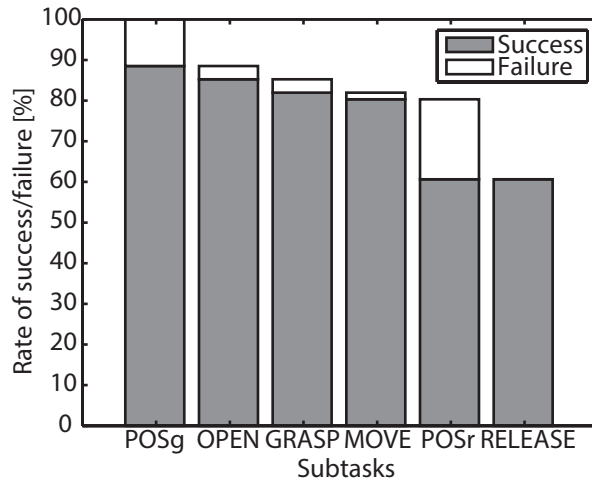
successful outside the robot, however when the arm was placed in the arm cuff of the robot, the finger flexors did not respond to the stimulation anymore, likely due to skin/electrode movement with respect to the muscle. Therefore when this observation was made the other objects were not evaluated to save time as this would not provide new information. In S2 the stimulation of grasp and release was relatively successful, however the middle finger had high tonus and did not extend sufficiently which caused pushing away of the larger objects. Therefore evaluation of the largest cube was omitted. For the small cube, reach was mainly successful but the grip was not firm enough to prevent slippage of the object.

As shown by table 6.2, the reach, grasp and release movements provided by the system were not always successful. To investigate the failures in more detail, figure 6.5 shows the successes and failures of all trials in healthy subjects and stroke subjects distributed over the different subtasks. In healthy and stroke subjects positioning of the robot had high failure rates. In the stroke subjects, hand opening was only successful in a few trials and none of the objects was successfully grasped. For the stroke subjects, no data was available for moving the object, positioning the hand for release and releasing the object, since all trials had failed before object movement could occur.

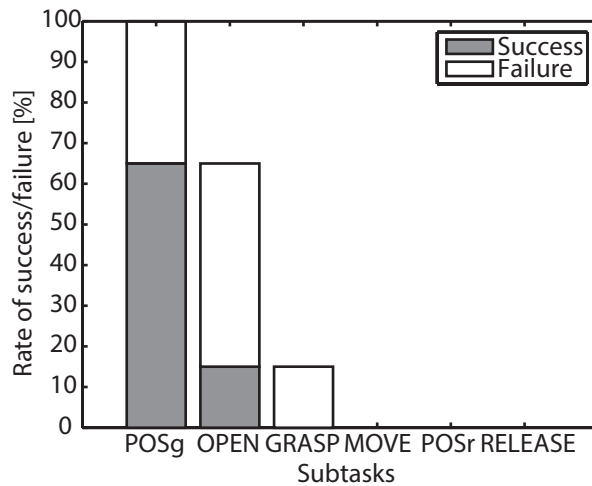
6

6.3.2 Tracking performance

Figure 6.6 shows time series of arm/hand movement and finger movement during multiple trials in subject H1 and S2. The performance of tracking the reference positions was evaluated separately for arm movement and finger movement. The arm position tracking RMS errors averaged over all trials was 69.6 ± 17.5 and 145.1 ± 27.8 for healthy subjects and stroke subjects respectively. Thus the positioning errors in stroke patients were about twice as large as in the healthy subjects. Steady state errors for opening the hand for grasp in healthy subjects were $14.6 \pm 11.0^\circ$, $18.8 \pm 16.2^\circ$ and $19.1 \pm 11.6^\circ$ for index, middle and ring finger respectively and $18.5 \pm 12.6^\circ$ and $21.4 \pm 14.4^\circ$ for thumb abduction and extension respectively. In the stroke subjects hand opening steady state errors were $32.5 \pm 9.1^\circ$, $25.5 \pm 7.7^\circ$ and $11.2 \pm 6.3^\circ$ for index, middle and ring finger respectively and $8.2 \pm 6.3^\circ$ and $6.9 \pm 3.6^\circ$ for thumb abduction and extension respectively. Angular errors of $\sim 20^\circ$ will lead to a displacement of $\sim 3\text{cm}$ at the finger tips, depending on the finger length.

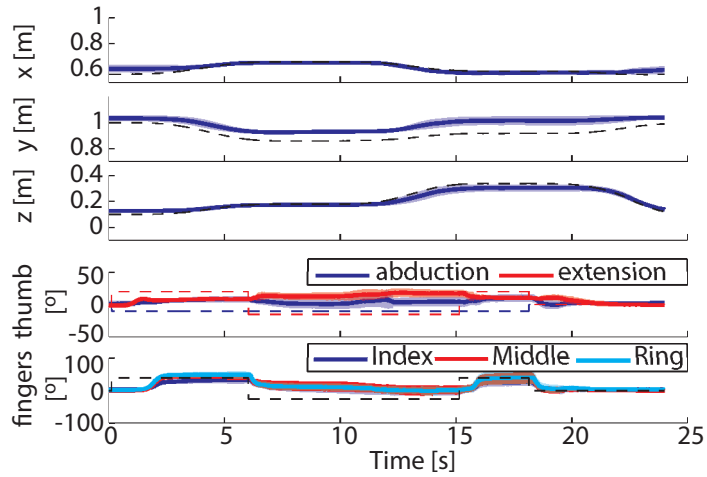


(a)

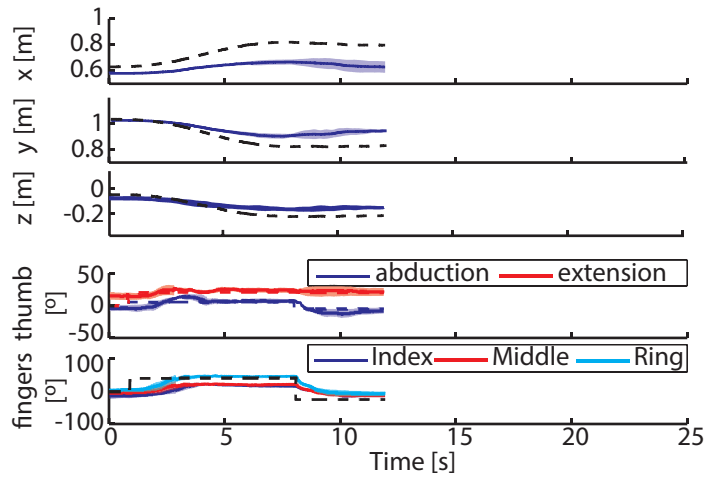


(b)

Figure 6.5: Causes of failure in healthy subjects (a) and stroke subjects (b). Bars indicate occurrences of successful trials (gray) and failures (white) for each of the following subtasks: positioning hand for grasping (POSg), opening hand for grasping (OPEN), grasping the object (GRASP), hold and move the object (HOLD), position the hand for object release at the target position (POSr) and release the object at the target position (RELEASE).



(a)



(b)

Figure 6.6: Measured arm/hand positions and finger angles (solid) compared to reference positions and angles (dashed) for trials with a 5cm cube for subjects H1 (top) and S2 (bottom). For S2 only the reach to grasp part is shown, trials were aborted due to ineffective grasp. Thumb and finger angles are reported relative to the subject's neutral position. Angles were defined zero when the subject relaxed his hand and stimulation was off.

6.3.3 Subject passiveness

For technical evaluation of the combined system of robotics and electrical stimulation, it is important to know the performance independent of any user interaction. Therefore, subjects were instructed to relax. In addition, the healthy subjects were blindfolded to remove information on object location and type. To check whether the subjects were indeed passive during the trials, the total work during each trail was calculated for the healthy subjects and corrected for the potential energy change due to the measured height difference at beginning and end of the trial. The average corrected work done by the robot on the user during the trial is $0.1 \pm 0.5J$ and $1.3 \pm 0.8J$ for subjects H1 and H2 respectively. These negligible values indicate that the combination of robot and subject behaved conservatively.

6.4 Discussion

Our aim was to show the feasibility of using a system combining robotics and functional electrical stimulation for functional tasks in which the subject was passive. From our results we can conclude that the current system was not applicable for (these) chronic stroke subjects, as we were unable to complete the tasks successfully. However, the combination of robotics and FES was shown technically feasible in healthy subjects. The high success rates in healthy subjects, together with the fact that the failure rate in stroke subjects was partially influenced by technical limitations, indicate the potential of the system for application in post stroke rehabilitation.

6.4.1 Technical limitations

Two technical limitations can be identified after evaluation of the current system: 1) a possible mismatch in programmed object locations and actual object locations and 2) interference of the robotic arm cuff with the electrical stimulation outcome.

In the current setup the object location was pre-programmed in the robot controller. Therefore performance was prone to small deviations in manual object placement or in robot movement. Currently the applied virtual stiffness was relatively low. An increased robot virtual stiffness might improve robot positioning. Currently, this virtual stiffness was limited by the noise level within the analog communication between the robot's embedded computer and the xPC target computer. Even with an increased stiffness, small errors in object repositioning could still lead to grasp failures, since objects were manually positioned at a marked position and the robot was calibrated to move to that same marked position. For future systems we suggest to incorporate active user involvement (desired in rehabilitation) in combination with intention detection to improve the positioning accuracy and reduce the number of failures. Additional feedback of object/target positions within the system could also lead to a reduction of positioning errors, as the user can then actively steer the system to the desired position.

In subject S1, the arm connection of the robot might have influenced the electrical stimulation responses. Currently, the cuff of the robot is attached over

the middle of the forearm. Thereby, it is placed over the electrodes and muscle bellies, which is likely to influence the stimulation responses. Redesign of the arm connection, such that it is attached only near the elbow and near the wrist, will remove the problem of interfering with the stimulation and is therefore suggested to increase outcome.

The healthy subjects were blindfolded to reduce the possibility of voluntary interaction. Since object positions were constant over trials, subjects might have learned the positions and could still have actively contributed to the movement based on their proprioception. However, the small values for the net work done by the robot during the trials are an indication that active user involvement is minimal during the trials.

6.4.2 Clinical implications

Fully supporting the reach, grasp and release movements will be a first step towards an integrated system for rehabilitation after stroke. To apply this system in the clinic or in a home environment, robot positioning and arm interface should be improved as described above. In addition, four important modifications are necessary before the system can have clinical merit: 1) donning and doffing time should be reduced, 2) a more mobile finger measurement system should be used, 3) support should be tailored to the ability of the individual patient instead of full support and 4) the user should be given control by detection of his/her intention. Suggestions for these modifications are discussed in the next paragraphs.

To reduce donning time, array electrodes (Popović-Bijelić et al. 2005; Kuhn et al. 2009; Malešević et al. 2012) could be included to automatically search for the best positions and possibly compensate for altered stimulation responses due to skin or nearby muscle movement. To reduce model initialization time, intelligent solutions are needed to start training early and improve the model during the training session. This could be achieved by a form of initial automated electrode testing (Malešević et al. 2012) and recursive model estimation (e.g. Moon et al. 2005). In addition, models obtained from previous sessions might be used as a starting point. Further research to find the optimal tradeoff between short model initialization time and high model accuracy is needed.

A VisualEyez optical motion system was used in the experiments reported in the current paper. This is perfectly suited for a laboratory setup, however for a clinical application such a system is not desired. For clinical application a more compact and more plug and play solution is needed. Measurement gloves (Williams et al. 2000; Simone and Kamper 2005; Veltink et al. 2009; Oess et al. 2012) or commercially available devices like Microsoft Kinect (Chang et al. 2011) or LEAP motion (Weichert et al. 2013) might be used as a more portable solution for feedback of finger angles.

Forcing a passive subject in a specific movement path without voluntary effort does not result in relearning of movement (Reinkensmeyer et al. 2009). To promote motor relearning, the amount of support should be based on patient performance such that the patient is maximally active and still able to complete the task (Wol-

brecht et al. 2008). Therefore iterative learning control (Freeman et al. 2009) or other assist-as-needed approaches (e.g. Wolbrecht et al. 2008) are necessary to use the current system successfully for rehabilitation.

For rehabilitation purposes, it is desired that the patient can control the movement (Huang and Krakauer 2009), therefore the system should be able to detect the patient's intention. The measured interaction force might be used for this purpose. Due to inertia in the system, measured interaction forces indicate intended movement by the user when the system itself is not moving. The system can be programmed to provide support either when a certain force threshold is exceeded or proportional to the measured force. Admittance control schemes have been applied for similar systems to let the system respond to a detected interaction force with movement based on a dynamic model (Spenko et al. 2006; Duchaine and Gosselin 2009; Huo et al. 2010). By changing parameters in the dynamic model, the support can be adjusted to a desired level while leaving the user in control of the movement.

With the mentioned further improvements, the current system has great potential for support of movement during post-stroke functional training. Due to the compactness of the system, future versions might also become applicable in a home environment, allowing for intensive therapy. However, as currently only passive movement was evaluated, the therapeutic effects need further investigation.

6.5 Conclusion

A combination of Model Predictive Control of FES and robotic arm support can be successful in supporting functional tasks. Currently, we have evaluated passive reach and grasp with the combined system. The approach was successful in complete functional reach, grasp and release of objects in only 37% of the trials. The main cause of failure was position mismatch between the robot and the object/target position. Based on high success rates of the subtasks we expect to improve performance even further by increasing the virtual stiffness of the robot and by closing the positioning loop, i.e. feedback of the exact object position to the robot. This could be achieved either by artificial measurement of object position or by allowing the user to steer the robot, which removes the need of preprogramming the positions.

For therapy after stroke, the current approach should be extended towards an assist-as-needed approach with user intention detection to maximize patient involvement. Benefits and feasibility of such an approach should be further investigated. However, since passive movement has been shown technically feasible, we are confident that reducing the support to engage the patients will be also feasible with the current system.



General discussion

Stroke is a major cause of morbidity in the western world. As life styles in less developed countries are changing, stroke spreads more throughout the entire world (Ovbiagele and Nguyen-Huynh 2011). The number of stroke survivors is likely to increase further due to graying of society and continuously improving health-care. Graying of society also leads to a reduced number of available caregivers. Thus, stroke not only has a huge impact on an individual's life, but also causes a large burden for the health care system due to the importance of intensive training to promote recovery.

Technological innovation could be a solution to reduce the stress on the health-care system. Conventional stroke therapy (Langhorne et al. 2009) focuses on training movement of the affected limb. The assistance of functional movement often applied by physical therapists might be partially taken over and intensified by an automated system. The role of a physiotherapist will then become more supervisory, which allows for simultaneous training of multiple patients or even training at home and thereby increased health-care efficiency. Effectiveness in post stroke rehabilitation is the subject of numerous studies in the fields of rehabilitation robotics (Lum et al. 2002; Prange et al. 2006; Krebs et al. 2008; Kwakkel et al. 2008; Loureiro et al. 2011) and functional electrical stimulation (FES) (de Kroon et al. 2002; Sheffler and Chae 2007). The effects of these techniques have been shown as effective as conventional therapy. A combination of techniques with focus on functional movements might even be superior to conventional therapy.

The aim of this thesis was to develop and evaluate methods for proper control of an automated hybrid rehabilitation system: combining robotics for reach assistance and FES for grasp & release to allow functional upper limb movement training. For successful clinical application, such a device should be safe and easy to use by a non-expert and should allow for fast donning and doffing to maximize available time for training.

Functional grasp and release is essential for manipulation of real objects, however without successful positioning of the arm (reaching out), grasp and release becomes virtually useless from a functional point of view. The focus of the thesis lies mainly on technical feasibility of such a combined system and its individual components. The obtained knowledge will be discussed in the following sections. It will contribute to future developments of stroke rehabilitation systems, which address full functional arm movements.

7.1 Selective electrical stimulation of grasp and release

Dexterous hand movement and ease of manipulation of objects with different shapes and sizes is an important function which distinguishes human beings from most other mammals. FES allows to externally activate muscles and assist movement (Micera et al. 2010). For rehabilitation purpose, surface FES is desirable due to its non-invasiveness and thereby easier donning and doffing. However, with surface FES selectivity of muscle activation becomes theoretically limited due to spread of the applied charge. In chapter 2 the possibility and variability of finding stimulation locations on the forearm to extend individual fingers was evaluated in healthy

subjects. From the results it was concluded that although it is possible to find appropriate locations for each degree of freedom, the exact positions of these locations are highly variable between subjects. A subject specific approach is therefore advocated.

Subject specific methods are further investigated in chapters 3 and 4. In chapter 3 methods for modeling and control of FES for force generation are presented and evaluated for thumb force control in healthy subjects and in chronic stroke subjects. The results indicate that a subject specific approach describing muscle force direction by a single direction and describing force amplitude by a nonlinear sigmoidal curve is feasible to predict muscle force responses stimulated by surface FES. In addition, the feasibility of using the obtained model in two dimensional force control was shown. However, in our study the chronic stroke patients' fatigue and small force ranges are limiting factors. Nevertheless performance will likely improve with more training or application earlier after stroke. The use of a feedback controller in addition to the feed forward path, shows superior results to using feedforward only, which leads to the conclusion that performance monitoring during stimulation and closed loop control is desired for accurate force control.

Control of muscles based on individualized models was shown feasible in chapter 3, however tuning of all the individual controller parameters can be cumbersome and time-consuming. Therefore, in chapter 4 steps towards a more automated approach were taken and applied for movement control in grasp and release. Again an individualized model is obtained. This model relates the stimulation amplitude of muscles responsible for finger flexion, finger extension, thumb opposition, thumb flexion and thumb abduction to angular movement of the fingers. To optimize control inputs such that given setpoint angles for all joints are reached, a model predictive controller was implemented and evaluated. This controller was shown capable of tracking setpoint angles and furthermore suitable for functional grasp and release of real objects of different sizes. Assisted interaction with real objects provides the opportunity of functional task training, which is believed to be more effective than movement training alone (Timmermans et al. 2009). Chapter 4 shows that this interaction is feasible with the presented model predictive controller and is therefore a big step towards more functional task training.

7.2 Robotic support of reaching

Grasp and release movement is only functional when combined with a proper reaching movement. In collaboration with project partners a prototype robotic arm manipulator was developed. The device and the control methods are presented in chapter 5 together with the technical evaluation of the device. The system has the technical ability to compensate the user's arm weight and to support the arm during movement. Due to its inherent safety and ease of use, the system has potential to make the final step to clinical application, or even home use. However, for clinical application, an integrated system which not only addresses reach training but also training of grasp and release will be more beneficial, as such a system could be used to support functional arm movement during rehabilitation.

7.3 Integrated system for support of reach, grasp and release

In the study described in chapter 6, the system for grasp and release support (chapter 4) and for assistance of arm movement (chapter 5) were combined for training of functional tasks. The system was evaluated during passive functional movement tasks in healthy subjects and severely affected chronic stroke subjects. From a technical point of view, full support of the movement (i.e. the subject is completely passive) is the most demanding task. In addition, severely affected chronic stroke subjects are the most demanding group, as these subjects often have very limited function and increased joint stiffness (Kwakkel et al. 2004). Performance of the system in these subjects is currently not sufficient for complete functional movement support. None of the trials in the stroke subjects were completed successfully, partially due to inaccurate arm positioning and partially due to limited response to the electrical stimulation of hand muscles. However, in healthy subjects high success rates were achieved. The success rates of the movement subtasks in healthy subjects are high (76%-100%). Analysis of the non-successful trials revealed that robot positioning accuracy is a critical factor, which needs improvement in a future version. This could be solved by a higher virtualstiffness, feedback of object position and/or active control of robot position by the user. The high success rate in healthy subjects show the feasibility of an integrated system to support functional movement tasks. The fact that success in severely affected chronic stroke subjects was influenced partially by technical limitations show the potential of the system for application in post stroke rehabilitation.

7.4 Towards clinical application

The robotic manipulator presented in chapter 5 was shown effective for both gravity compensation and active three dimensional assistance. Thereby, the device allows for training of more severely affected patients compared to devices which only provide gravity support or two dimensional assistance (Hogan et al. 1992; Sanchez et al. 2006; Stienen et al. 2009b). The device is less powerful than strong exoskeletal based devices (Perry et al. 2007; Nef et al. 2007) which makes it more compact, light-weight and safe while its power is still sufficient for assistance of functional movement tasks. In addition, FES based on the model predictive control approach presented in chapter 4 was shown successful for functional grasp and release tasks in stroke patients. The main focus for improving this methodology should therefore lie on the practical implementation. Currently, electrode positioning and model identification is time consuming and dependent on extensive anatomical knowledge as appropriate positions for selective muscle activation vary largely between subjects (chapter 2).

A system to properly target motor relearning should address the following three aspects: 1) active user involvement, 2) detection of user intention and 3) allow for frequent training. The current evaluation of the final integrated system presented in chapter 6 focused only on technical feasibility of passive movements. To be clinically applicable, it is important that the user is not passive during training.

Motor relearning is promoted only when the user is active and allowed to make mistakes (Reinkensmeyer et al. 2009). When the user is as active as possible (i.e. operating at the limit of his/her ability) learning is expected to be maximal. Therefore it is important that the system can adapt and is minimally active during the functional tasks. Preferably the system is just sufficiently active to allow the user to complete the task, which will increase motivation (Timmermans et al. 2009). To allow the user to be maximally active and make mistakes, the user should also be allowed to initiate and steer movements during the task (Huang and Krakauer 2009). Therefore the system should "know" the intention of the user. For frequent training, an ideal solution would be to place the training device at the patient's home. Recommendations for modifications and extensions of the currently presented methods in light of these three aspects are discussed in the next subsections.

7.4.1 Active user involvement

To maximize patient activity and thereby motor learning, assistance should be minimized. Wolbrecht et al. (2008) suggested assist as needed algorithms with a forgetting factor and a learning factor. In this approach the system learns the ability of the patient by gradually reducing assistance over time and detecting movement failure. Upon failure, assistance is increased again to complete the given task. When tasks have a repetitive nature, like walking or cycling, a similar approach could be used to adjust the assistance during each iteration (Bristow et al. 2006; Freeman et al. 2009). Such an iterative learning control (ILC) approach could also apply for training of repetitive reach and grasp tasks. However, the objective of reach and grasp tasks is to manipulate objects and thereby the specific path toward the object is less important. ILC is usually based on reference trajectories for the whole cycle. To be applicable for functional task training ILC should update the provided assistance only based on the success of the manipulation task. When the task is unsuccessful, there is a need to automatically analyze the previous trial and identify which parts of the movement cause the failure and need additional support (e.g. Veltink et al. 1992; Franken et al. 1995). Further research into such an approach is recommended before application in a system as described in chapter 6. However, ILC based on minimum jerk reference trajectories (Shadmehr and Wise 2005) could already improve the therapeutic effect of such a system although it may penalize jerky movement more than necessary to achieve the task goal.

7.4.2 Detection of user intention

Voluntary initiation of movement needs a system which detects start of movement by the user and responds accordingly. Detection of user intention can be based on several biological signals like brain activity, muscle activity or skeletal movement. For application in the current hybrid system, signal detection at the interface between system and user seems the most logical, which leaves either muscle activity (EMG), arm movement or interaction force. Corbett et al. (2011) compared detec-

tion of EMG and force for control of a prosthetic hand and obtained similar results for both interfaces. As FES is also applied during the movement, the electrical field evoked by FES will also influence the EMG recordings. Although it is possible to filter out these stimulation artefacts (Sennels et al. 1997; Langzam et al. 2006), measurement of the interaction forces seems more straightforward, especially since interaction forces are already measured. Based on the measured interaction force the system can provide assistance either when a certain force threshold is exceeded or proportional to the measured force, to make movement easier. Admittance control schemes have been applied for similar systems to detect an interaction force and let the system respond with movement based on a dynamic model (Spenko et al. 2006; Duchaine and Gosselin 2009; Huo et al. 2010). By changing parameters in the dynamic model, movement assistance can be adjusted.

7.4.3 Therapy at home

Stroke therapy in the patient's home environment might be a solution to simultaneously increase training intensity and release the stress on the health care system. As described in chapter 5, the robotic system presented in this thesis already has great potential for applicability in a home environment, due to its inherent safety (decoupling of motor and load) and ease of use by a non-expert. However, for at home application of the integrated system as presented in chapter 6 several improvements are desired. Main concern of the present system is the time to setup. Ideally the time to setup should only be a fraction of the training session duration and setup should be doable by the patient themselves. Currently, electrode placement is cumbersome and time consuming and also model initialization takes too long to be practically feasible.

Electrode placement is mainly time consuming due to the variability between subjects as described in chapter 2. Therefore each electrode is placed individually and then responses are observed to verify proper placement. This is neither time efficient nor suitable for performance by the patients themselves. In the past decade, several attempts have been made to apply array electrodes, covering a large skin surface together with an automated algorithm to detect appropriate stimulation sites (DB Popović and MB Popović 2009; Keller et al. 2006; Malešević et al. 2012). This would be an ideal solution for proper electrode placement without requiring experienced operators or extensive time.

Estimation of the input-output relation between stimulation amplitude and movement response is time consuming because of the relatively large number of channels and the repetitions needed to increase model certainty. If array electrodes would be used, even more channels will be available. Therefore intelligent solutions are needed to start training early and improve the model during the training session. This could be achieved by a form of initial automated electrode testing (Malešević et al. 2012) and recursive model estimation (e.g. Moon et al. 2005). In addition, models obtained from previous sessions might be used as a starting point. Further research into such solutions is needed and should also address the separation of voluntary and artificial activity. When voluntary activity is present

(section 7.4.1) it is essential to subtract the voluntary activity to properly model the artificial contribution to the movement. The other way around, a model of voluntary ability would be even more useful, to predict the performance beforehand and update the provided assistance accordingly.

7.5 Conclusion

Ideally, rehabilitation of upper extremities focuses at frequent functional movement training (Timmermans et al. 2009) with maximized patient activity (Wolbrecht et al. 2008; Reinkensmeyer et al. 2009). An automated system can provide this type of training when it addresses arm and hand simultaneously, provides a workspace similar to daily living tasks and allows the patient to make mistakes. In this thesis, technical feasibility of an automated system combining robotic reach support with FES based support of grasp and release was demonstrated (chapter 6). The system uses subject specific control approaches (chapters 2, 3 and 4) and a novel robotic end-point manipulator aimed at functional therapy in a home environment (chapter 5). Several technical improvements to increase the ease of use and tailor assistance to ability are needed. But, importantly, the feasibility was shown and therefore the commercial market is encouraged to implement such technology in everyday health-care. Thereby, acceptance of technology applied in health care should further increase: partially by more evidence of effects of the applied technology (Loureiro et al. 2011) and partially by focusing on ease of use (Hidler and Lum 2011). Only with efficient cooperation of therapists, physicians, engineers and scientists, the future of stroke rehabilitation will improve. The technologic possibilities of combining robotics and FES in a subject specific approach presented here contribute to a future with a healthy health-care system, while maximizing functional independence of stroke survivors.

References

-
- Barsi, GI, DB Popović, IM Tarkka, T Sinkjær, and MJ Grey (2008). "Cortical excitability changes following grasping exercise augmented with electrical stimulation." *Experimental brain research* 191 (1), pp. 57–66 (cit. on pp. 4, 6, 13, 101).
- Bastian, AJ (2008). "Understanding sensorimotor adaptation and learning for rehabilitation." *Current opinion in neurology* 21 (6), p. 628 (cit. on p. 5).
- Beer, RF, MD Ellis, BG Holubar, and JPA Dewald (2007). "Impact of gravity loading on post-stroke reaching and its relationship to weakness." *Muscle and Nerve* 36 (2), pp. 242–250 (cit. on pp. 81, 95).
- Bemporad, A, M Morari, and NL Ricker (2010). *Model Predictive Control Toolbox 3 User's Guide*. Tech. rep. The MathWorks, Inc. (cit. on pp. 63, 64).
- Besio, WG (1997). *Command Generation for FES Enhanced Grasping Utilizing Surface EMG in Persons with Cervical Spinal Cord Injury*. University of Miami (cit. on p. 74).
- Bolte Taylor, J (2009). *My Stroke of Insight*. Hachette UK (cit. on p. 3).
- Brainin, M (2013). "Poststroke spasticity: Treating to the disability." *Neurology* 80 (3 Supplement 2), S1–S4 (cit. on p. 74).
- Brewer, BR, SK McDowell, and LC Worthen-Chaudhari (2007). "Poststroke upper extremity rehabilitation: A review of robotic systems and clinical results." *Topics in Stroke Rehabilitation* 14 (6), pp. 22–44 (cit. on p. 79).
- Bristow, DA, M Tharayil, and AG Alleyne (2006). "A survey of iterative learning control." *IEEE Control Systems* 26 (3), pp. 96–114 (cit. on p. 119).
- Camacho, EF and C Bordons Alba (2004). *Model Predictive Control*. Second. Springer (cit. on p. 103).
- Cameron, T, K McDonald, L Anderson, and A Prochazka (1999). "The effect of wrist angle on electrically evoked hand opening in patients with spastic hemiplegia." *IEEE Transactions on Rehabilitation Engineering* 7 (1), pp. 109–111 (cit. on p. 13).
- Carda, S, C Cisari, and M Invernizzi (2013). "Sarcopenia or muscle modifications in neurologic diseases: a lexical or pathophysiological difference?" *European Journal of Physical and Rehabilitation Medicine (Europa Medicophysica)* February;49(1):119-30 (1973-9087 (Linking)), pages (cit. on p. 74).
- Chan, MK, RK.-y Tong, and KY.-k Chung (2009). "Bilateral Upper Limb Training With Functional Electric Stimulation in Patients With Chronic Stroke." *Neurorehabilitation and Neural Repair* 23 (4), pp. 357–365 (cit. on p. 57).
- Chang, Y.-J, S.-F Chen, and J.-D Huang (2011). "A Kinect-based system for physical rehabilitation: A pilot study for young adults with motor disabilities." *Research in developmental disabilities* 32 (6), pp. 2566–2570 (cit. on pp. 73, 112).

- Corbett, EA, EJ Perreault, and TA Kuiken (2011). "Comparison of electromyography and force as interfaces for prosthetic control." *Journal of Rehabilitation Research and Development* 48 (6), pp. 629–42 (cit. on p. 119).
- Crago, PE, N Lan, P Veltink, JJ Abbas, and C Kantor (1996). "New control strategies for neuroprosthetic systems." *Journal of Rehabilitation Research and Development* 33 (2), pp. 158–172 (cit. on p. 72).
- Crago, PE, RJ Nakai, and H Chizeck (1991). "Feedback regulation of hand grasp opening and contact force during stimulation of paralyzed muscle." *IEEE Transactions on Biomedical Engineering* 38 (1), pp. 17–28 (cit. on p. 31).
- Daanen, HAM, AJ Krul, and JFM Molenbroek (2003). *DINED*. Uitgeverij Kerckebosch (cit. on p. 83).
- de Kroon, JR, JH van der Lee, MJ IJzerman, and GJ Lankhorst (2002). "Therapeutic electrical stimulation to improve motor control and functional abilities of the upper extremity after stroke: a systematic review." *Clinical Rehabilitation* 16 (4), pp. 350–360 (cit. on pp. 6, 101, 116).
- DeLisa, J (1988). *Rehabilitation medicine: principles and practice*. Lippincott (cit. on p. 57).
- Donnan, GA, M Fisher, M Macleod, and SM Davis (2008). "Stroke." *The Lancet* 371 (9624), pp. 1612–1623 (cit. on p. 3).
- Dovat, L, O Lambercy, R Gassert, T Maeder, T Milner, TC Leong, E Burdet, et al. (2008). "HandCARE: a cable-actuated rehabilitation system to train hand function after stroke." *IEEE Transactions on Neural Systems and Rehabilitation Engineering* 16 (6), pp. 582–591 (cit. on pp. 7, 101).
- Duchaine, V and C Gosselin (2009). "Safe, stable and intuitive control for physical human-robot interaction." *IEEE International Conference on Robotics and Automation, Kobe, Japan*. IEEE, pp. 3383–3388 (cit. on pp. 113, 120).
- Elsaify, A (2005). "A self optimising portable FES system using an electrode array and movement sensors." PhD thesis. University of Leicester (cit. on p. 73).
- Enoka, RM and AJ Fuglevand (2001). "Motor unit physiology: Some unresolved issues." *Muscle and Nerve* 24 (1), pp. 4–17 (cit. on pp. 25, 26).
- Ethier, C, ER Oby, MJ Bauman, and LE Miller (2012). "Restoration of grasp following paralysis through brain-controlled stimulation of muscles." *Nature* 485, pp. 368–371 (cit. on p. 74).
- Ferreau, H, H Bock, and M Diehl (2008). "An online active set strategy to overcome the limitations of explicit MPC." *International Journal of Robust and Nonlinear Control* 18 (8), pp. 816–830 (cit. on p. 38).
- Flanagan, JR, MK Burstedt, and RS Johansson (1999). "Control of fingertip forces in multidigit manipulation." *Journal of Neurophysiology* 81 (4), pp. 1706–1717 (cit. on p. 50).

-
- Franken, HM, PH Veltink, G Baardman, RA Redmeyer, and HBK Boom (1995). "Cycle-to-cycle control of swing phase of paraplegic gait induced by surface electrical stimulation." *Medical and Biological Engineering and Computing* 33 (3), pp. 440–451 (cit. on p. 119).
- Freeman, CT, A.-M Hughes, JH Burrige, PH Chappell, PL Lewin, and E Rogers (2009). "Iterative learning control of FES applied to the upper extremity for rehabilitation." *Control Engineering Practice* 17 (3), pp. 368–381 (cit. on pp. 101, 113, 119).
- Happee, R (1994). "Inverse dynamic optimization including muscular dynamics, a new simulation method applied to goal directed movements." *Journal of Biomechanics* 27 (7), pp. 953–960 (cit. on pp. 31, 34).
- Hara, Y (2008). "Neurorehabilitation with new functional electrical stimulation for hemiparetic upper extremity in stroke patients." *Journal of Nippon Medical School* 75 (1), pp. 4–14 (cit. on pp. 14, 57, 74).
- Hart, RL, KL Kilgore, and PH Peckham (1998). "A comparison between control methods for implanted FES hand-grasp systems." *IEEE Transactions on Rehabilitation Engineering* 6 (2), pp. 208–218 (cit. on p. 72).
- Hidler, J and PS Lum (2011). "The road ahead for rehabilitation robotics." *Journal of Rehabilitation Research and Development* 48 (4), pp. vii–x (cit. on p. 121).
- Hincapie, JG and RF Kirsch (2007). "EMG-based control for a C5/C6 spinal cord injury upper extremity neuroprosthesis." *2007 Annual International Conference of the IEEE Engineering in Medicine and Biology Society, Lyon, France 2007*, pp. 2432–2435 (cit. on p. 74).
- Hoffmann, U, M Deinhofer, and T Keller (2012). "Automatic determination of parameters for multipad functional electrical stimulation: Application to hand opening and closing." *2012 Annual International Conference of the IEEE Engineering in Medicine and Biology Society, San Diego, CA, USA*, pp. 1859–1863 (cit. on p. 73).
- Hogan, N, HI Krebs, J Charnnarong, P Srikrishna, and A Sharon (1992). "MIT-MANUS: a workstation for manual therapy and training. I." *Proceedings of the IEEE International Workshop on Robot and Human Communication, Tokyo, Japan. IEEE*, pp. 161–165 (cit. on pp. 6, 79, 118).
- Hu, XL, KY Tong, R Li, M Chen, JJ Xue, SK Ho, and PN Chen (2011). "Post-stroke wrist rehabilitation assisted with an intention-driven functional electrical stimulation (FES)-robot system." *2011 IEEE International Conference on Rehabilitation Robotics (ICORR), Zurich, Switzerland*, pp. 1–6 (cit. on p. 74).
- Hu, X, K Tong, R Li, M Chen, JJ Xue, SK Ho, and PN Chen (2010). "Effectiveness of functional electrical stimulation (FES)-robot assisted wrist training on persons after stroke." *2010 Annual International Conference of the IEEE Engi-*

- neering in Medicine and Biology Society, Buenos Aires, Argentina*, pp. 5819–5822 (cit. on p. 57).
- Huang, VS and JW Krakauer (2009). “Robotic neurorehabilitation: a computational motor learning perspective.” *Journal of NeuroEngineering and Rehabilitation* 6 (1), p. 5 (cit. on pp. 113, 119).
- Huo, W, J Huang, Y Wang, and J Wu (2010). “Control of a rehabilitation robotic exoskeleton based on intentional reaching direction.” *2010 International Symposium on Micro-NanoMechatronics and Human Science (MHS), Nagoya, Japan*, pp. 357–362 (cit. on pp. 113, 120).
- Johansson, BB (2000). “Brain plasticity and stroke rehabilitation The Willis lecture.” *Stroke* 31 (1), pp. 223–230 (cit. on p. 4).
- Kamikawa, Y and T Maeno (2008). “Underactuated five-finger prosthetic hand inspired by grasping force distribution of humans.” *IEEE/RSJ International Conference on Intelligent Robots and Systems, Nice, France*, pp. 717–722 (cit. on p. 26).
- Kandel, ER, JH Schwartz, and TM Jessell (2000). *Principles of neural science*. 4th ed. McGraw-Hill, New York, USA (cit. on p. 4).
- Kaufman, KR, KN An, WJ Litchy, WP Cooney, E Chao, et al. (1999). “In-vivo function of the thumb muscles.” *Clinical Biomechanics* 14 (2), pp. 141–150 (cit. on p. 31).
- Keller, T, B Hackl, M Lawrence, and A Kuhn (2006). “Identification and control of hand grasp using multi-channel transcutaneous electrical stimulation.” *11th Annual Conference of the International Functional Electrical Stimulation Society, Zao, Japan*. Zao, Japan, pp. 29–31 (cit. on pp. 14, 25, 58, 73, 120).
- Klamroth-Marganska, V, J Blanco, K Campen, A Curt, V Dietz, T Ettl, M Felder, B Fellinghauer, M Guidali, A Kollmar, et al. (2013). “Three-dimensional, task-specific robot therapy of the arm after stroke: a multicentre, parallel-group randomised trial.” *The Lancet Neurology* (cit. on p. 79).
- Kooij, H van der, EHF van Asseldonk, and FC van der Helm (2005). “Comparison of different methods to identify and quantify balance control.” *Journal of Neuroscience Methods* 145 (1&2), pp. 175–203. ISSN: 0165-0270 (cit. on p. 79).
- Kozin, SH (1998). “The anatomy of the recurrent branch of the median nerve.” *The Journal of Hand Surgery* 23 (5), pp. 852–858 (cit. on p. 50).
- Krabben, T, BI Molier, A Houwink, JS Rietman, JH Burke, and GB Prange (2011). “Circle drawing as evaluative movement task in stroke rehabilitation: an explorative study.” *Journal of NeuroEngineering and Rehabilitation* 8 (1), p. 15 (cit. on p. 95).
- Krabben, T, GB Prange, BI Molier, AHA Stienen, MJA Jannink, JH Burke, and JS Rietman (2012). “Influence of gravity compensation training on synergistic

-
- movement patterns of the upper extremity after stroke, a pilot study." *Journal of NeuroEngineering and Rehabilitation* 9 (1), p. 44 (cit. on pp. 81, 95).
- Krakauer, JW (2006). "Motor learning: its relevance to stroke recovery and neurorehabilitation." *Current Opinion in Neurology* 19, pp. 84–90 (cit. on pp. 5, 13).
- Krebs, HI, L Dipietro, S Levy-Tzedek, S Fasoli, A Rykman-Berland, J Zipse, J Fawcett, J Stein, H Poizner, A Lo, B Volpe, and N Hogan (2008). "A paradigm shift for rehabilitation robotics." *IEEE Engineering in Medicine and Biology Magazine* 27 (4), pp. 61–70 (cit. on pp. 7, 116).
- Kuhn, A, T Keller, M Lawrence, and M Morari (June 2010). "The Influence of Electrode Size on Selectivity and Comfort in Transcutaneous Electrical Stimulation of the Forearm." *IEEE Transactions on Neural Systems and Rehabilitation Engineering* 18 (3), pp. 255–262 (cit. on pp. 15, 25, 35).
- Kuhn, A, T Keller, S Micera, and M Morari (2009). "Array electrode design for transcutaneous electrical stimulation: a simulation study." *Medical engineering and physics* 31 (8), pp. 945–951 (cit. on pp. 25, 112).
- Kwakkel, G, BJ Kollen, and HI Krebs (2008). "Effects of robot-assisted therapy on upper limb recovery after stroke: a systematic review." *Neurorehabilitation and Neural Repair* 22 (2), pp. 111–121 (cit. on pp. 7, 79, 116).
- Kwakkel, G, BJ Kollen, and E Lindeman (2004). "Understanding the pattern of functional recovery after stroke: facts and theories." *Restorative Neurology and Neuroscience* 22 (3), pp. 281–299 (cit. on p. 118).
- Kwakkel, G and CG Meskers (2013). "Effects of robotic therapy of the arm after stroke." *The Lancet Neurology* (cit. on p. 79).
- Lamercy, O, L Dovat, R Gassert, E Burdet, CL Teo, and T Milner (2007). "A haptic knob for rehabilitation of hand function." *IEEE Transactions on Neural Systems and Rehabilitation Engineering* 15 (3), pp. 356–366 (cit. on p. 7).
- Lang, CE, SL DeJong, and JA Beebe (2009). "Recovery of Thumb and Finger Extension and Its Relation to Grasp Performance After Stroke." *Journal of Neurophysiology* 102 (1), pp. 451–459 (cit. on p. 13).
- Lang, CE and MH Schieber (2004). "Human Finger Independence: Limitations due to Passive Mechanical Coupling Versus Active Neuromuscular Control." *Journal of Neurophysiology* 92 (5), pp. 2802–2810 (cit. on pp. 14, 24).
- Lang, CE and MH Schieber (2004). "Reduced Muscle Selectivity During Individuated Finger Movements in Humans After Damage to the Motor Cortex or Corticospinal Tract." *Journal of Neurophysiology* 91 (4), pp. 1722–1733 (cit. on p. 13).
- Langhorne, P, F Coupar, and A Pollock (2009). "Motor recovery after stroke: a systematic review." *The Lancet Neurology* 8 (8), pp. 741–754 (cit. on p. 116).

- Langzam, E, E Isakov, and J Mizrahi (2006). "Evaluation of methods for extraction of the volitional EMG in dynamic hybrid muscle activation." *Journal of NeuroEngineering and Rehabilitation* 3 (1), p. 27 (cit. on pp. 74, 120).
- Lawrence, ES, C Coshall, R Dundas, J Stewart, AG Rudd, R Howard, and CDA Wolfe (2001). "Estimates of the Prevalence of Acute Stroke Impairments and Disability in a Multiethnic Population." *Stroke* 32 (6), pp. 1279–1284 (cit. on p. 4).
- Lawrence, M, GP Gross, M Lang, A Kuhn, T Keller, and M Morari (2008). "Assessment of finger forces and wrist torques for functional grasp using new multi-channel textile neuroprostheses." *Artificial Organs* 32 (8), pp. 634–638 (cit. on p. 13).
- Leijnse, JNAL, S Carter, A Gupta, and S McCabe (2008). "Anatomic Basis for Individuated Surface EMG and Homogeneous Electrostimulation With Neuroprostheses of the Extensor Digitorum Communis." *Journal of Neurophysiology* 100 (1), pp. 64–75 (cit. on pp. 14, 24).
- Ljung, L (2013). *System Identification Toolbox User's Guide*. Tech. rep. The MathWorks, Inc. (cit. on p. 66).
- Loureiro, RC, WS Harwin, K Nagai, and M Johnson (2011). "Advances in upper limb stroke rehabilitation: a technology push." *Medical and Biological Engineering and Computing* 49 (10), pp. 1103–1118 (cit. on pp. 79, 101, 116, 121).
- Lujan, JL and PE Crago (2009). "Automated optimal coordination of multiple-DOF neuromuscular actions in feedforward neuroprostheses." *IEEE Transactions on Biomedical Engineering* 56 (1), pp. 179–187 (cit. on pp. 31, 49, 51).
- Lum, PS, CG Burgar, PC Shor, M Majmundar, and MV der Loos (2002). "Robot-assisted movement training compared with conventional therapy techniques for the rehabilitation of upper-limb motor function after stroke." *Archives of Physical Medicine and Rehabilitation* 83 (7), pp. 952–959 (cit. on pp. 7, 79, 116).
- Lum, PS, CG Burgar, M Van der Loos, PC Shor, M Majmundar, R Yap, et al. (2006). "MIME robotic device for upper-limb neurorehabilitation in subacute stroke subjects: A follow-up study." *Journal of Rehabilitation Research and Development* 43 (5), p. 631 (cit. on p. 79).
- Lynch, CL and MR Popovic (2008). "Functional electrical stimulation." *IEEE Control Systems* 28 (2), pp. 40–50 (cit. on p. 101).
- Maciejowski, JM (1989). *Multivariable feedback design*. Vol. 8. Addison-Wesley Wokingham (cit. on p. 88).
- Malešević, NM, LZP Maneski, V Ilić, N Jorgovanović, G Bijelić, T Keller, DB Popović, et al. (2012). "A multi-pad electrode based functional electrical stim-

-
- ulation system for restoration of grasp.” *Journal of NeuroEngineering and Rehabilitation* 9 (1), p. 66 (cit. on pp. 52, 73, 112, 120).
- Malhotra, S, S Rosewilliam, H Hermens, C Roffe, P Jones, and AD Pandyan (2012). “A randomized controlled trial of surface neuromuscular electrical stimulation applied early after acute stroke: effects on wrist pain, spasticity and contractures.” *Clinical Rehabilitation* (cit. on pp. 6, 101).
- Mao, Y and S Agrawal (2012). “Design of a Cable-Driven Arm Exoskeleton (CAREX) for Neural Rehabilitation.” *IEEE Transactions on Robotics* 28 (4), pp. 922–931. ISSN: 1552-3098 (cit. on p. 81).
- Micera, S, T Keller, M Lawrence, M Morari, and DB Popović (2010). “Wearable neural prostheses.” *IEEE Engineering in Medicine and Biology Magazine* 29 (3), pp. 64–69 (cit. on pp. 14, 31, 72, 101, 116).
- Micera, S, MC Carrozza, E Guglielmelli, G Cappiello, F Zaccone, C Freschi, R Colombo, A Mazzone, C Delconte, F Pisano, et al. (2005). “A simple robotic system for neurorehabilitation.” *Autonomous Robots* 19 (3), pp. 271–284 (cit. on p. 79).
- Monster, AW and H Chan (1977). “Isometric force production by motor units of extensor digitorum communis muscle in man.” *Journal of Neurophysiology* 40 (6), pp. 1432–1443 (cit. on p. 27).
- Moon, S.-M, RL Clark, and DG Cole (2005). “The recursive generalized predictive feedback control: theory and experiments.” *Journal of Sound and Vibration* 279 (1), pp. 171–199 (cit. on pp. 112, 120).
- Muller-Putz, GR, R Rupp, and G Pfurtscheller (Oct. 2008). “Graz Brain-Computer Interface: Control of neuroprostheses for the upper extremity.” *1st International Symposium on Applied Sciences on Biomedical and Communication Technologies, Aalborg, Denmark*, pp. 1–2 (cit. on p. 74).
- Nathan, RH (1979). “Functional electrical stimulation of the upper limb: charting the forearm surface.” *Medical and Biological Engineering and Computing* 17 (6), pp. 729–736 (cit. on p. 13).
- Nathan, RH (1990). “FNS of the upper limb: targeting the forearm muscles for surface stimulation.” *Medical and Biological Engineering and Computing* 28 (3), pp. 249–256 (cit. on pp. 13, 14, 25).
- Nef, T, M Mihelj, and R Riener (2007). “ARMin: a robot for patient-cooperative arm therapy.” *Medical and Biological Engineering and Computing* 45 (9), pp. 887–900 (cit. on pp. 6, 79, 118).
- Nudo, RJ (2006). “Mechanisms for recovery of motor function following cortical damage.” *Current opinion in Neurobiology* 16 (6), pp. 638–644 (cit. on p. 5).

- Nudo, RJ, EJ Plautz, and SB Frost (2001). "Role of adaptive plasticity in recovery of function after damage to motor cortex." *Muscle and nerve* 24 (8), pp. 1000–1019 (cit. on p. 4).
- Oblak, J and Z Matjacic (2011). "Design of a series visco-elastic actuator for multi-purpose rehabilitation haptic device." *Journal of NeuroEngineering and Rehabilitation* 8 (1), p. 3 (cit. on p. 85).
- O'Dwyer, SB, DT O'Keefe, S Coote, and GM Lyons (Mar. 2006). "An electrode configuration technique using an electrode matrix arrangement for FES-based upper arm rehabilitation systems." *Medical Engineering and Physics* 28 (2), pp. 166–176 (cit. on p. 73).
- Oess, N, J Wanek, and A Curt (2012). "Design and evaluation of a low-cost instrumented glove for hand function assessment." *Journal of NeuroEngineering and Rehabilitation* 9 (1), p. 2 (cit. on pp. 73, 112).
- Otten, A, HC Voort, AHA Stienen, EHF van Asseldonk, RGKM Aarts, and H van der Kooij (2014). "LIMPACT: A Hydraulically Powered Self-Aligning Upper Limb Exoskeleton." *In preparation* (cit. on p. 79).
- Ovbiagele, B and M Nguyen-Huynh (2011). "Stroke Epidemiology: Advancing Our Understanding of Disease Mechanism and Therapy." *Neurotherapeutics* 8 (3). 10.1007/s13311-011-0053-1, pp. 319–329 (cit. on pp. 31, 116).
- Park, H.-S, Y Ren, and L.-Q Zhang (2008). "IntelliArm: An exoskeleton for diagnosis and treatment of patients with neurological impairments." *2nd IEEE RAS & EMBS International Conference on Biomedical Robotics and Biomechanics (BioRob)*, Scottsdale, AZ, USA. IEEE, pp. 109–114 (cit. on p. 79).
- Pearlman, JL, SS Roach, and FJ Valero-Cuevas (2004). "The fundamental thumb-tip force vectors produced by the muscles of the thumb." *Journal of Orthopaedic Research* 22 (2), pp. 306–312 (cit. on p. 31).
- Penfield, W and T Rasmussen (1950). "The cerebral cortex of man; a clinical study of localization of function." (cit. on p. 4).
- Perry, JC, J Rosen, and S Burns (2007). "Upper-limb powered exoskeleton design." *IEEE/ASME Transactions on Mechatronics* 12 (4), pp. 408–417 (cit. on pp. 6, 79, 118).
- Pfurtscheller, G, GR Müller-Putz, J Pfurtscheller, and R Rupp (2005). "EEG-based asynchronous BCI controls functional electrical stimulation in a tetra-plegic patient." *EURASIP Journal on Applied Signal Processing* 2005, pp. 3152–3155 (cit. on p. 74).
- Popović, DB and MB Popović (2009). "Automatic determination of the optimal shape of a surface electrode: selective stimulation." *Journal of Neuroscience Methods* 178 (1), pp. 174–181 (cit. on pp. 13, 31, 73, 120).

-
- Popović, DB, T Sinkjær, and MB Popović (2009). "Electrical stimulation as a means for achieving recovery of function in stroke patients." *NeuroRehabilitation* 25 (1), pp. 45–58 (cit. on pp. 13, 57).
- Popović-Bijelić, A, G Bijelić, N Jorgovanović, D Bojanić, MB Popović, and DB Popović (2005). "Multi-Field Surface Electrode for Selective Electrical Stimulation." *Artificial organs* 29 (6), pp. 448–452 (cit. on pp. 13, 112).
- Powell, J, AD Pandyan, M Granat, M Cameron, and DJ Stott (1999). "Electrical stimulation of wrist extensors in poststroke hemiplegia." *Stroke* 30 (7), pp. 1384–1389 (cit. on pp. 5, 101).
- Prange, GB, MJA Jannink, CGM Groothuis-Oudshoorn, HJ Hermens, and MJ IJzerman (2006). "Systematic review of the effect of robot-aided therapy on recovery of the hemiparetic arm after stroke." *Journal of Rehabilitation Research and Development* 43 (2), pp. 171–184 (cit. on pp. 7, 79, 116).
- Prange, GB, T Krabben, GJ Renzenbrink, MJ IJzerman, HJ Hermens, and MJ Jannink (2012). "Changes in muscle activation after reach training with gravity compensation in chronic stroke patients." *International Journal of Rehabilitation Research* 35 (3), pp. 234–242 (cit. on pp. 81, 95).
- Pratt, GA and MM Williamson (1995). "Series elastic actuators." *Proceedings of the IEEE/RSJ International Conference on Intelligent Robots and Systems, Edmonton, Canada*. Vol. 1, 399–406 vol.1 (cit. on p. 84).
- Prilutsky, BI and VM Zatsiorsky (2002). "Optimization-based models of muscle coordination." *Exercise and Sport Sciences Reviews* 30 (1), p. 32 (cit. on pp. 31, 34).
- Prochazka, A, M Gauthier, M Wieler, and Z Kenwell (1997). "The bionic glove: An electrical stimulator garment that provides controlled grasp and hand opening in quadriplegia." *Archives of Physical Medicine and Rehabilitation* 78 (6), pp. 608–614 (cit. on pp. 14, 57).
- Reinkensmeyer, DJ, OM Akoner, DP Ferris, and KE Gordon (2009). "Slacking by the human motor system: Computational models and implications for robotic orthoses." *2009. Annual International Conference of the IEEE Engineering in Medicine and Biology Society, Minneapolis, MN, USA*, pp. 2129–2132 (cit. on pp. 73, 81, 101, 112, 119, 121).
- Riener, R, T Nef, and G Colombo (2005). "Robot-aided neurorehabilitation of the upper extremities." *Medical and Biological Engineering and Computing* 43 (1), pp. 2–10 (cit. on p. 79).
- Roby-Brami, A, A Feydy, M Combeaud, EV Biryukova, B Bussel, and MF Levin (2003). "Motor compensation and recovery for reaching in stroke patients." *Acta Neurologica Scandinavica* 107 (5), pp. 369–381 (cit. on p. 4).

- Rosati, G, P Gallina, S Masiero, and A Rossi (2005). "Design of a new 5 d.o.f. wire-based robot for rehabilitation." *2005 International Conference on Rehabilitation Robotics (ICORR)*, Chicago, IL, USA, pp. 430–433 (cit. on p. 81).
- Rosewilliam, S, S Malhotra, C Roffe, P Jones, and AD Pandyan (2012). "Can surface neuromuscular electrical stimulation of the wrist and hand combined with routine therapy facilitate recovery of arm function in patients with stroke?" *Archives of Physical Medicine and Rehabilitation* 93 (10), pp. 1715–1721 (cit. on pp. 5, 101).
- Roth, EJ and RL Harvey (2002). Braddom, RL. *Physical medicine and rehabilitation*. Elsevier Health Sciences. Chap. Rehabilitation of Stroke Syndromes, pp. 1055–1078 (cit. on p. 3).
- Sanchez, RJ, J Liu, S Rao, P Shah, R Smith, T Rahman, SC Cramer, JE Brown, and DJ Reinkensmeyer (2006). "Automating Arm Movement Training Following Severe Stroke: Functional Exercises With Quantitative Feedback in a Gravity-Reduced Environment." *IEEE Transactions on Neural Systems and Rehabilitation Engineering* 14 (3), pp. 378–389 (cit. on pp. 79, 118).
- Scheerer, EM, Y.-W Liao, EJ Perreault, MC Tresch, and LK M. (2012). "Optimal sampling of recruitment curves for functional electrical stimulation control." *34th Annual International Conference of the IEEE EMBS*, pp. 329–332 (cit. on p. 50).
- Scheerer, EM, Y.-W Liao, EJ Perreault, MC Tresch, WD Memberg, RF Kirsch, and KM Lynch (2012). "System identification for 3D force control of a human arm neuroprosthesis using functional electrical stimulation." *Robotics and Automation (ICRA)*, 2012 IEEE International Conference on, pp. 3698–3705 (cit. on p. 51).
- Schiele, A and G Hirzinger (2011). "A new generation of ergonomic exoskeletons-The high-performance X-Arm-2 for space robotics telepresence." *2011 IEEE/RSJ International Conference on Intelligent Robots and Systems (IROS)*, San Francisco, CA, USA. IEEE, pp. 2158–2165 (cit. on p. 79).
- Schneiders, M, M Rohm, and R Rupp (2011). "Towards Non-invasive BCI Controlled Grasp Neuroprostheses - Systematic Analysis of FES-induced Artefacts on EEG-signals." *International Journal of Bioelectromagnetism* 13(2), pp. 98–99 (cit. on p. 74).
- Schouten, AC, E de Vlught, JJB van Hilten, and FC van der Helm (2006). "Design of a torque-controlled manipulator to analyse the admittance of the wrist joint." *Journal of Neuroscience Methods* 154 (1-2), pp. 134–141 (cit. on p. 88).
- Seber, GAF and CJ Wild (2003). *Nonlinear Regression*. Hoboken, NJ: Wiley-Interscience (cit. on p. 37).
- Sennels, S, F Biering-Sorensen, OT Andersen, and SD Hansen (1997). "Functional neuromuscular stimulation controlled by surface electromyographic signals pro-

-
- duced by volitional activation of the same muscle: adaptive removal of the muscle response from the recorded EMG-signal." *IEEE Transactions on Rehabilitation Engineering* 5 (2), pp. 195–206 (cit. on pp. 74, 120).
- Shadmehr, R and SP Wise (2005). *The computational neurobiology of reaching and pointing: a foundation for motor learning*. The MIT press (cit. on pp. 95, 119).
- Sheffler, LR and J Chae (2007). "Neuromuscular electrical stimulation in neurorehabilitation." *Muscle and nerve* 35 (5), pp. 562–590 (cit. on pp. 5, 6, 101, 116).
- Shimada, Y, S Chida, T Matsunaga, A Misawa, H Ito, T Sakuraba, M Sato, K Hatakeyama, and E Itoi (2003). "Grasping power by means of functional electrical stimulation in a case of C6 complete tetraplegia." *Tohoku Journal of Experimental Medicine* 201 (2), pp. 91–96 (cit. on p. 13).
- Shindo, K, T Fujiwara, J Hara, H Oba, F Hotta, T Tsuji, K Hase, and M Liu (2011). "Effectiveness of Hybrid Assistive Neuromuscular Dynamic Stimulation Therapy in Patients With Subacute Stroke: A Randomized Controlled Pilot Trial." *Neurorehabilitation and Neural Repair* 25 (9), pp. 830–837 (cit. on p. 57).
- Simone, L and D Kamper (2005). "Design considerations for a wearable monitor to measure finger posture." *Journal of NeuroEngineering and Rehabilitation* 2 (1), p. 5 (cit. on pp. 73, 112).
- Singh, G, S Boddu, I Chakravorty, GM Bairy, and M Ganesh (2013). "An instrumented glove for monitoring forces during object manipulation." *2013 IEEE Point-of-Care Healthcare Technologies (PHT), Bangalore, India*, pp. 212–215 (cit. on p. 50).
- Sinkjær, T, M Haugland, A Inmann, M Hansen, and KD Nielsen (2003). "Biopotentials as command and feedback signals in functional electrical stimulation systems." *Medical Engineering and Physics* 25 (1), pp. 29–40 (cit. on p. 74).
- Snoek, GJ, MJ IJzerman, TS Stoffers, and G Zilvold (2000). "Use of the NESS handmaster to restore handfunction in tetraplegia: clinical experiences in ten patients." *Spinal Cord* 38 (4), pp. 244–249 (cit. on pp. 5, 101).
- Spenko, M, H Yu, and S Dubowsky (2006). "Robotic personal aids for mobility and monitoring for the elderly." *IEEE Transactions on Neural Systems and Rehabilitation Engineering* 14 (3), pp. 344–351 (cit. on pp. 113, 120).
- Stein, RB and V Mushahwar (2005). "Reanimating limbs after injury or disease." *Trends in Neurosciences* 28 (10), pp. 518–524 (cit. on p. 6).
- Stienen, AHA, EEG Hekman, GB Prange, MJA Jannink, AMM Aalsma, FCT van der Helm, and H van der Kooij (2009a). "Dampace: Design of an Exoskeleton for Force-Coordination Training in Upper-Extremity Rehabilitation." *Journal of Medical Devices* 3 (3), p. 031003 (cit. on pp. 6, 79).

- Stienen, AHA, EEG Hekman, GB Prange, MJA Jannink, FCT van der Helm, and H van der Kooij (2009b). "Freebal: Design of a Dedicated Weight-Support System for Upper-Extremity Rehabilitation." *Journal of Medical Devices* 3 (4) (cit. on pp. 6, 79, 118).
- Stienen, AHA, JG McPherson, AC Schouten, and JPA Dewald (2011). "The ACT-4D: A novel rehabilitation robot for the quantification of upper limb motor impairments following brain injury." *2011 IEEE International Conference on Rehabilitation Robotics (ICORR)*. IEEE, pp. 1–6 (cit. on p. 79).
- Sukal, TM, MD Ellis, and JPA Dewald (2007). "Shoulder abduction-induced reductions in reaching work area following hemiparetic stroke: neuroscientific implications." *Experimental Brain Research* 183 (2), pp. 215–223 (cit. on p. 95).
- Tavella, M, R Leeb, R Rupp, and JR del Millan (2010). "Towards natural non-invasive hand neuroprostheses for daily living." *2010 Annual International Conference of the IEEE Engineering in Medicine and Biology Society, Buenos Aires, Argentina 2010*, pp. 126–129 (cit. on p. 74).
- Thorsen, R, M Ferrarin, R Spadone, and C Frigo (1999). "Functional control of the hand in tetraplegics based on residual synergistic EMG activity." *Artificial Organs* 23 (5), pp. 470–473 (cit. on p. 14).
- Thrasher, TA, V Zivanovic, W McIlroy, and MR Popovic (2008). "Rehabilitation of Reaching and Grasping Function in Severe Hemiplegic Patients Using Functional Electrical Stimulation Therapy." *Neurorehabilitation and Neural Repair* 22 (6), pp. 706–714 (cit. on p. 57).
- Timmermans, AAA, HAM Seelen, R Willmann, and H Kingma (2009). "Technology-assisted training of arm-hand skills in stroke: concepts on reacquisition of motor control and therapist guidelines for rehabilitation technology design." *Journal of NeuroEngineering and Rehabilitation* 6 (1), p. 1 (cit. on pp. 5, 117, 119, 121).
- Timmermans, AAA, AI Spooren, H Kingma, and HA Seelen (2010). "Influence of task-oriented training content on skilled arm-hand performance in stroke: a systematic review." *Neurorehabilitation and Neural Repair* 24 (9), pp. 858–870 (cit. on pp. 73, 83, 87).
- Van der Linde, RQ, P Lammertse, E Frederiksen, and B Ruiters (2002). "The Haptic-Master, a new high-performance haptic interface." *Proceedings of Eurohaptics, München, Germany*, pp. 1–5 (cit. on p. 6).
- van Duinen, H, WS Yu, and SC Gandevia (2009). "Limited ability to extend the digits of the human hand independently with extensor digitorum." *The Journal of Physiology* 587 (20), pp. 4799–4810 (cit. on p. 14).
- Veltink, PH, HM Franken, JA Van Alste, and HB Boom (1992). "Modelling the optimal control of cyclical leg movements induced by functional electrical stim-

-
- ulation.” *The International Journal of Artificial Organs* 15 (12), pp. 746–755 (cit. on p. 119).
- Veltink, PH, HG Kortier, and HM Schepers (2009). “Sensing power transfer between the human body and the environment.” *IEEE Transactions on Biomedical Engineering* 56 (6), pp. 1711–1718 (cit. on p. 112).
- Veltink, PH, HG Kortier, HM Schepers, VI Sluiter, RA Brookhuis, TSJ Lammerink, and RJ Wiegerink (2012). “PowerGlove, Concepts and current results.” *Proceedings of XII International Symposium on 3D Analysis of Human Movement, Bologna, Italy*. Ed. by A Leardini and R Stagni. Bologna, Italy: Universita di Bologna, pp. 42–45 (cit. on p. 73).
- Weichert, F, D Bachmann, B Rudak, and D Fisseler (2013). “Analysis of the Accuracy and Robustness of the Leap Motion Controller.” *Sensors* 13 (5), pp. 6380–6393 (cit. on pp. 73, 112).
- Westerveld, AJ, A Kuck, A Schouten, P Veltink, and H van der Kooij (2012). “Grasp and release with surface functional electrical stimulation using a Model Predictive Control approach.” *2012 Annual International Conference of the IEEE Engineering in Medicine and Biology Society, San Diego, CA, USA*, pp. 333–336 (cit. on pp. 50, 52, 57).
- Williams, NW, JMT Penrose, CM Caddy, E Barnes, DR Hose, and P Harley (2000). “A goniometric glove for clinical hand assessment construction, calibration and validation.” *Journal of Hand Surgery (British and European Volume)* 25 (2), pp. 200–207 (cit. on pp. 73, 112).
- Wolbrecht, ET, V Chan, DJ Reinkensmeyer, and JE Bobrow (2008). “Optimizing compliant, model-based robotic assistance to promote neurorehabilitation.” *IEEE Transactions on Neural Systems and Rehabilitation Engineering* 16 (3), pp. 286–297 (cit. on pp. 8, 31, 73, 101, 112, 113, 119, 121).
- Worsnopp, TT, MA Peshkin, JE Colgate, and DG Kamper (2007). “An actuated finger exoskeleton for hand rehabilitation following stroke.” *IEEE 10th International Conference on Rehabilitation Robotics, Noordwijk, The Netherlands*. IEEE, pp. 896–901 (cit. on pp. 7, 101).
- Yamaguchi, H, D Nishikawa, W Yu, M Maruishi, H Yokoi, Y Mano, and Y Kakazu (1999). “EMG control switching system for FES.” *8th IEEE International Workshop on Robot and Human Interaction, Pisa, Italy*, pp. 7–12 (cit. on p. 74).
- Ziegler, JG and NB Nichols (1942). “Optimum Settings for Automatic Controllers.” *Transactions of the American Society of Mechanical Engineers* 64, pp. 759–768 (cit. on pp. 37, 49).

Summary

Reach, grasp and release is part of many functional movements. Every day we manipulate objects without thinking how to coordinate our muscles in order to move our arms and fingers. Over 75% of stroke survivors have upper limb motor deficits, which makes functional arm and hand movements difficult and limits their functional independence. Upper limb therapies after stroke focus on regaining functional ability and independence.

Graying of society leads to more stroke victims and fewer health care professionals. Technology might be a solution to support certain rehabilitation therapies in future health care. Robotic systems have been developed for support of arm and hand movements and functional electrical stimulation (FES) has been applied to activate arm and hand muscles. Therapeutic effects of both techniques have been shown similar to conventional therapies. In addition, the application of these technologies allows for more frequent training with less physical effort for therapists. Therefore, technology could reduce the burden on the health care system caused by graying of society.

Repetitive practice of functional tasks has been shown beneficial for rehabilitation after stroke. Simultaneous support of reach, grasp and release is desired to increase functional outcome. Robotics has been applied successfully for arm support. Support of grasp and release with external mechanics requires high complexity, which makes hand robotics currently not very suitable for functional movement training. FES, however, has been applied successfully for activation of hand muscles. A hybrid approach, combining FES support of grasp and release with robotic reach support could be an excellent solution for enabling functional task training.

The aim of this thesis is to develop and evaluate methods for control of an automated hybrid rehabilitation system combining robotics for reach assistance and FES for grasp and release to allow functional arm and hand training. For successful clinical application, such a device should be safe and easy to use by a non-expert and should allow for fast donning and doffing to maximize available time for training. By the use of an automated system for stroke rehabilitation, which is also applicable in the patient's home, therapy can be intensified even further.

For successful application of a hybrid system, solutions for individual components have first been explored. In chapter 2, the possibilities for selective activation of individual fingers by FES were explored and related to electrode placement in healthy subjects. Although it was shown possible to find appropriate locations for each degree of freedom, the exact positions of these locations are highly variable between subjects. A subject specific approach for FES application is therefore desired.

The human muscular system is redundant: more muscles than degrees of freedom are present. In chapter 3, subject specific control methods for a redundant muscle system with FES were presented and evaluated. A subject specific model relating the stimulation parameters of thumb muscles to the evoked thumb forces is used to predict thumb forces in both healthy subjects and stroke subjects. Subsequently, the individualized muscle models were used to control the thumb force towards target force vectors by sharing the load among the individual muscles. The approach was shown feasible in both healthy and stroke subjects, however the

number of tunable parameters makes the approach somewhat cumbersome and time-consuming for clinical application.

To reduce the number of tunable parameters, steps towards an automated model based method were taken and applied for controlling the movement of the thumb and fingers during grasp and release of actual objects (chapter 4). The relation between muscle stimulation and movement of individual fingers was measured and modeled. A model predictive controller was implemented to use the estimated model to predict the movement and calculate the required stimulation parameters based on desired finger joint angles. This controller was shown capable of tracking set point angles. Furthermore successful grasp and release of real objects of different sizes was demonstrated in both healthy and stroke subjects. Thereby, chapter 4 demonstrates that controlled interaction with real objects using FES is feasible, which is a big step towards more functional task training.

Grasp and release movement is only functional with proper reach movement. In collaboration with project partners a prototype robotic arm manipulator was developed. The device and its control methods were presented in chapter 5 together with the technical evaluation of the device. The system has the technical ability to compensate the user's arm weight and to support arm movements. Due to its inherent safety and ease of use, the system has potential to make the final step to clinical application, and even home use. However, for clinical application, an integrated system which not only addresses reach training but also training of grasp and release will be more beneficial, as such a system could be used to support functional arm movement during rehabilitation.

The systems for grasp and release support (chapter 4) and for assistance of arm movement (chapter 5) were combined for training of functional tasks. The system was evaluated during passive functional movement tasks in healthy subjects and severe chronic stroke subjects (chapter 6). From a technical point of view, full support of the movement (i.e. the subject is completely passive) is the most demanding task. In healthy subjects high success rates were achieved. The success rates of the movement subtasks in healthy subjects were also high (76%-100%). The success rates in healthy subjects show the potential of the system for functional task support. However, performance of the system in preliminary tests with stroke subjects is currently not satisfactory. None of the trials in the stroke subjects were completed successfully. Partially due to positioning inaccuracies relative to the object and partially due to limited finger movement with FES. However, the included stroke subjects were severely affected and in a chronic state. To be conclusive on post stroke applicability of the current system, additional evaluation in a broader range of stroke subjects is required.

Ideally, an automated rehabilitation system should only support when necessary, put the patient in control and allow for high intensive training. These additional requirements will challenge the individual patient to his maximum capacity and thereby maximize therapy outcome. In this thesis the technical feasibility and performance was evaluated and therefore the subjects were asked to relax in the experiments described in this thesis (i.e. no voluntary movement). A passive subject will be the most demanding situation for the system and was therefore used

as evaluation setting. In chapter 7 possible directions for active user involvement, detection of user intention and training in a home environment allowing for intensive training were discussed. Firstly, assistance may be minimized based on patient performance and task success rates. Secondly, the user's intention could be detected from the measured interaction forces. And finally, the use of array electrodes allows for electrode placement by a non-experienced user and improves practical applicability by reducing donning/doffing time. With such extensions the system could be taken to a next level, allowing for frequent functional movement training with maximized patient activity.

This thesis demonstrates the technical feasibility of an automated rehabilitation system, which combines robotics and FES. The commercial market is encouraged to implement such technology in everyday health-care. Thereby, acceptance of technology applied in health care should further increase. The technologic possibilities of combining robotics and FES in a subject specific approach presented here will contribute to a sustainable health-care system, while maximizing functional independence of stroke survivors.

Samenvatting

Elke dag manipuleren we objecten zonder na te denken over de coördinatie van individuele spieren om onze armen en vingers te bewegen. Meer dan 75% van de CVA patiënten heeft een beperkte functie van de bovenste extremiteit. Hierdoor worden functionele arm- en handbewegingen bemoeilijkt, hetgeen hen functioneel afhankelijk maakt. De nadruk van therapie na een beroerte ligt op het verhogen van onafhankelijkheid door functionele bewegingen te trainen.

Vergrijzing van de samenleving leidt tot meer CVA slachtoffers en minder zorg professionals. Technologie kan een oplossing zijn om bepaalde onderdelen van de gezondheidszorg in de toekomst te ondersteunen. Er zijn robotsystemen ontwikkeld voor ondersteuning van de arm en handbewegingen en ook functionele elektrische stimulatie (FES) wordt toegepast voor activatie van arm en hand spieren. Effect van beide technieken is aangetoond en vergelijkbaar met conventionele therapieën. Bovendien biedt de toepassing van technologische systemen de mogelijkheid om vaker te trainen met minder lichamelijke inspanning voor therapeuten. Daarom zou technologie de last op de gezondheidszorg als gevolg van vergrijzing van de samenleving kunnen verminderen.

Herhaaldelijk oefenen van functionele taken gunstig is voor revalidatie na een beroerte. Gelijktijdige ondersteuning van reik en grijpbewegingen is gewenst om het effect van therapie te verhogen. Voor arm ondersteuning is robotica reeds succesvol toegepast. Echter vereist ondersteuning van de vingers met externe mechanica een hoge complexiteit, hetgeen hand robotica momenteel minder toepasbaar maakt voor bewegingstraining. FES daarentegen is in het verleden met succes toegepast voor de activering van handspieren. Een hybride aanpak, die FES ondersteuning van grijpen en loslaten combineert met robotica voor ondersteuning van reikbewegingen zou een uitstekende oplossing kunnen om het trainen van functionele taken mogelijk te maken.

Het doel van dit proefschrift is om methoden voor de aansturing van een geautomatiseerd hybride revalidatie systeem te ontwikkelen en te evalueren. Door robot ondersteuning voor reiken te combineren met FES ondersteuning voor grijpen wordt functionele arm en hand training mogelijk. Voor een succesvolle klinische toepassing, dient een dergelijk apparaat veilig en eenvoudig te gebruiken zijn door een leek. Het revalidatieproces kan nog verder worden geïntensiveerd indien een geautomatiseerd systeem geschikt is voor thuisgebruik.

Voor een succesvolle toepassing van een hybride systeem, zijn oplossingen voor de afzonderlijke onderdelen eerst onderzocht. In hoofdstuk 2, werden de mogelijkheden voor selectieve activering van afzonderlijke vingers door FES onderzocht bij gezonde proefpersonen en gerelateerd aan plaatsing van de elektroden. Hoewel het mogelijk is om geschikte locaties te vinden voor elke vrijheidsgraad werd aangetoond dat de exacte posities van deze locaties zeer variabel zijn tussen verschillende personen. Een individuele aanpak voor de toepassing van FES is daarom gewenst.

Het menselijk spierstelsel is redundant: er zijn meer spieren dan vrijheidsgraden aanwezig. In hoofdstuk 3 zijn geïndividualiseerde methoden gepresenteerd en geëvalueerd om een redundant spierstelsel aan te sturen met FES. Een individueel model werd gebruikt om stimulatieparameters van de duimspieren te relateren aan de opgewekte duimkrachten. Vervolgens werden de geïndividualiseerde spiermo-

dellen gebruikt om de duimkracht naar een doelkracht (vector) te regelen door het verdelen van de belasting over de afzonderlijke spieren. Deze aanpak is haalbaar gebleken bij zowel gezonde proefpersonen als mensen die een CVA hebben gehad. Echter, maken het aantal instelbare parameters de aanpak enigszins omslachtig en tijdrovend voor klinische toepassing.

Om het aantal instelbare parameters te verminderen, zijn stappen genomen richting een meer geautomatiseerde methode die is toegepast voor het regelen van de beweging van de duim en de vingers tijdens pakken en weer los laten van verschillende objecten (hoofdstuk 4). De relatie tussen spierstimulatie en beweging van individuele vingers werd gemodelleerd. Een zogenoemde model predictive controller (MPC) werd gebruikt om het geschatte model te gebruiken om de beweging te voorspellen en om de benodigde stimulatieparameters te berekenen op basis van de gewenste referentiehoeken voor de vingers. Deze regelaar bleek geschikt voor het volgen van referentiehoeken. Daarnaast werd aangetoond dat de methode bruikbaar is voor het succesvol pakken en weer loslaten van echte voorwerpen met verschillende afmetingen in zowel gezonde proefpersonen als CVA patiënten. Daarmee toont hoofdstuk 4 aan dat gecontroleerde interactie met echte objecten haalbaar is, hetgeen een grote stap is op weg naar training van functionele taken.

Handbeweging is alleen functioneel met de juiste armbeweging. In samenwerking met projectpartners werd een prototype robot ontwikkeld. Het apparaat en de aansturingmethoden zijn gepresenteerd in hoofdstuk 5, samen met de technische evaluatie van het apparaat. Het systeem beschikt over de technische mogelijkheden om het armgewicht van de gebruiker te compenseren en armbewegingen te ondersteunen. Vanwege de inherente veiligheid en het gebruiksgemak, heeft het systeem de potentie om de laatste stap naar een klinische toepassing, of zelfs thuisgebruik, te maken. Voor klinische toepassing is een geïntegreerd systeem dat zich niet alleen richt op armtraining maar ook op training van grijpen en loslaten gunstiger, aangezien een dergelijk systeem gebruikt kan worden om functionele armbewegingen te ondersteunen tijdens revalidatie.

De systemen voor het aansturen van de vingers met FES (hoofdstuk 4) en voor ondersteuning van de armbeweging (hoofdstuk 5) zijn gecombineerd voor de ondersteuning van functionele taken. Het systeem werd geëvalueerd tijdens passieve functionele bewegingen bij gezonde proefpersonen en bij ernstige chronische CVA patiënten (hoofdstuk 6). Vanuit een technisch oogpunt is volledige ondersteuning van de beweging (de persoon is volledig passief) de meest veeleisende taak. Bij gezonde proefpersonen werden hoge succespercentages behaald. Ook de percentages van de deeltaken bij gezonde proefpersonen waren hoog (76 % -100 %). De percentages bij gezonde proefpersonen tonen de mogelijkheden van het systeem aan voor het ondersteunen van functionele taken. Echter, de prestaties van het systeem bij chronische CVA patiënten is nog niet goed genoeg. Geen van de testen in de CVA patiënten werden volledig succesvol afgerond. Ten dele door onnauwkeurigheden in arm positionering en deels door beperkt resultaat van handopening en grijpen. De geïnccludeerde CVA patiënten waren zwaar getroffen en in een chronische toestand. Extra evaluatie in een bredere groep CVA patiënten is vereist om goede conclusies te kunnen trekken aangaande toepasbaarheid van het

huidige systeem.

Idealiter zou een geautomatiseerd systeem de beweging alleen ondersteunen wanneer dat nodig is, kan de patiënt het systeem zelf aansturen en biedt het systeem mogelijkheden voor intensieve taak training. Deze extra eisen maximaliseren de inspanning voor de patiënt en daardoor het therapieresultaat. In dit proefschrift is de technische haalbaarheid geëvalueerd en daarom werden de proefpersonen gevraagd om volledig te ontspannen in de in dit proefschrift beschreven experimenten (geen vrijwillige beweging). Het bewegen van een passief persoon is voor het systeem de meest veeleisende taak en is daarom gebruikt als uitgangspunt voor de evaluaties. In hoofdstuk 7 zijn mogelijke oplossingen voor actieve betrokkenheid van de gebruikers, detectie van de gebruikersintentie en training in een thuisomgeving voor hogere intensiteit besproken. Ten eerste, kan de ondersteuning worden beperkt op basis van de prestaties van patiënten en taak scores. Ten tweede zou de intentie van de gebruiker bepaald kunnen worden uit de gemeten interactie krachten. Tenslotte, zou het gebruik van elektrode arrays ervoor zorgen dat elektroden door een onervaren gebruiker geplaatst kunnen worden. Met dergelijke uitbreidingen kan het systeem naar een hoger niveau worden getild, waardoor hoogfrequente training van functionele bewegingen met maximale activiteit van de patiënt mogelijk gemaakt wordt.

Dit proefschrift laat de technische haalbaarheid zien van een geautomatiseerd systeem dat revalidatie robotica en FES combineert. Het is nu aan de commerciële markt om dergelijke technologie in de dagelijkse gezondheidszorg te implementeren. Daarvoor dient acceptatie van technologie in de gezondheidszorg verder toe te nemen. De technologische mogelijkheden van het combineren van robotica en FES met een geïndividualiseerde aanpak die zijn gepresenteerd in dit proefschrift zullen bijdragen aan een duurzame gezondheidszorg, terwijl functionele onafhankelijkheid van CVA patiënten wordt gemaximaliseerd.

Dankwoord

U bent begonnen met lezen van het dankwoord. Wellicht het meest gelezen gedeelte van dit proefschrift. Een proefschrift dat er niet was geweest zonder de hulp van vele anderen en waarvan de totstandkoming op zijn minst een stuk onaangenamer was geweest zonder de steun van vele anderen. Eenieder die op welke manier dan ook een bijdrage heeft geleverd aan dit proefschrift of het proces daar naartoe wil ik hartelijk danken. Een aantal personen wil ik hieronder in het bijzonder noemen.

Allereerst wil ik alle vrijwilligers (al dan niet met een beperking ten gevolge van een beroerte) hartelijk danken voor hun tijd en moeite om deel te nemen aan de verschillende experimenten. Zonder jullie had ik geen data gehad om te analyseren en had dit proefschrift niet kunnen bestaan.

Zonder prof. dr. ir. Van der Kooij was dit proefschrift er ook zeker niet geweest. Mogelijk had ik dan niet eens overwogen om aan een promotieonderzoek te beginnen. Beste Herman, jij bent degene die me op deze mogelijkheid heeft gewezen en die me er warm voor heeft weten te maken om voor deze positie te kiezen. Terugkijkend op de afgelopen vijf jaar heb ik daar geen spijt van gehad, heel erg bedankt voor jouw inspanningen hiervoor. Ook tijdens het onderzoek zelf stond je altijd klaar (al dan niet fysiek, gezien je Zwitserse avontuur) met goede suggesties (soms wat in overvloed) en een kritische blik. Je hebt me de ruimte gegeven om mijn eigen onderzoek te leiden en was in staat om me waar nodig bij te sturen door mij met kleine opmerkingen naar nieuwe inzichten te leiden. Enorm bedankt daarvoor!

Prof. dr. ir. Veltink, als co-promotor heb jij ook een belangrijke rol gespeeld in de invulling van mijn onderzoek. Beste Peter, mijn eerste ervaringen met FES waren op jouw kantoor. Jij leerde me hoe ik de verschillende stimulatieparameters kon instellen en wat het effect van de verschillende parameters is. Gaandeweg mijn promotieonderzoek bleek jij behalve van FES, van veel meer dingen veel verstand te hebben. Ik dank je graag voor je scherpe blik, heldere feedback en nuttige suggesties zowel tijdens het opzetten van de verschillende studies als bij het verwerken van de data en het schrijven van de artikelen. Dankjewel!

Beste Alfred, als assistent-promotor was ook jouw hulp van groot belang. Ik heb me verbaasd over het gemak waarmee jij tijdens het oplossen van praktische (robot-)problemen (uitdagingen) in het lab schakelt tussen de praktijk en je grote theoretische kennis. Even alles rustig bekijken op een rijtje zetten en beredeneren en dan was de oplossing vaak snel binnen handbereik. Dank ook voor je nuchtere kijk en vaak rake opmerkingen die voor mij weer als eyeopener konden dienen. Tijdens het schrijven stond je klaar met goede suggesties om het verhaal nog helderder en meer to the point te maken. Bedankt voor dit alles!

Lieve Lianne, volgens mij kan de vakgroep Biomedische Werktuigbouwkunde (BW) zich geen betere secretaresse wensen. Als duizendpoot sta je altijd klaar voor iedereen en wil en kan je alles regelen. Daarnaast ben je ook nog altijd geïnteresseerd in de thuissituatie en zorg je voor gezelligheid in de vakgroep. Dankjewel voor al je organisatorische hulp.

Voor het realiseren van meetopstellingen moest ik regelmatig terugvallen op het technisch ondersteunende personeel. Met name Geert en later Wouter hebben mij

hierbij grote diensten bewezen. Hoewel ik het zelf ook altijd leuk vond om dingen te klussen, was het fijn om iemand in de buurt te hebben die er ook echt verstand van heeft. Geert, jammer dat je geen deel meer uitmaakt van de vakgroep. Ik heb je aanwezigheid altijd als zeer prettig ervaren, zowel qua persoonlijkheid als voor hulp bij het realiseren van opstellingen.

Alexander, Floor en Tjitske, samen vormden we de gezellige kamer. Dank jullie wel voor het creëren van een prettige werksfeer, de welkome afleiding. Ook bedankt voor de gezellige etentjes (met zijn vieren op stap in Alex' Camaro zal vrees ik niet meer gaan lukken, althans niet met droge voeten). Fijn dat ik bij jullie terecht kon voor suggesties, tips of babypraat.

Ook alle andere collega's van BW wil ik bedanken voor alle gezelligheid en bruikbare tips. In het bijzonder wil ik nog het BW futsal team en de lunchwandelaars noemen. Het was heerlijk om tussendoor even je zinnen te kunnen verzetten door samen een balletje te trappen of een frisse neus te halen. BW is de laatste jaren flink uitgedijd, maar steeds gezellig gebleven. Allemaal bedankt! Thank you all!

Also I would like to gratefully thank our German MIAS-ATD project partners TIC and Use-Lab. Christian you have been very helpful in designing and troubleshooting the electrical stimulator. Many thanks for all your prompt answers and all the help in developing/modifying the stimulators. For the people at Use-Lab many thanks for all the good discussions during meetings, the help in evaluating the robot and the offers to assist me with my experiments.

Ook de Nederlandse projectpartners wil ik danken voor alle hulp en de prettige bijeenkomsten. De mensen van Demcon en RRD ontzettend bedankt voor alle hulp en prettige bijeenkomsten. Thijs, jij valt inmiddels in beide categorieën. Jou wil ik in het bijzonder bedanken voor het sparren en de hulp en suggesties die je had voor mijn onderzoek. Ik wens je heel veel succes met de laatste lodjes van jouw promotieonderzoek! Ook Gerdienke en Jaap wil ik hartelijk danken voor het mij (samen met Cindy Lammertink namens de UT) wegwijs maken in METC-land. Zonder jullie hulp had het ongetwijfeld een stuk langer geduurd voordat ik überhaupt met mijn experimenten kon beginnen.

Dear Alex, although I learned German in high-school and grew up very close to the German border, English has always been the common denominator in our communication. I owe you many thanks in whatever language. You started your career in Enschede with an internship within my PhD project, decided to stay and help me out as student-assistant and finally did your MSc assignment on the same topic, which even resulted in a chapter of this thesis. We had nice discussions on how to interpret results or improve setups and algorithms. I had a lot of fun with you in the lab and I'm very happy to have you as my paranimph. Vielen Dank für die angenehme Zusammenarbeit!

Beste Janneke, ik ben ook erg blij met jou als paranimf. We kennen elkaar al een hele tijd, het blijft leuk om je een beetje te stangen, maar eigenlijk ben ik gewoon blij om jou tot mijn vriendenkring te kunnen rekenen. Fijn dat je zonder na te hoeven denken (en zonder goed te weten wat van je verwacht wordt) direct 'ja' zei op mijn verzoek om paranimf te worden. Dankjewel dat je dit voor me

doet. Ik wens je heel veel succes met je eigen promotieonderzoek!

Alle vrienden en familie wil ik danken voor de nodige afleiding die jullie me geboden hebben. Papa en mama bedankt voor de wetenschap dat ik altijd op jullie terug kan vallen en ook voor het organiseren van de gezellige familieweekenden. Thijs, Patrick, Helma, Dirk en Harm bedankt voor het mede creëren van de gezelligheid in die weekenden. Lieve brusters, we zien elkaar niet altijd even veel (misschien wel te weinig?) maar als we samen zijn is het altijd weer als vanouds: gezellig. Bedankt voor de nodige afleiding de afgelopen jaren. Henk, Ineke, Sanne en Frans, fijn dat jullie altijd zo geïnteresseerd waren in mij en mijn onderzoek. Bedankt voor de warmte en gezelligheid die jullie gebracht hebben de afgelopen jaren. Hanne, Marie en Bent, Freek en David bedankt dat ik jullie oom mag zijn en dank jullie wel voor het plezier dat jullie op de momenten dat we elkaar zagen gebracht hebben met jullie onuitputtelijke energie.

Judi, mijn lief, zonder jou was dit boekje er niet geweest. Dankjewel voor al je handreikingen. Dank je wel voor het brengen van rust op momenten van twijfel. Dank je wel dat ik altijd heb kunnen rekenen op jou onvoorwaardelijke steun en liefde. Ik geniet van het leven met jou. Zo mogelijk nog meer nu Emma en Sep erbij zijn. Lieve Emma dank je wel voor al je verstopspelletjes, lekkere knuffels, leuke dansjes en heerlijke lach. Lieve Sep, dankjewel voor je aanwezigheid, leuke lach en het feit dat je me nu de tijd gunt om dit dankwoord te schrijven. Judi, Emma en Sep, het spijt me dat ik de afgelopen tijd regelmatig (al dan niet fysiek) afwezig was. Ik zal er voor zorgen dat ik niet meer opeens 'uit' sta, nu het proefschrift bijna af is.

Curriculum Vitae



Ard Westerveld was born in 1984 in Gendringen, The Netherlands. He received his high school diploma in 2002 from the 'Christelijk College Schaersvoorde' in Aalten. The same year he started studying computer science at the University of Twente. In December 2003, he switched to studying biomedical engineering with neural and motor systems as specialization. During his internship he went to the Sint Maartenskliniek Research Development & Education in Nijmegen, where he developed methodologies for auto-detection of EMG onset times for the EMG analysis in varus/valgus gait before and after a double osteotomy. In March 2009, he received his Master's degree in biomedical engineering after a final project on the development and evaluation of methodology for studying calf muscle length changes during human balance control with ultrasound imaging and a custom-built perturbation device. Shortly thereafter, he started his PhD research project in the laboratory of biomechanical engineering at the University of Twente under the supervision of prof. dr. ir. H. van der Kooij, prof. dr. ir. P.H. Veltink and dr. ir. A.C. Schouten. The research focused on the evaluation of control algorithms for a hybrid rehabilitation system combining robotics and functional electrical stimulation, aimed at functional arm and hand therapy after stroke. This thesis is the result of this research.

In 2010, Ard married to Judi Rougoor and they have two children. Their daughter Emma was born in 2011 and their son Sep was born in 2013. Since January 2014, he is working as a mechatronical engineer at FWD Mechatronical Solutions BV in Varsseveld, The Netherlands.

Publications

Journal publications

- Westerveld, AJ**, AC Schouten, PH Veltink, and H van der Kooij (2012). "Selectivity and resolution of surface electrical stimulation for grasp and release." *IEEE Transactions on Neural Systems and Rehabilitation Engineering*. 20 (1), pp. 94–101.
- Westerveld, AJ**, AC Schouten, PH Veltink, and H van der Kooij (2013). "Control of thumb force using surface functional electrical stimulation and muscle load sharing." *Journal of NeuroEngineering and Rehabilitation* 10 (1), p. 104.
- Kuck, A, **AJ Westerveld**, PH Veltink, and H van der Kooij (2013). "Grasp control in stroke patients using functional electrical stimulation and model predictive control." *submitted*.
- Westerveld, AJ**, BJ Aalderink, W Hagedoorn, M Buijze, AC Schouten, and H van der Kooij (2013). "A damper driven robotic endpoint manipulator for functional rehabilitation exercises after stroke." *submitted*.
- Westerveld, AJ**, AC Schouten, PH Veltink, and H van der Kooij (2013). "Passive Reach and Grasp with Functional Electrical Stimulation and Robotic Arm Support." *submitted*.

Conference publications

- Kooij, H van der, EHF van Asseldonk, **AJ Westerveld**, and AC Schouten (2009). "Measurement of calf muscle length during perturbed standing." *Society for Neuroscience conference, Chicago (IL), USA*.
- Boonstra, TA, **AJ Westerveld**, and H van der Kooij (2009). "Assessment of reflex modulation during perturbed standing." *Society for Neuroscience conference, Chicago (IL), USA*.
- Westerveld, AJ**, H van der Kooij, PH Veltink, and AC Schouten (2009). "Influences of experienced gravitational stiffness on ankle joint stabilization during standing." *IEEE Engineering in Medicine and Biology Society Benelux meeting, Enschede, The Netherlands*.
- Westerveld, AJ**, AC Schouten, PH Veltink, and H van der Kooij (2010). "Selectivity of electrical stimulation for grasping support." *The XVIII congress of the International Society of Electrophysiology and Kinesiology, Aalborg, Denmark*.
- Westerveld, AJ**, AC Schouten, PH Veltink, and H van der Kooij (2011). "Selectivity and of electrical stimulation of finger muscles for grasping support." *3rd Dutch Biomedical Engineering Conference, Egmond aan Zee, The Netherlands*.
- Westerveld, AJ**, AC Schouten, PH Veltink, and H van der Kooij (2012). "Adaptive control of thumb tip position by multi-channel functional electrical stimulation." *3rd Annual Conference of the International Functional Electrical Stimulation Society UK and Ireland Chapter, Birmingham, UK*.

- Westerveld, AJ**, A Kuck, AC Schouten, PH Veltink, and H van der Kooij (2012). "Grasp and release with surface functional electrical stimulation using a Model Predictive Control approach." *2012 Annual International Conference of the IEEE Engineering in Medicine and Biology Society, San Diego, USA*, pp. 333–336.
- Westerveld, AJ**, AC Schouten, PH Veltink, and H van der Kooij (2013). "Subject specific assistance of reach, grasp and release after stroke." *4th Dutch Biomedical Engineering Conference, Egmond aan Zee, The Netherlands*.
- Westerveld, AJ**, AC Schouten, PH Veltink, and H van der Kooij (2013). "Thumb force control: muscle load sharing with functional electrical stimulation." *COST Action TD1006 symposium on Rehabilitation Robotics, Enschede, The Netherlands*.
- ¹**Westerveld, AJ**, A Kuck, AC Schouten, PH Veltink, and H van der Kooij (2013). "Passive Reach and Grasp with Functional Electrical Stimulation and Robotic Arm Support." *18th annual conference of the International Functional Electrical Stimulation Society, Donastia-San Sebastian, Spain*.
- Beekhuis, H, **Westerveld, AJ**, AHA Stienen, and H van der Kooij (2013). "Design of a self-aligning 3-DOF actuated exoskeleton for diagnosis and training of wrist and forearm after stroke." *IEEE International Conference on Rehabilitation Robotics, 2013, Seattle, United States*.

¹Received a Vodovnik award for second best student paper